

ISTANBUL TECHNICAL UNIVERSITY ★ GRADUATE SCHOOL OF SCIENCE
ENGINEERING AND TECHNOLOGY

**SELF-HEALING OF HIGH-PERFORMANCE FIBRE-REINFORCED
CEMENTITIOUS COMPOSITES**

M.Sc. THESIS

**Ömer KAYA
(501071089)**

Department of Civil Engineering

Structural Engineering Programme

Thesis Advisor: Prof. Dr. Mehmet Ali TAŞDEMİR

NOVEMBER 2011

İSTANBUL TEKNİK ÜNİVERSİTESİ ★ FEN BİLİMLERİ ENSTİTÜSÜ

**YÜKSEK PERFORMANSLI FİBER DONATILI ÇİMENTO ESASLI
KOMPOZİTLERİN KENDİ KENDİNİ İYİLEŞTİRMESİ**

YÜKSEK LİSANS TEZİ

**Ömer KAYA
(501071089)**

İnşaat Mühendisliği Anabilim Dalı

Yapı Mühendisliği Programı

Tez Danışmanı: Prof. Dr. Mehmet Ali TAŞDEMİR

KASIM 2011

Ömer Kaya, a **M.Sc.** student of **ITU Graduate School of Science, Engineering and Technology** student ID **501071089**, successfully defended the **thesis** entitled **“SELF-HEALING OF HIGH-PERFORMANCE FIBRE-REINFORCED CEMENTITIOUS COMPOSITES** which he prepared after fulfilling the requirements specified in the associated legislations, before the jury whose signatures are below.

Thesis Advisor : **Prof. Dr. Mehmet Ali TAŞDEMİR**
İstanbul Technical University

Co-advisor : **Prof.Dr. Viktor MECHTCHERINE**
TU Dresden

Jury Members : **Prof. Dr. Turan ÖZTURAN**
Boğaziçi University

Prof. Dr. Hulusi ÖZKUL
İstanbul Technical University

Doç. Dr. Yılmaz AKKAYA
İstanbul Technical University

Date of Submission : 31 October 2011

Date of Defense : 26 November 2011

To my mum in the heaven,

FOREWORD

I would like to thank my thesis supervisors Prof. Dr.-Ing. Viktor Mechtcherine and Prof. Dr. Mehmet Ali Taşdemir for providing me the opportunity to complete my thesis and for their support and guidance that made my thesis work possible. I also want to thank my thesis advisory committee.

I would also like to thank all my colleagues in Institute for Construction Materials at TU Dresden and in ISTON Corporation for their help.

For the non-scientific side of my thesis, I particularly want to thank my family, Frau Beesemann and all my friends in Germany and Turkey for their continuous support.

November 2011

Ömer KAYA

TABLE OF CONTENTS

	<u>Page</u>
FOREWORD	ix
TABLE OF CONTENTS	xi
ABBREVIATIONS	xiii
LIST OF TABLES	xv
LIST OF FIGURES	xvii
SUMMARY	xxii
ÖZET	xxiiiv
1. INTRODUCTION	1
1.1 Purpose of Thesis	1
1.2 Literature Review	2
1.2.1 Self-Healing phenomena.....	2
1.2.1.1 Why self-healing in cement based materials.....	2
1.2.1.2 Intelligence levels of materials.....	4
1.2.2 Definitions of self-healing	5
1.2.2.1 Self-closing	6
Experimental evidence on autogenic self-closing.....	8
1.2.2.2 Self-healing	11
1.2.3 Textile reinforced concrete	25
1.2.4 Superabsorbent polymers	26
2. EXPERIMENTAL STUDY	31
2.1 Materials.....	31
2.1.1 Cement	31
2.1.2 Aggregates	32
2.1.2.1 Sand.....	32
2.1.3 Pozzolanas.....	34
2.1.3.1 Fly ash	34
2.1.3.2 Silica fume	35
2.1.4 Admixtures.....	35
2.1.5 Water	36
2.1.6 Textile reinforcement.....	36
2.1.7 Superabsorbent polymer	37
2.2 Mixture Composition, Specimen Preparation, Curing and Testing Program...	38
2.3 Fresh Concrete Properties	40
2.4 Experimental Procedure	40
2.4.1 Uniaxial tension tests	41
2.4.2 Microscopic analyses	42
2.4.2.1 Electron scanning microscopy	42
2.4.2.2 Optical microscopy	42
2.4.2.3 Mercury intrusion porozimeter test.....	43
2.4.2.4 EDX analysis.....	43

3. EXPERIMENTAL RESULTS AND DISCUSSION	45
3.1 Mechanical Properties of Specimens.....	45
3.1.1 Preliminary work.....	46
3.1.2 Final work	51
3.2 Microscopic Analyses	62
3.2.1 Optical microscopy analysis.....	62
3.2.1.1 Two weeks curing	62
3.2.1.2 Four weeks curing	65
3.2.1.3 Thin sections.....	68
3.2.2 SEM and EDX analysis.....	75
3.2.3 MIP analysis.....	81
4. CONCLUSIONS AND RECOMMENDATIONS	85
REFERENCES	87
CURRICULUM VITAE	93

ABBREVIATIONS

C-S-H	: Tobermorit
SEM	: Scanning Electron Microscope
<i>k</i>	: Coefficient of Permeability
FRCC	: Fibre Reinforced Cementitious Composites
PE	: Polyethylene
SC	: Steel Cord
ECC	: Engineered Cementitious Composites
EDS	: Energy Dispersive Spectroscopy System
BFSC	: Blast Furnace Slag Cement
OPC	: Ordinary Portland Cement
RH	: Relative Humidity
UHPC	: Ultra High-Performance Concrete
AR	: Alkali Resistant
TRC	: Textile Reinforced Concrete
SAP	: Superabsorbent Polymers
EDX	: Energy Dispersive X-ray
ESEM	: Environmental Scanning Electron Microscope
MIP	: Mercury Intrusion Porozimeter
UV	: Ultraviolet

LIST OF TABLES

	<u>Page</u>
Table 1.1 : Classification of aimed service life	3
Table 1.2 : Definitions of self-healing terms.	6
Table 1.3 : Composition of the mortar mixes giving weight of each constituent.	9
Table 1.4 : Permissible crack width for self-closing	11
Table 1.5 : Mix proportion of FRCC specimens	13
Table 1.6 : Maximum crack width evaluated by means of microscope observation.	14
Table 2.1 : Properties of cement types used in experiments	31
Table 2.2 : Properties of CEM I 32.5 R	32
Table 2.3 : Properties of CEM III/B 32,5.....	32
Table 2.4 : Sieve total pass (%) of sand 0/1	33
Table 2.5 : Properties of quartz sand (0,06-0,2)mm	33
Table 2.6 : Typical grain size and grain characteristics and typical grain size related properties of Millisil.....	34
Table 2.7 : Physical and Chemical Properties of Millisil W3.....	34
Table 2.8 : Properties of fly ash	35
Table 2.9 : Properties of silica fume	35
Table 2.10 : Properties of super plasticizer	36
Table 2.11 : Properties of textile reinforcement.....	36
Table 2.12 : Material description and properties of commercial filament.....	36
Table 2.13 : Material amounts for 1 m ³ concrete mixture	39
Table 3.1 : Table of specimens' naming according to various concrete composition and curing conditions	46
Table 3.2 : Table of specimens' naming according to various concrete composition, curing conditions and durations	51

LIST OF FIGURES

	<u>Page</u>
Figure 1.1 : Performance and costs with elapse of time for normal and high quality structures.....	4
Figure 1.2 : Hierarchy of materials based on different levels of intelligence.....	5
Figure 1.3 : Different causes of autogenic self-closing.	6
Figure 1.4 : Calcite crystals on a crack face after opening the crack.....	7
Figure 1.5 : Influence of crack width on flow relative to initial flow.....	8
Figure 1.6 : Initial flow through cracks of various widths for 1 m length.....	9
Figure 1.7 : Decrease in water permeability coefficient k [m/s] due to autogenous closing of the crack in specimens with different crack widths.....	11
Figure 1.8 : Microscopic observation of self-healing products at a crack surface....	14
Figure 1.9 : Time dependence of mean size of self-healing products attached at the crack surface	15
Figure 1.10 : Influence of time dependence of water permeability coefficient due to type of FRCC	16
Figure 1.11 : Comparison of tensile property of specimens before and after 28 days of self-healing.....	17
Figure 1.12 : Resonant frequency recovery of ECC specimens pre-loaded	19
Figure 1.13 : Optical micrograph of healing product in ECC cement and SEM micrograph of a healed crack.....	20
Figure 1.14 : Load-Displacement behaviour of virgin specimen and reloading after 3 weeks in air.....	23
Figure 1.15 : Load-Displacement behaviour of cured and non-cured specimens.....	23
Figure 1.16 : Steel reinforced concrete hyper-shell	26
Figure 1.17 : Schematic view of the test setup for gas permeability and water permeability.....	26
Figure 1.18 : Dry and swollen SAP particle	27
Figure 1.19 : SAP based on polyacrylic acid.....	27
Figure 1.20 : Autogenous shrinkage of fine and coarse grained UHPC measured starting after the final set.....	29
Figure 2.1 : Grain size curve of sand 0/1 mm.....	33
Figure 2.2 : Grain size distribution of fly ash	35
Figure 2.3 : Biaxial textile reinforcement made of carbon multifilament yarns.....	37
Figure 2.4 : Particle-size-distribution of SAP material.....	37
Figure 2.5 : Geometry of TRC tension test specimen.....	38
Figure 2.6 : Loading of a TRC tension test specimen.....	39
Figure 2.7 : Slump test equipment	40
Figure 2.8 : Uniaxial tension test machine.....	41
Figure 3.1 : Stress-strain curve of C1WD and 2C1WD.....	46
Figure 3.2 : Stress-strain curve of C1A and 2C1A	47
Figure 3.3 : Stress-strain curve of C1W and 2C1W	47

Figure 3.4 : Stress-strain curve of C3WD and 2C3WD.....	48
Figure 3.5 : Stress-strain curve of C3A and 2C3A.....	49
Figure 3.6 : Stress-strain curve of C3W and 2C3W.....	49
Figure 3.7 : Stress-strain curve of SAPWD and 2SAPWD	50
Figure 3.8 : Stress-strain curve of SAPA and 2SAPA	50
Figure 3.9 : Stress-strain curve of SAPW and 2SAPW	50
Figure 3.10 : Stress-strain curve of C1A22-2C1A22.....	52
Figure 3.11 : Stress-strain curve of C1A42-2C1A42.....	52
Figure 3.12 : Stress-strain curve of C3A21-2C3A21.....	52
Figure 3.13 : Stress-strain curve of C3A41-2C3A41.....	53
Figure 3.14 : Stress-strain curve of SAPA21-2SAPA21	53
Figure 3.15 : Stress-strain curve of SAPA41-2SAPA41	54
Figure 3.16 : Stress-strain curve of C1W22-2C1W22.....	54
Figure 3.17 : Stress-strain curve of C1W41-2C1W41	55
Figure 3.18 : Stress-strain curve of C3W22-2C3W22.....	55
Figure 3.19 : Stress-strain curve of C3W43-2C3W43.....	56
Figure 3.20 : Stress-strain curve of SAPW21-2SAPW21.....	56
Figure 3.21 : Stress-strain curve of SAPW43-2SAPW43.....	56
Figure 3.22 : Stress-strain curve of C1WD121-2C1WD121	57
Figure 3.23 : Stress-strain curve of C1WD142-2C1WD142	57
Figure 3.24 : Stress-strain curve of C3WD123-2C3WD123	58
Figure 3.25 : Stress-strain curve of C3WD142-2C3WD142	58
Figure 3.26 : Stress-strain curve of SAPWD121-2SAPWD121.....	59
Figure 3.27 : Stress-strain curve of SAPWD141-2SAPWD141.....	59
Figure 3.28 : Stress-strain curve of C1WD223-2C1WD223	60
Figure 3.29 : Stress-strain curve of C1WD24-2C1WD243	60
Figure 3.30 : Stress-strain curve of C3WD221-2C3WD221	60
Figure 3.31 : Stress-strain curve of C3WD243-2C3WD243	61
Figure 3.32 : Stress-strain curve of SAPWD223-2SAPWD223.....	61
Figure 3.33 : Stress-strain curve of SAPWD243-2SAPWD243.....	62
Figure 3.34 : Optical microscope photos of C1A, C1W,C1WD1 and C1WD2 specimens.....	63
Figure 3.35 : Optical microscope photos of C3A, C3W, C3WD1 and C3WD2 specimens.....	64
Figure 3.36 : Optical microscope photos of SAPA, SAPW, SAPWD1 and SAPWD2 specimens.....	65
Figure 3.37 : Optical microscope photos of C1A, C1W, C1WD1 and C1WD2 specimens.....	66
Figure 3.38 : Optical microscope photos of C3A, C3W, C3WD1 and C3WD2 specimens.....	67
Figure 3.39 : Optical microscope photos of SAPA, SAPW, SAPWD1 and SAPWD2 specimens.....	68
Figure 3.40 : The optical microscope photo of CEM I reference specimen	69
Figure 3.41 : The photos of CEM I specimens exposed to water and wet-dry curing for 2 and 4 weeks, which were taken under UV light	69
Figure 3.42 : The photos of CEM III specimens exposed to water and wet-dry curing for 2 and 4 weeks, which were taken under UV light	70
Figure 3.43 : The optical microscope photos of CEM III specimens after various exposures	71

Figure 3.44 : The photos of CEM III specimens exposed to water and wet-dry curing for 2 and 4 weeks, which were taken under UV light	73
Figure 3.45 : The optical microscope photos of SAP group specimens after various exposures	74
Figure 3.46 : SEM picture of a crack and EDX analysis of the specimen C1W4	75
Figure 3.47 : EDX analysis of the specimen C1WD14	76
Figure 3.48 : SEM picture of a crack and EDX analysis of the specimen C3W4	76
Figure 3.49 : SEM picture of a crack and EDX analysis of the specimen SAPW4..	77
Figure 3.50 : SEM pictures of CEM I group specimens.....	78
Figure 3.51 : SEM pictures of CEM III group specimens	80
Figure 3.52 : SEM pictures of CEM III group specimens	81
Figure 3.53 : Total pore size distribution of C1 group specimens.....	82
Figure 3.54 : Total pore size distribution of C3 group specimens.....	82
Figure 3.55 : Total pore size distribution of SAP group specimens	83

SELF-HEALING OF HIGH-PERFORMANCE FIBRE-REINFORCED CEMENTITIOUS COMPOSITES

SUMMARY

Cracks in the concrete have many negative effects on durability and mechanical properties. Shrinkage and freezing-thawing can be mentioned as some reasons of cracks. They may cause loss of performance and decrease service life of concrete. Preventing cracks is important especially for watertight structures and for prolonging the service life. Many researchers have searched self-healing in recent years and it has become a common method for preventing cracks and recovery of strength and durability properties of concrete. Self-healing of concrete increases the service life of structures and durability properties of concrete structures. However self-healing of concrete is an economic and ecologic solution. The mechanism of self-healing mostly depends on continued hydration and formation of calcites in the cracks with the presence of water.

The self-healing of high performance fiber reinforced concrete was investigated in this study. Four layered textile reinforced concrete specimens were chosen as high performance fiber reinforced concrete. Two concrete mixtures were designed for production of specimens. The binder in the first mixture was pure Portland cement (CEM I) and in the second mixture the binders were CEM III, fly ash and silica fume. Super absorbent polymers were added to the first composition as the third mixture group to observe the effect of super absorbent polymers to self-healing. Specimens were cast as rectangular prisms with the dimensions of 500x100x14 mm. After demoulding they were wrapped in plastic foil and kept in the climate room for 28 days. Tensile test was chosen for controlled pre-cracking, the displacement ratio was 3mm/m. After pre-cracking specimens were exposed to different curing conditions and durations for 2 and 4 weeks. Two types of wet-dry cycles were chosen to simulate the outdoor environment conditions. Specimens were exposed to air, water, wet-dry cycle-I (water curing during 1 hour then laboratory climate during 23 hours) and wet-dry-II (water curing during 1 hour then laboratory climate during 71 hours). The curing durations were 2 and 4 weeks. Mechanical tests and microscopic analysis were done for observing self-healing. Uniaxial tensile test, optical microscope analysis, thin sections analysis, scanning electron microscopy, EDX analysis and MIP tests were performed in the study. It can be concluded that self-healing products, which were attached to cracks after water and wet-dry exposures, are leading to recovery of mechanical performance. Air curing showed no self-healing in all groups. Longer curing is increasing mechanical healing performance for water curing and wet-dry cycling. Specimens that were produced with CEM I cement and cured for longer time showed the best self-healing behavior because of unhydrated cement left after hydration. Addition of SAP materials supported further hydration and showed positive mechanical effect for less time wet-dry cycle. Presence of water in the crack is the most important factor for self-healing.

However, the healing capacity for pure Portland cement was the highest. Newly formed self-healing products in the cracks were mostly combination of C-S-H phases and calcites. Denser structures were observed after self-healing exposures in MIP tests.

YÜKSEK PERFORMANSLI FİBER DONATILI ÇİMENTO ESASLI KOMPOZİTLERİN KENDİ KENDİNİ İYİLEŞTİRMESİ

ÖZET

Beton yapımının kolay ve ucuz olmasının yanında istenen yapı malzemesi özelliklerini de karşılayabilmesi sonucu dünyada en çok kullanılan yapı malzemesi olmuştur. Son yıllarda beton teknolojisinde önemli gelişmeler yaşanmıştır. Betonun mekanik özelliklerinin gelişmiş olmasına rağmen dürabilite betonda en önemli problemlerden biri olmaya devam etmektedir. Betonda son yıllarda mukavemete göre tasarımdan çok dürabiliteye göre tasarım önem kazanmıştır.

Yapılan tanımlamalara göre malzemeler çevresel tepki verebilme yeteneklerine göre 3 ana gruba ayrılmışlardır. En büyük grupta yer alan temel malzemeler çevrelerinde oluşan değişikliklere herhangi bir cevap veremezler. Buna ters olarak şekil hafızasına sahip malzemeler veya sıcaklığa tepki veren polimerler gibi akıllı malzemeler çevrelerindeki değişimlere faydasal birtakım tepkiler verebilirler. Bunlara ek olarak, en üst grupta yer alan yetenekli ve akıllı malzemeler çevrelerinde oluşan birtakım değişikliklerden kaynaklı verileri işleyebilir ve oluşan bu değişikliğe tepki verebilirler. Deri ve kemik gibi organik maddeler bu grupta yer almasına karşın benzer maddelerin insanlar tarafından yapım araştırmaları ise henüz çok başlardadır. Aynı fikirlerden hareketle betondaki çatlakların betonun mekanik özelliklerine ve durabilitesine pek çok negatif etkisi olduğu bilinmektedir. Rötne ve donma-çözülme gibi bazı olaylar çatlakların oluşma sebepleri arasında gösterilebilir. Çatlaklar betonda performans düşüklüğüne ve betonun servis ömrünün azalmasına neden olabilir. Çatlakların engellenmesi yapıların servis ömrünün uzamasını sağlamak ve özellikle su geçirimsiz yapılarda büyük önem arz etmektedir. Herhangi bir malzemenin kendi kendini iyileştirmesi genelde malzemedeki herhangi bir sebeple oluşan kusurların kaldırılması ve iyileştirilmesi olarak tanımlanır. Birçok araştırmacı son yıllarda betonun kendi kendini iyileştirmesi konusunda araştırma yapmaktadır. Betonun kendi kendini iyileştirmesi yöntemi çatlakların engellenmesi ve mekanik ve dürabilite özelliklerinin geri kazandırılması konusunda bilinen bir metod haline gelmiştir. Betonun kendi kendini iyileştirmesi yapıların servis ömrünü uzattığı gibi dürabilite özelliklerini de iyileştirmektedir. Böylece yapıların tamir masraflarının ve yeni yapı ve hammadde ihtiyaçlarının azaltılması bakımından bu metod ekonomik ve çevreci bir çözüm oluşturmaktadır. Betonun kendi kendini iyileştirmesi mekanizması çoğunlukla çatlak boyunca suyun mevcudiyetiyle beton içerisinde hidrate olmamış çimentonun hidrate olmasına ve kalsit oluşumuna dayanmaktadır. Çatlaklar bazı durumlarda dürabilite özellikleri için problem oluşturmaktadır. Çatlakların sadece kapanmasının yeterli olduğu durumlarda çatlak kapanmasından bahsedilebilir. Diğer durumlarda ise, betonun mekanik özelliklerini geri kazanması betonun kendi kendini iyileştirmesi olarak tanımlanır. Betonun kendi kendini iyileştirmesi eğer beton karışımına giren malzemelerin çeşitli kimyasal ve fiziksel olayları sonucu gerçekleşiyorsa otojenik; eğer reçine dolgulu kırılğan lifler gibi mühendislik malzemelerinin dışarıdan eklenmesiyle oluşuyorsa otonomik kendi kendini iyileştirme adını alır.

Bu çalışmada yüksek performanslı fiber donatılı betonların kendi kendini iyileştirmesi araştırılmıştır. Bu tez çalışmasında 4 tabakalı karbon tekstil donatılı betonlar yüksek performanslı fiber donatılı beton olarak seçilmiştir. Numune üretimi

için iki farklı beton karışımı kullanılmıştır. Birinci grup beton karışımında bağlayıcı malzeme olarak CEM I çimentosu ikinci grup beton karışımında ise CEM III, uçucu kül ve silis dumanı kullanılmıştır. Üçüncü grup karışımlarda ise süper absorban (su emici) polimerlerin betonun kendi kendini iyileştirmesine etkisinin incelenmesi için söz konusu polimerler birinci grup beton karışımı ile aynı içeriğe sahip olan karışımlar üretilmiştir. Çalışmada yuvarlak şekilli doğal kumun yanında 0,06-0,2 mm boyutlara sahip farklı bir çeşit kuvars kumu ve silis kumundan üretilmiş ince kum agrega olarak kullanılmıştır. Kıvam kontrolü için karışımlarda 1,2 kg/lt özgül ağırlıklı naftalin sülfonat esaslı akışkanlaştırıcı katkı kullanılmıştır. Deney numuneleri 500x100x14 mm boyutlara sahip dikdörtgen prizmalardır. Numuneler kalıptan alındıktan sonra plastik folyolar ile kaplanmış ve laboratuvar şartlarında 28 gün bekletilmişlerdir. Sonrasında numunelerde kontrollü çatlakların sağlanması için eksenel çekme testi 3mm/m deformasyon kontrollü olarak gerçekleştirilmiştir. Çalışmanın ilk kısmında numuneler laboratuvar şartlarında bırakılma, su içerisinde bırakılma ve ıslanma-kuruma çevrimine 2 hafta boyunca tabi tutulmuşlardır. Bununla birlikte çalışmanın ikinci kısmında, iki çeşit ıslanma kuruma çevrimi söz konusu betonların karşılaşılabileceği çevresel koşulları temsil etmektedir. Çalışmanın bu kısmında numuneler laboratuvar koşullarında bekletilme, su içerisinde bekletilme, ıslanma kuruma çevrimi-I (numunelerin 1 saatlik su kürünün ardından laboratuvar şartlarında 23 saat bekletilmesi) ve ıslanma kuruma çevrimi-II (numunelerin 1 saatlik su kürünün ardından laboratuvar şartlarında 71 saat bekletilmesi) kür koşullarına maruz bırakılmıştır. Numuneler bu kür koşullarında 2 ve 4 hafta kürlenmiştir. Betonun kendi kendini iyileştirmesinin gözlemlenmesi amacıyla çalışmanın ilk kısımda sadece mekanik testler, ikinci kısmında ise mekanik testlerin yanında mikroskobik analizler de yapılmıştır. Bu amaçla çalışmada eksenel çekme testleri, optik mikroskop analizleri, taramalı electron mikroskobu çalışmaları, EDX analizleri ve civalı porozimetre testleri (MIP) yürütülmüştür. Çalışmada ulaşılan sonuçlar şöyle özetlenebilir: Betonun kendi kendini iyileştirmesi sonucu çatlaklarda oluşan maddeler su kürü ve ıslanma kuruma çevrimleri sonucu oluşmuştur ve bu maddeler betonun mekanik özelliklerini geri kazanmasında etkili olmuşlardır. Laboratuvar şartlarına maruz bırakılan numunelerde herhangi bir kendi kendini iyileştirme aktivitesi görülmemiştir. Daha uzun süreli su kürü ve ıslanma kuruma çevrimleri, numunelerin mekanik özelliklerinin geri kazanılmasında kısa süreli kür ve çevrimlere göre daha etkili olmuştur. Bağlayıcı malzemesi CEM I çimentosu olup 4 hafta boyunca su kürü ve ıslanma kuruma çevrimine maruz bırakılan numuneler en iyi kendi kendini iyileştirme özelliğini göstermişlerdir. Numunelerde bulunan çatlaklar içerisinde su varlığı ile devam eden çimento hidratasyonu bunun en önemli nedenidir. Süper absorban polimerlerin beton karışımına eklenmesi çatlaklarda kür sonucu devam eden hidratasyonu desteklemesinin yanında daha az sayıda ıslanma kuruma çevrimlerinde betonun mekanik özelliklerinin geri kazanılmasında etkili olmuştur. Betonda oluşan çatlaklarda suyun bulunması betonun kendini iyileştirmesi için en önemli faktördür. Çünkü betonun kendi kendini iyileştirmesinde ve çatlakların kapatılmasında gerekli kimyasal reaksiyonlar ve ince malzemelerin taşınması su ile mümkün olabilmektedir. Tüm çimento bağlayıcılı karışımlarda reaksiyona girmemiş çimentonun hidratasyonu mevcuttur ve puzolanik reaksiyonların betonun kendini iyileştirmesini desteklediği görülmüştür. Bunun yanında sadece Portland çimentosunun kullanıldığı karışımların kendi kendini iyileştirme kapasitesi en yüksektir. Betonun kendini iyileştirmesi sonucu çatlaklarda oluşan maddeler SEM fotoğraflarından tam olarak ayırt edilememesinin yanında EDX analizleri ile yapılan eşleştirmelere göre genellikle C-S-H fazı ve kalsittir.

Civalı porozimetre testinde ise tüm kr kořullarında atlaklarda oluřan yeni maddelerin numunelerin genel yapısını pozitif etkilediđi grlmřtir. Bunun yanında kr uygulanmıř numunelerin kr uygulanmamıř numunelere gre daha kk bořluk boyutu dađılımına ve daha yođun bir i yapıya sahip olduđu gzlemlenmiřtir. Yapılan alıřmaların genel deđerlendirilmesinde ise betonun atlaklarını kapatması ve kendi kendini iyileřtirmesi ortamda su ve yeterli miktarda hidrate olmamıř imentonun bulunduđu durumlarda aıkca gzlemlendiđi sonucuna varılmıřtır.

1. INTRODUCTION

Concrete is the most widely-used construction material in the world because of its easy and cheap production and desirable material properties as well. In the last years there have been great developments in concrete technology. The mechanical properties of concrete have been improving, on the other hand; durability is the main problem of concrete. Nowadays, it is more important to design concrete according to durability instead of strength properties.

Durability is very important to fulfill the service life of concrete structures. Cracks, which can be caused by loading, shrinkage etc., may reduce the durability of concrete structures. Methods for preventing cracks like self-healing are important to increase the durability and service life of concrete. A relatively longer service life of concrete will reduce the demand for new structures and repair costs as well. This also procures reduction in using of raw materials, pollution, energy consumption and CO₂ production deviously.

Self-healing which is generally defined as the ability to remove or heal the damage of materials. For concrete structures, the phenomenon is mostly preventing cracks with newly formed matters in cracks. Self-healing of concrete increases the durability and service life. It generally depends on further hydration of unreacted cement in concrete and calcium carbonate crystallization. Self-healing phenomena seems to be an economic and ecologic method due to the reasons like CO₂ production as mentioned before.

1.1 Purpose of Thesis

In this thesis self-healing of 3 different concrete mixtures was investigated. These two groups are concrete mixtures which were produced with CEM I cement and CEM III cement and pozzolanas as binders. The last group has the same mixture as the first group but in addition; super absorbent polymers (SAP) were used in these mixtures as well. Specimens were pre-cracked then uni-axial tensile tests and

microscopic investigations were done before and after various curing conditions for self-healing. The curing conditions are exposure in air, water and two different wet-dry cycles for different time periods. However, microscopic investigations in this study are consisted of electron scanning microscopy (ESM), optical microscopy, mercury intrusion porozimeter test and energy dispersive X-ray (EDX) analysis.

1.2 Literature Review

1.2.1 Self-Healing phenomena

Engineering materials is basically depends on the idea [1] that one way to make strong and stiff materials is assembling as many atoms with a high bond strength to neighbouring atoms in as small as possible. According to this idea, diamond is the stiffest and possibly the strongest material because of its densely packed small carbon atoms and each having high-covalent bonds.

Strength is the ability of a material to sustain high load without disintegrating and forming new surfaces [2]. Loads may cause permanent or plastic deformation due to displacements of atoms. Such displacements may also cause high internal defects then cracks and finally loosing function of materials. Damage prevention is the concept for stronger material design which is based on microstructures that oppose the formation or extension of micro-cracks. An alternative concept which forms the basis of the self-healing materials is damage management. In this paradigm formation of damage is not problematic as long as it is counteracted by removing or healing of damage. The final performance of self-healing material depends on rate of damage versus rate of healing of damage. The empty space of the defects has to be filled with new matter for self-healing materials however a healing trigger is also a must for beginning of self-healing process [2].

1.2.1.1 Why self-healing in cement based materials?

Concrete is the most widely used construction material in the world. Concrete is a quasi-brittle material, strong in compression but relatively weak in tension. The production of 1 ton cement produces approximately 1 ton of CO₂. Considering annually worldwide usage of cement is 2.35×10^9 tons, it is that estimated that 5-7% of total CO₂ production is because of cement production [2]. Service life of a concrete structure is the necessary time for the fulfilment of performance of the

structure; however the performance is the ability to meet the requirements of owners, all authorities and users of the structure [3]. Different types of service life definitions are used depending of the type of construction. According to DuraCrete [4] three different service life are defined as follows:

- a) The technical service life is the service life time till the damages are acceptable.
- b) The functional service life of the structure is the service life that functional performance of the construction meets the needs of all related parties and owners.
- c) The economic service life is the service life till using reinforced concrete structure for another purpose instead of current state. According to standard EN 1991-1 [5] classification of aimed service life can be given below:

Table 1.1 : Classification of aimed service life [5].

Class	Target Service Life (years)	Example
1	1-5	Temporary structures
2	25	Interchangeable concrete elements like roof truss and railway ties
3	50	Buildings and other general constructions
4	100	Monumental structures, bridges and other civil engineering constructions

A relatively long service life of concrete structures is going to reduce the demand for new structures. Long service life of structures will provide significant economic and environmental contributions. This situation will also be beneficial for using fewer raw materials, reduction in pollution, energy consumption and total CO₂ production in the world. Some statistics show that enormous amounts of money are being spent due to the lack of quality and durability of concrete structures. In the USA reconstruction of bridges has been estimated between \$20 billion and \$200 billion and average annual maintenance cost for bridges is estimated at \$5.2 billion [6]. In the Netherlands approximately 33% of annual budget for large civil engineering works is spent for inspection, monitoring, maintenance, upgrading and repair. In the UK over 45% of the annual expenditure on construction is for repair and maintenance costs [7].

These examples of costs above show that service life of a concrete structure is an important issue to search. In the following figure, relationship between performance

of structures and elapsed time is presented. For normal quality structures mostly two or more repairs are needed during the service life of concrete structure. With an initial higher cost, high quality structures need mostly one repair or less than normal quality concrete structures. As seen in figure (1.1.b) after two or more repairs general maintenance and repair costs are higher than high quality structures at the end of service life. Curve (1.1.c) schematically shows the performance of a structure with self-repairing materials will regain initial level of performance after occurring and healing process of cracks and such deformations. By using such kind of materials, maintenance and repair costs will be nearly at the same level during all service life of self-healing concrete structure [8].

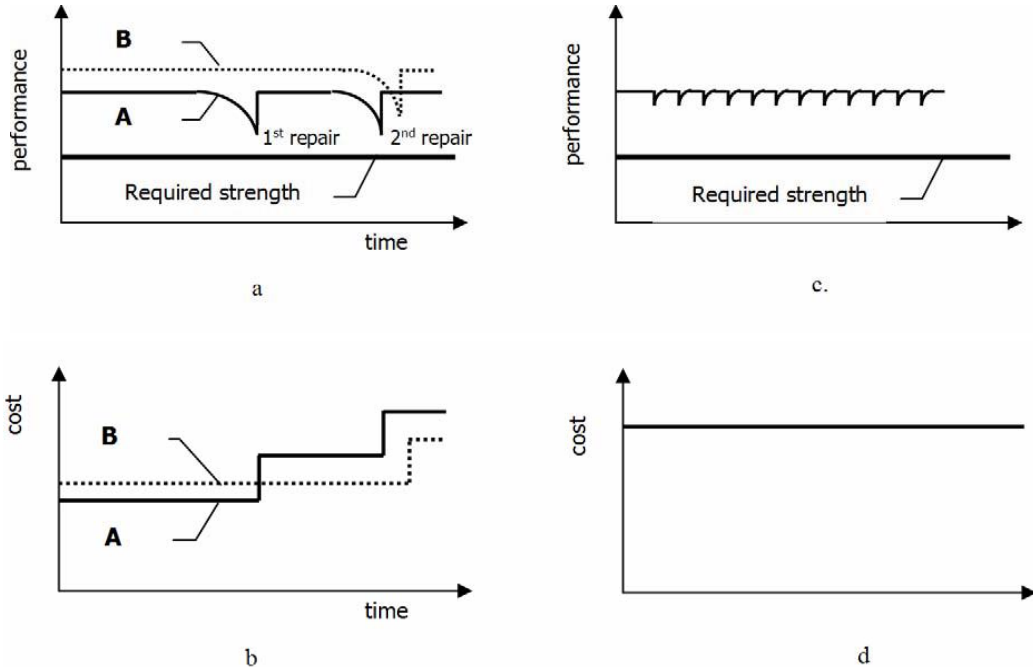


Figure 1.1 : Performance (a) and costs (b) with elapse of time for normal and high quality structures. Performance (c) and cost (d) of a structure made with self-healing material (concrete) with elapse of time. [8].

1.2.1.2 Intelligence levels of materials

In the RILEM report materials are categorized into 3 groups based on different levels of intelligence as seen in the following figure [2]. The biggest group of materials called ‘basic materials’ has no response to changes in surrounding environment. Contrarily, smart materials like piezoelectric materials, shape memory materials and temperature-responsive polymers are engineered materials that are able to give a beneficial response to some changes in their environments. Moreover, the highest level is intelligent materials. It is defined intelligent materials as "materials which

incorporate the notion of information as well as physical index such as strength and durability" [9]. Intelligent materials can get the information, process the information and react to change in the surround. Similar behaviours exhibited by natural materials like skin and bones and the man-made intelligent materials are still at the early stage of investigation.

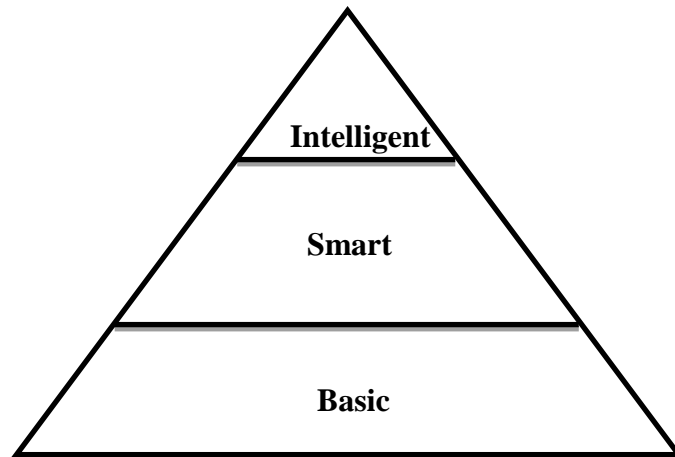


Figure 1.2 : Hierarchy of materials based on different levels of intelligence [2].

1.2.2 Definitions of self-healing

Mechanism of the self-healing in concrete is usually defined with further hydration of unreacted cement, expansion of concrete in the cracks (swelling of C-S-H), calcium carbonate crystallization, closing of cracks by solid matter in the water and closing of cracks by concrete particles resulting from crack spelling [10]. However, in the RILEM state of art report about self-healing, this phenomena in cement based materials addressed the difference between crack closure and restoring initial mechanical properties. In some cases cracks are problematic for durability reasons and simply leakage and crack closure would be sufficient. This situation is called as self-closing. However in other cases restoring mechanical properties would be possible with self-healing [2].

Autogenic process is defined for the situations when self-healing or self-closing is a result of processes involving the original materials components and these components have not been intentionally introduced to initiate self-healing or self-closing. On the other hand when closing or healing process is due to engineered additions like resins contained brittle fibers or immobilized microorganisms the process termed 'autonomic' [2]. The following table will give brief information about these terms.

Table 1.2 : Definitions of self-healing terms [2].

Process	Self-closing	Self-healing
Autogenic	Own generic material closes cracks	Own generic material restore properties
Autonomic	Engineered additions close cracks	Engineered additions restore properties

1.2.2.1 Self-closing

Self-closing is one the mechanism of reducing the width of the cracks in concrete. It is the expression for the fact that width of a through-crack diminishes with the time [2]. There are three main causes of self-closing in concrete as seen in the following figure [11].

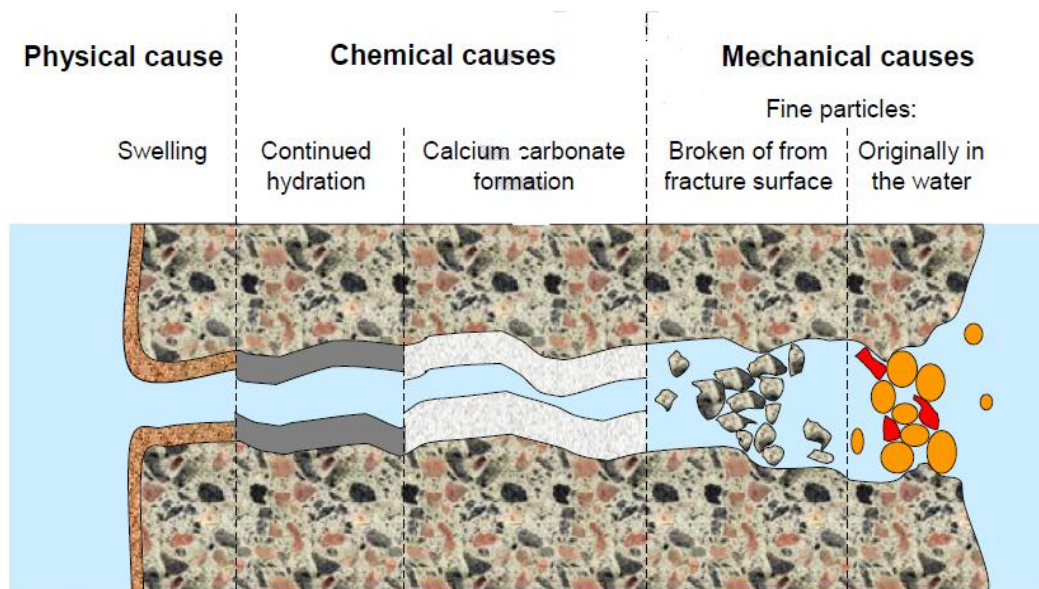


Figure 1.3 : Different causes of autogenic self-closing [11].

In the physical cause, swelling occurs when water is absorbed by hydrated cement paste and reaches the space between the constituents of hydrated cement paste. The effect swelling is reduction of the fluid flow is less than 10% [2].

One of the chemical causes of self-closing is continued hydration of cement in the concrete. These new reaction products grow into the free space of the crack but the continued hydration of cement cannot be responsible for a complete self-closing. The second chemical process is the formation calcium carbonate and growth of these crystals on the crack faces. According to this chemical process, calcium ions from the pore water of concrete (Ca^{2+}) react with the carbonate ions of the water in the crack (CO_3^{2-}) and combine CaCO_3 to which precipitates in the crack. In a study, it is

shown that this mechanism is by far the most important contribution to self-closing [12].

The mechanical effects have minor importance than the other effects. In this type of self-closing fine particles, broken from fracture surface or already present in water, may reduce the crack width [2].

Concrete is a compound of matrix and aggregates and when the cement hydrates calcium silicate hydrates (C-S-H), aluminates and calcium hydroxide are formed. In addition, calcium hydroxide is soluble in water and it is necessary for the formation of calcium carbonate in the cracks. In composite cements, a part of calcium hydroxide is used for the formation of hydration products by the second constituent like fly ash and pozzolanas. Mostly pozzolanas use calcium hydroxide as an activator. Portland cement has relatively more calcium hydroxide than other cement composites with fly ash or blast furnace slag. Moreover the type of aggregates like limestone may positively affect self-closing. The shape of aggregates grains and the grading curve can influence the crack geometry and so self-closing. Finally, water is the most important factor for self-closing. Water is important for chemical reactions and for the transport of fine particles that are mentioned in self-closing phenomena. With the presence of water calcium carbonate are formed and grows on the crack surface and the calcite crystals (CaCO_3), as seen in the figure below [11], form a dense layer which blocks the flow of water, [12].

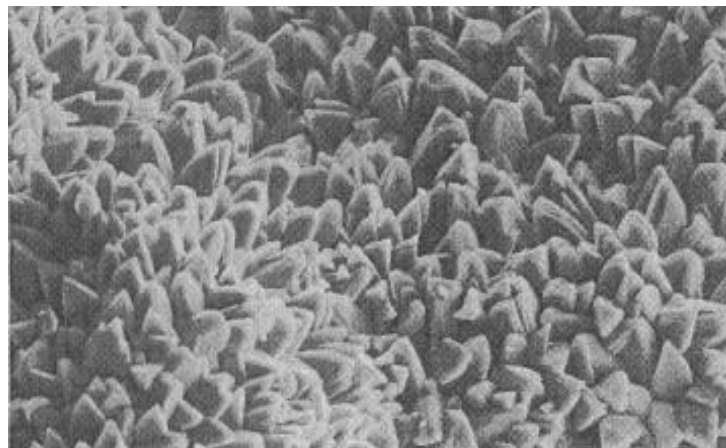


Figure 1.4 : Calcite crystals on a crack face after opening the crack [11].

Experimental evidence on autogenic self-closing

It was reported in a study [13] that after the experiments on the cement lining in steel pipes that the cracks of 0,05 mm closed completely after 60 hours and bigger cracks

of 0,1 mm closed after one year. However it is concluded after study [14] that continued hydration was the cause for recovery. It is also found that moisture supply is the most important factor for self-closing and age at the first cracking time is also essential [14,15]. In the investigation [16], there was no effect from the type of cement and a slow increase of the pressure gradient during water exposure has a positive effect for self-closing. As cause of self-closing, blocking of the cracks by fine particles and the precipitation of calcium carbonate are assumed. It is reported that the most important parameters for self-closing were crack width and water pressure gradient [17]. In the study [18], filling cracks by fine particles and forming of calcium carbonate on the crack faces were the sources of self-closing. It was also added that coarse aggregates yield a rougher crack surface and therefore a better self-closing effect.

Water permeability tests were performed on small specimens with a single tensile through crack [11]. The effects of water source (hardness), type of addition in concrete, type of aggregate, pressure gradient and the crack width were studied. The first three parameters have nearly no effect and the effect of crack width and pressure gradient are shown in the following figures. As seen in the figure 1.5 and 1.6, the crack width of 0,1 mm has generally the best self-closing. Evaluating these figures together makes it possible to conclude that the reduction of flow in absolute sense is strongest for the larger crack width. The self-closing effect by crystallization of CaCO_3 in the cracks was explained [11]. X-ray diffraction experiments from crack faces show CaCO_3 is the main element for the self-closing.

Relative flow [%]

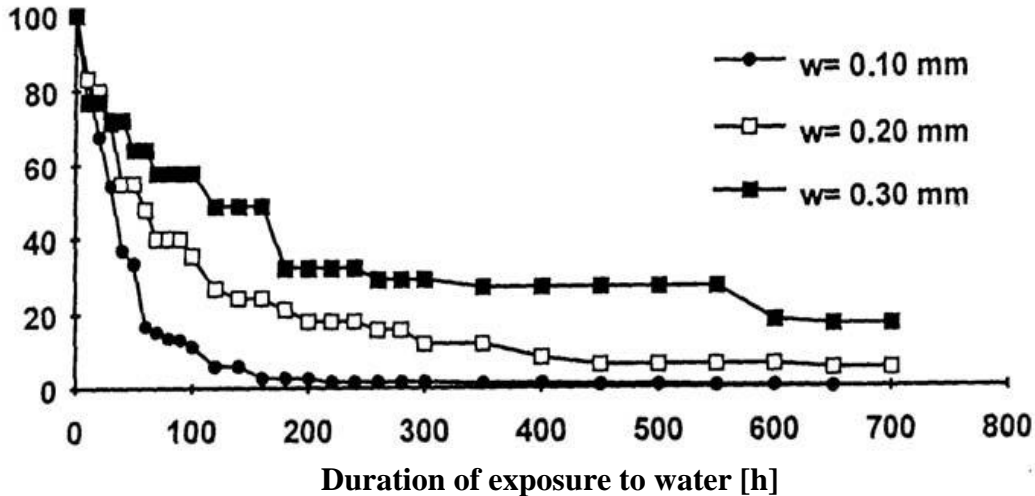


Figure 1.5 : Influence of crack width on flow relative to initial flow [11].

Initial flow q_0 [L/(h m)]

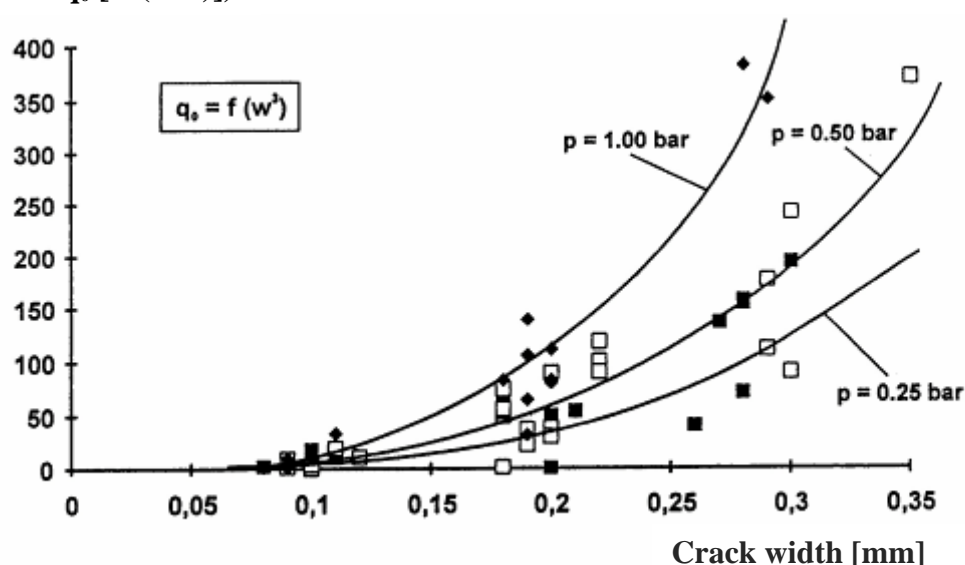


Figure 1.6 : Initial flow through cracks of various widths for 1 m length [11].

In an investigation about self-closing, potential of different mix composition of cementitious materials was studied [19]. Mortar specimens with 8 different compositions containing CEM I, CEM II, CEM III, fly ash and blast furnace slag were prepared. In compositions ordinary Portland cement was replaced by fly ash and blast furnace slag in different percentages. All the mixtures were prepared with water to binder ratio of 0,4 except the one mixture with 0,5. The composition of each mixtures is shown in the following table.

Table 1.3 : Composition of the mortar mixes giving weight of each constituent in gram [19].

	Sand	Cement			Fly ash	Blast furnace slag	Water
	DIN 196-1	CEM I 52.5 N	CEM II/B-M 32.5 N	CEMIII/B 32.5 HSR/LA			
CEMI-0.4	1350	450					180
CEMI-0.4-30FA	1350	315			135		180
CEMI-0.4-50FA	1350	225			225		180
CEMI-0.4-50BFS	1350	225				225	180
CEMI-0.4-70BFS	1350	135				315	180
CEMII-0.4	1350		450				180
CEMIII-0.4	1350			450			180
CEMI-0.5	1350	450					225

Specimens were cured for one and half month and then they were fractured in a crack opening controlled splitting test. Subsequently, the crack width of each sample was measured at different locations, equally divided along the crack length. The average value was used to characterize the crack width of each specimen. The effect of the mortar composition on the self-closing potential was investigated by measuring the change of water permeability of the cracked specimens. A low pressure permeability test setup was used and water permeability coefficient k was calculated according to Darcy's law. Permeability coefficients were measured at the beginning and the end of first 5 days and at the end of 15 days. As shown in the following figure, during the test, water flow through the specimens decreased. It was determined that for increasing crack widths, the difference in water permeability coefficient and consequently the self-closing potential also increased [19]. It was supposed that mixes with a higher amount of cement particles or lower water to binder ratio would contain more unhydrated particles and thus result in a higher degree of self-closing. But there was no big difference in self-closing between the water to binder ratios 0,4 and 0,5. The degree of self-closing was higher when a higher amount of slag was used and there was no big decrease in water permeability in the case Portland clinker was replaced with fly ash. They stated that reaction of fly ash is slower than reaction of blast furnace slag. However it was concluded that the self-closing potential of cementitious materials may be changed by the changing of mixture composition. Another type of experiments was carried out [20,21] that consisted of damaging concrete cubes by rapid freeze-thaw cycles, and then storing them in 20 °C water for 3 months. Two types of concrete at water-cement ratio of 0.4, one with silica fume and the other without silica fume, were tested. Deterioration and healing was measured by resonance frequency (converted to dynamic modulus of elasticity) and compressive strength. Freeze-thaw cycles led to loss in both properties. Self-healing gave a substantial recovery of the frequency, but only a small recovery in compressive strength. It was explained by SEM observations that the cracks were only partly filled with new products. Most of the crystals seen in the cracks were newly formed C-S-H. Portlandite ($\text{Ca}(\text{OH})_2$) was also observed locally. The study showed that self-healing is less apparent in concrete containing silica fume than in concrete without silica fume.

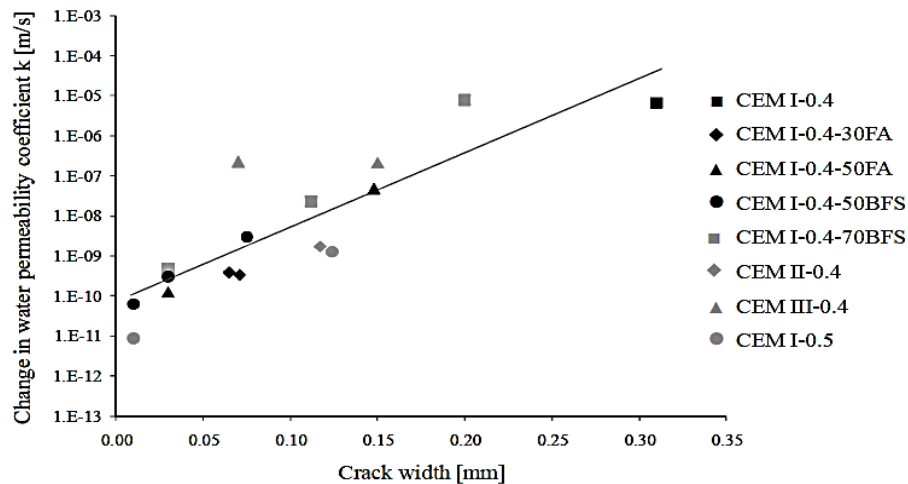


Figure 1.7 : Decrease in water permeability coefficient k [m/s] due to autogenous closing of the crack in specimens with different crack widths [mm] and with different mix compositions; the grey line indicates the mean change in water permeability [19].

There are several hypotheses about the maximum crack width which can heal. However young concrete heals faster and concrete with silica fume shows minor self-closing. There must always be water available and carbon dioxide because the main cause of self-closing seems to be the formation and precipitation of calcium carbonate. A survey was made and came to the conclusion that a through-crack, which is the most dangerous in water-retaining structures, of 0,2 mm can heal completely [22]. The same value is supported by another study [23]. It was found that a crack of 0,3 mm can still heal [11]. In the design proposal, it was differentiated between water head (hydraulic gradient), crack width, and occurring movement of the crack [12,24]. The proposal is shown in Table 1.4.

Table 1.4 : Permissible crack width for self-closing [12,24].

Hydraulic gradient, m/m	Design crack width, mm With 10 % movement	With 10 to 20 % movement
40	0.10-0.15	0.10
25	0.15-0.20	0.10-0.15
15	0.20-0.25	0.15-0.20

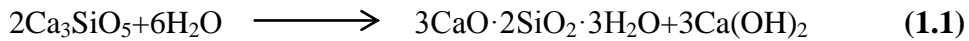
1.2.2.2 Self-healing

Autogenic self-healing

Mechanisms of self-healing

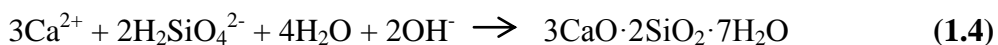
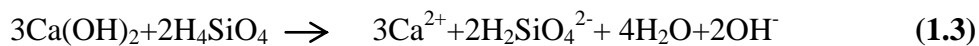
Cracks, that have many negative effects on durability and mechanical properties of concrete, can occur at any stage of service life of concrete elements [10]. Shrinkage,

over loading, design errors, thermal strains, creep, plastic settlement and deterioration mechanisms such as alkali-silicate reaction and freezing and thawing cycles are some of the reasons for cracks in concrete. Because of the significant loss of performance, preventing cracks is often studied issue in the last years. In 1836, the ability of small cracks in concrete to heal themselves in the presence of moisture was observed by the French Academy of Science [25]. Preventing cracks is important for watertight structures and for prolonging the service life of infrastructure [26]. Self-healing of concrete is one of the ways to regain this loss of performance due to cracks. Production of C-S-H is the main mechanism of self-healing [27]. This reaction occurs when tricalcium silicate (C3S/alite), (Equation 1.1) and dicalcium silicate (C2S/belite),(Equation 1.2) react with water to form C-S-H and calcium hydroxide (CH/portlandite), the generalized equations are:



Alite and belite are the main binder components of cement. Alite contains more reactive calcium than belite and it reacts more rapidly and gains early strength however belite reacts more slowly and responsible for the strength at later ages. During cement hydration, some grains of cement containing alite and belite do not totally react, resulting in unhydrated cores surrounded by hydrated C-S-H and CH material a natural encapsulation of chemicals uniformly dispersed in the concrete. During cracking, these naturally encapsulated particles are exposed to the atmosphere and begin to hydrate when exposed to water, which causes a volumetric expansion capable of completely closing micro cracks [2].

The continued hydrations of unreacted cement are present in all binders based on Portland cement. For cementitious systems containing significant additions of aluminosilicate materials such as fly ash, blast furnace slag, silica fume, or clay, the pozzolanic reaction may also provide a degree of self-healing. In alkaline environments, silicate species can dissolve from the pozzolanic material to create silicic acid (H_4SiO_4 , or SH). Silicic acid can react with dissolved portlandite, the result of which is C-S-H and water:



Pozzolanic reaction may also support self-healing. The C-S-H produced during the pozzolanic reaction can then heal fine cracks in the same manner as the C-S-H produced from the hydration of unreacted cement particles (e.g., volumetric change.) Because the rate of the pozzolanic reaction is coupled to the pH, it is substantially slower than the hydration of unreacted cement. In a cracked specimen, it is likely that the pozzolanic reaction will support self-healing even on the longest timescales. Since the service life of infrastructure can be on the order of decades, the inclusion of pozzolans may ensure self-healing in structures undergoing repeated damaging even after available unreacted cement has been consumed [2].

Effect of fibres on self-healing

As literally taken from RILEM report [2]; a wide investigation was made on effect of fibres on self-healing [28]. Table 1.5 shows the mix proportions of materials used in the study. They studied three types of fibre reinforced cementitious composites (FRCC): 1. Containing micro polyethylene fibre ($\phi=12\mu\text{m}$, length=6mm) (FRCC(PE)), 2. Containing steel cord fibre ($\phi=0.4\text{mm}$, length=32mm) (FRCC(SC)), and 3. Containing hybrid composite fibres (i.e. both of PE and SC fibres) (HFRCC).

In all series, four specimens of $25\times 75\times 75$ mm were prepared and pre-cracked with uniaxial tension test. During this test, each specimen was stretched to different strain levels in order to have different maximum crack widths. After the tension test, the crack surface was observed by a digital microscope and the crack width was measured, they can be seen in Table 1.6. The microscopic observation was repeated at 3, 14 and 28 days in order to investigate the effect of the self-healing of cracks.

Table 1.5 : Mix proportion of FRCC specimens investigated in [28].

Type of Mix	Water/Binder	Sand/Binder	Silica fume/Binder	SP/Binder	PE fiber (vol.%)	SC fiber (vol.%)	Fiber content (piece/m ³)
FRCC(SC)				-	-	0.75	187×10^4
FRCC(PE)	0.45	0.45	0.15	0.09	1.5	-	221×10^8
HFRCC				0.09	0.75	0.75	111×10^8

Table 1.6 : Max. crack width evaluated by means of microscope observation [28].

Types of Mixes	Number of Specimens and Widths (mm)			
	No. 1	No. 2	No. 3	No.4
FRCC(SC)	0.035	0.076	0.088	0.757
FRCC(PE)	0.019	0.038	0.119	0.368
HFRCC	0.017	0.081	0.407	0.710

In their microscopic observation it can clearly be seen in photographs that the crack surface of all specimens after the tension test is clear and there are no products on the surface. These photographs of the crack surface of FRCC(PE), FRCC(SC), and HFRCC can be seen in Figure 1.8. After 3 days the crack surfaces in FRCC(PE) and HFRCC were attached by self-healing products and the crack width decreased as the time passed. The crack surface in FRCC(SC) was not decreased by the self-healing products. It could be because there were too few fibers that self-healing products could attach to. On the other hand in the place where of a lot of micro PE fibers bridged over the crack, especially in most of FRCC(PE) specimens, there were many attachment of self-healing products. Even in case of FRCC(PE), however, if there were rather a few fibers, the attachment of self-healing products depended on the volume content of PE fibers. Therefore it was concluded that amount of the PE fiber per volume has a great influence on self-healing. After 3 days, it was seen that the steel cords on the crack surface in FRCC(SC) and HFRCC were corrosive and the volume expanded.

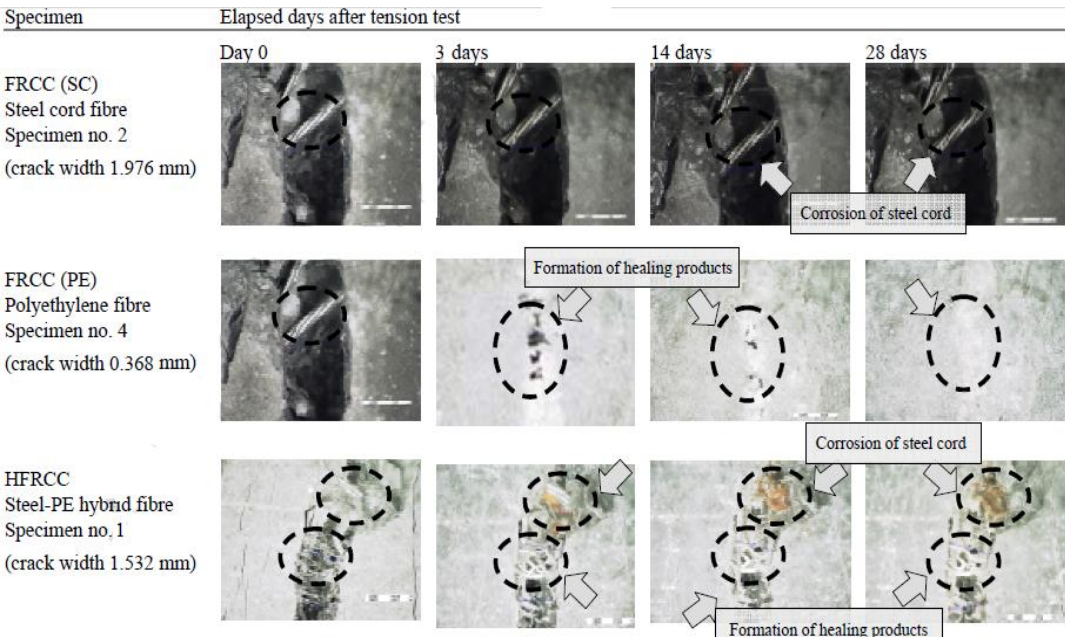


Figure 1.8 : Microscopic observation of self-healing products at a crack surface [28].

Size of self-healing products was also studied as a function of time. As seen in the following figure, the increasing rate of the mean size during the first 3 days is higher than after first 3 days. This may be because of decreasing Ca_2^+ diffusion speed from the inside of FRCC. Self-healing product layer made diffusion decreased. The amount of the attached products in was FRCC(PE) materials were the higher however number of mixed in fibres per volume in this group of specimens was the highest. Therefore it was concluded that the number of mixed in fibre per volume has a dominant influence on the crack self-closing effects.

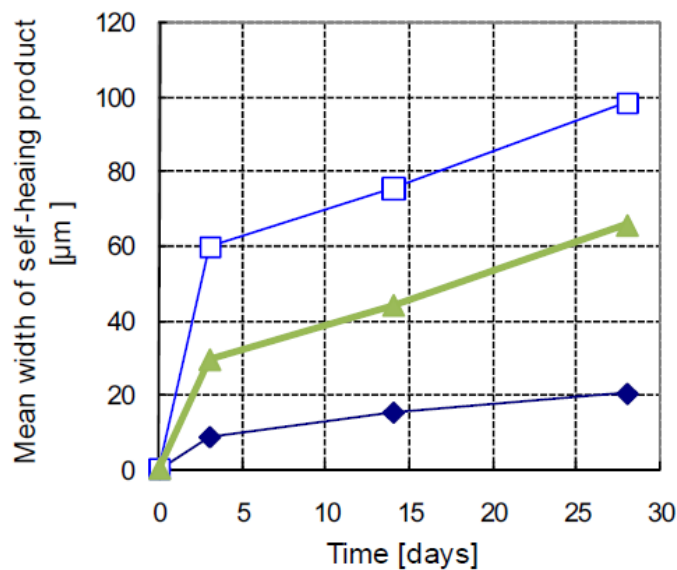


Figure 1.9 : Time dependence of mean size of self-healing products attached at the crack surface [28].

In the same study [28] the results of the water permeability test of the cracked and uncracked specimens can be seen in the following figure. The coefficient of water permeability for all specimens decreased until 3 days except for the uncracked specimens. After 3 days the decreasing rate of the coefficient of water permeability slowed down significantly in all specimens. This supports the microscopic observation results as shown in Figure 1.8 in which the self-healing products attaching speed is faster until 3 days than after 3 days. It can also be noticed that, in wider cracks, the coefficient of water permeability was almost constant after 3 days. Formation of calcium carbonate crystals in the wider cracks do not contribute to the self-healing mechanism. On the other hand, in case of specimens with a smaller crack width, the coefficient of water permeability decreased as time passed even after 3 days and in some cases reached to the same values with uncracked specimens. This can be explained that, in such a small crack width, the formation of calcium carbona-

te crystals has a great effect on self-healing of cracks. It can be seen in the Figure 1.10 that shows the influence of time dependence of water permeability coefficient due to type of FRCC, the decrease of the water permeability coefficient in FRCC(PE) and HFRCC is more than that in FRCC(SC). The self-healing products could attach to the crack surface more in FRCC(PE) and HFRCC than in FRCC(SC).

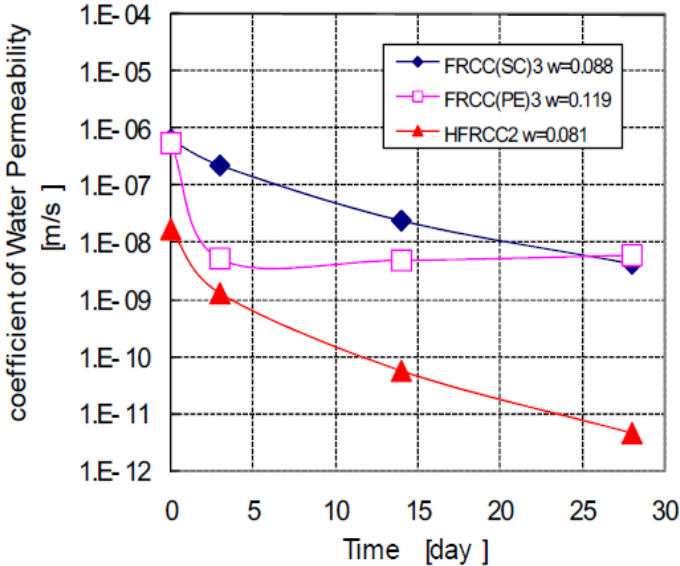


Figure 1.10 : Influence of time dependence of water permeability coefficient due to type of FRCC [28].

In order to evaluate the effect of self-healing on the tensile properties, the self-healed FRCC specimens were tested by uni-axial tension test again in the same study [28]. Figure 1.11 shows the tensile stress-elongation responses before and after the self-healing. As it can be seen in the figure, after self-healing period specimens gained their tensile strengths at different levels. It is surely because of new forming self-healing products. Calcium carbonate crystals attach the crack surface and fibers and this mechanism of self-healing may make tensile strength recoverable. In the HFRCC group, the elongation was less than 1,5 mm and the recovery rate was higher than 100%. This may be because of many newly formed calcium carbonate attached the crack surfaces with very fine fibers. Moreover, bond property of steel fibers might be healed by self-healing products. They also found in the crack surface investigation after tension test that, corrosion of steel fibers was both inside and outside in FRCC(SC) group. On the other hand, in HFRCC group corrosion was only outside. Lots of calcium carbonate crystals attached to the matrix around steel fibers may be cause of this situation and it corresponds with the increase of tensile strength after self-healing [28].

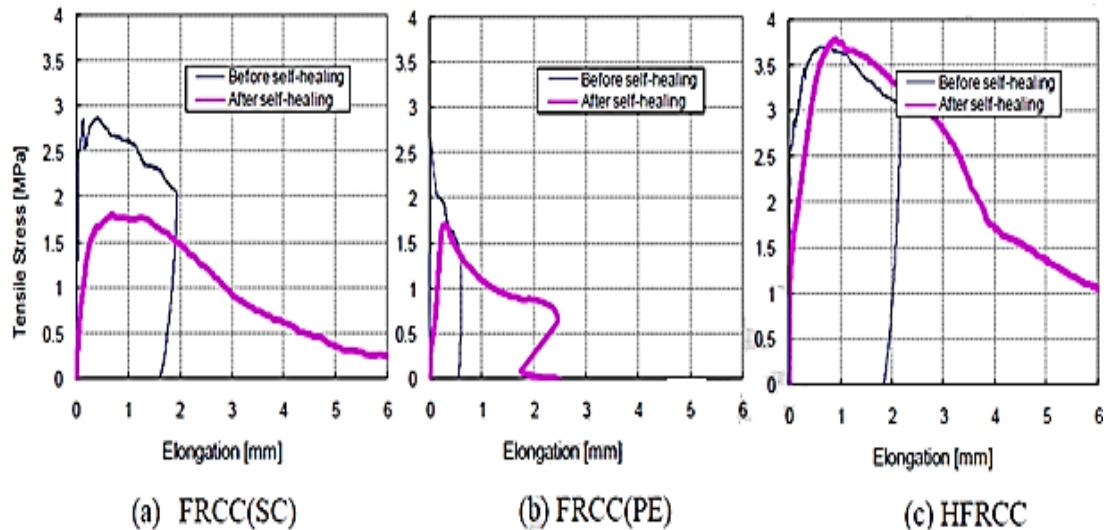


Figure 1.11 : Comparison of tensile property of specimens before and after 28 days of self-healing [28].

Self-healing in ECC

Engineered Cementitious Composite (ECC) is a unique type of high performance fiber reinforced cementitious composite and features high tensile strain capacity mostly with moderate fiber content [10]. As a result of desired small crack width, ECC concrete is suitable for observing healing of crack damage. Many investigations prove that presence of water and tight crack width are two important criteria for autogenic self-healing. In these studies tests were performed with the aim to establish the dependency of permeability and self-healing behaviour of cracked concrete on temperature. It has been shown that the decrease of the flow rate depends on crack width and temperature. Smaller cracks do heal faster than greater ones and a higher temperature favours a faster self-healing process [29-31]. Self-healing reactions can only occur when there is water in the environment of concrete crack. Moreover, without tight crack widths self-healing products were not able to fill the cracks completely.

For obtaining a “robust” self-healing concrete, six requirements were proposed [32]: Pervasiveness (the ability to heal as soon as, and wherever, a crack is present), stability (a healing mechanism that does not decrease effectiveness over time), economic feasibility, reliability (consistency of self-healing), quality (recovery of both self-closing and self-healing characteristics) and repeatability (ability to repair damage for multiple times). Although standard concrete meets some of these requirements, the brittle behaviour of normal concrete that makes controlling crack

width difficult.

Engineered cementitious composites (ECC) are micromechanically designed to suppress brittle fracture behaviour in favour of distributed micro cracking. This behaviour is supported from the interactions between cement and short fibers, without use of large aggregates, and has found use in a number of applications worldwide [33]. In ECC, crack width can be custom tailored to as low as 30 μm ; it has been shown that a crack width below 150 μm , and preferably below 50 μm , is critical to the self-healing of any cementitious system [32].

The fibers in ECC also encourage the production of healing products. Firstly, bridging fibers make the cross sectional area of a crack smaller, they also effectively raising the pH by diminishing flow. Secondly, for reasons arising purely from fluid dynamics, when water flows around the fiber, a turbulent zone is created on the leeward side. In this zone water velocity can stagnate, encouraging precipitation of healing product and creating a composite fiber/healing product material that bridges the crack [2].

In ECC due to the low water/binder ratio, there are notable amounts of unreacted cement and this increases self-healing capacity. Self-healing products on crack faces reducing the flow rate of water through cracks and lowers permeability coefficient.

In some investigations about the water permeability of self-healed ECC specimens, it was found that tight crack widths decreased continuously until reaching uncracked condition [34]. In the same study it was observed that in large cracks, self-healing products on crack faces was insufficient to fill the crack completely [34]. In a similar study, it was found the permeability of samples with crack widths below 150 μm decreased after 10 wet/dry cycles. However samples with crack widths of 150 μm or above did not improve [32].

It also has to be mentioned that water permeability tests accurately describe self-closing, in which cracks are blocked to water flow, but does not necessarily describe self-healing, which implies an improvement in mechanical properties. Because, during the test self-healing like swelling of C-S-H gel, or continued hydration of semi-hydrated cement may occur. Moreover, cracks may become blocked by particulate matter that reduce water flow but do not aid healing. In the study [10], ECC specimens were subjected to two wetting and drying cycling regime like

submersing specimens in water at 20°C for 24 h then drying in the laboratory at 21°C for 24 h and submersing in water at 20°C for 24 h then oven drying at 55°C for 22 h and finally cooling in the laboratory at 21°C for two hours. To quantify self-healing resonant frequency tests were conducted throughout wetting and drying cycles followed by uniaxial tensile testing of specimens. It was reported that crack damaged ECC specimens recovered 76% to 100% of their initial resonant frequency value, tensile strain capacity after pre-damaging with loading 3% tensile strain recovered close to 100% of virgin specimens without any preloading. It was also mentioned in the study that, temperature during wetting and drying cycles led to an increase in the ultimate strength but slight decrease in the tensile strain capacity of healed pre-damaged specimens and crack widths must be controlled below 150 μm preferably below 50 μm in order to engage noticeable self-healing behaviour.

In a study, resonant frequency recovery of ECC specimens were observed by pre-loading specimens between 0.30 and 3.0% strains after 10 wet/dry cycles [33]. As it can be seen in the following figure, specimens reached nearly same frequencies of virgin specimens except specimens which were pre-loaded 3%. However, tensile stress/strain relationships of ECC specimens pre-loaded to 3.0 and 2.0% before and after 10 wet/dry cycles were investigated. As seen in the figure recovery ratio of the specimens that were loaded to 2.0%, was higher than the specimens that were loaded to 3.0%.

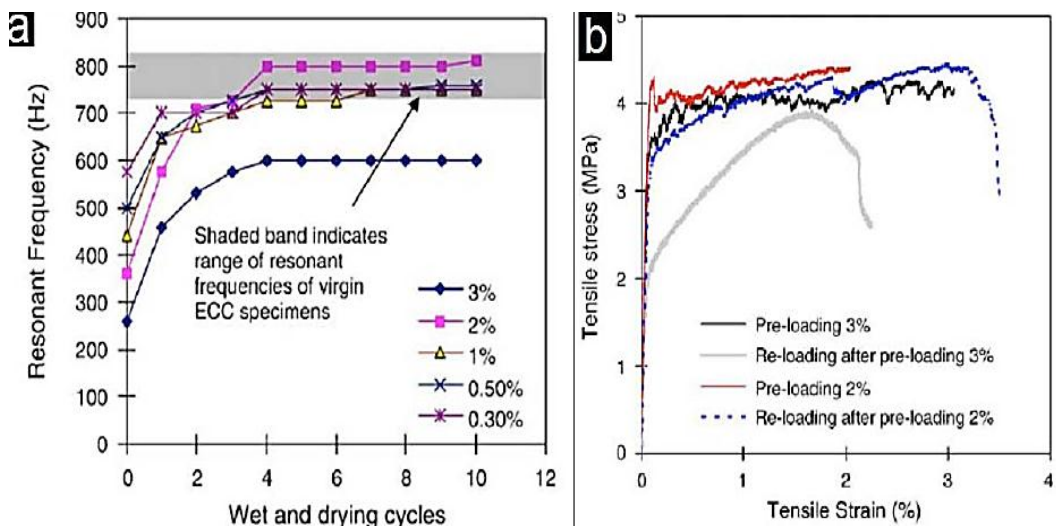


Figure 1.12 : a) Resonant frequency recovery of ECC specimens pre-loaded between 0.30 and 3.0% after 10 wet/dry cycles; b) tensile stress/strain relationships of ECC specimens pre-loaded to 3.0 and 2.0% before and after 10 wet/dry cycles [33].

In an investigation [34], specimens that contain both short polyethylene fibers and steel cords and they exhibited distributed micro-cracking behaviour. After 28 days water curing these specimens regained their mechanical properties. They attributed these self-healing to continued hydration products forming on fibers and crack faces.

In another search about the self-healing in ECC [26], it was observed that a significant improvement in resonant frequency during 4-5 wet-dry cycles. Specimens that had pre-loaded with 0.3-0.5% strain levels resonant frequency returned to nearly initial results. For the 1-2% pre-loading strain levels return of resonant frequency results was 90-95%.

In an observation [35] blast furnace slag and lime stone powder were used for production of self-healing ECC specimens. Ultimate deflection capacity related to flexural strength was 65-105% for the water cured specimens in comparison to virgin samples. For the air-cured specimens regain ratio was only 40-62%. They concluded that addition of blast furnace slag or lime stone powder did not negatively affect the self-healing capacity of ECC.

Healing products can be easily identified by optical microscopy (Figure 1.13a) or electron microscopy (Figure 1.13b); observation by eye is also possible in ECC. Micrographs of the healing products were made [36] and assuming it to be calcite based on the works [12,10,37]. Each concluded that the healing product to be calcite based on EDS spectra.

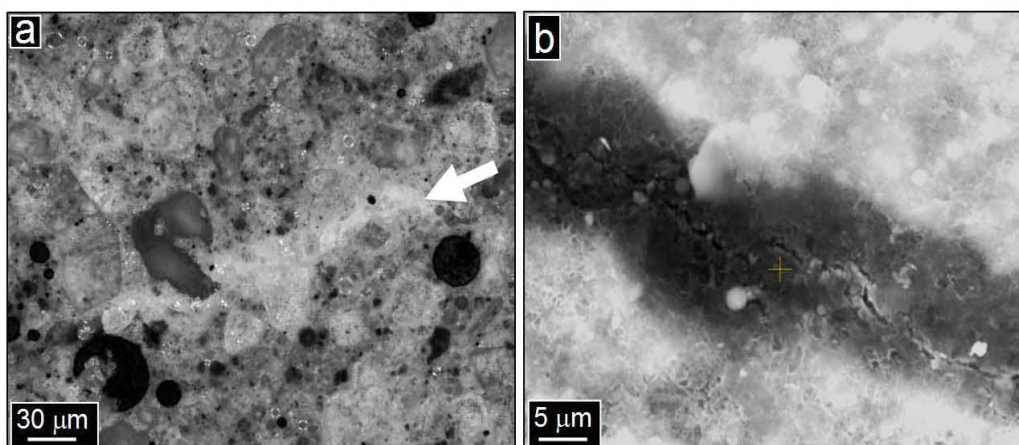


Figure 1.13 : a) optical micrograph of healing product in ECC cement (arrow); b) SEM micrograph of a healed crack [26].

In some other studies about identifying self-healing products [26], two distinct healing products in ECC materials by using scanning electron microscopy (SEM)

were observed. They saw that in very tight cracks, 'fiber-like' C-S-H was present and only in larger cracks 'stone like' calcite grains formed. The compositions of these self-healing products were confirmed by EDS, however, a large amount (10%) of Mg was also observed. They considered that this Mg could take the form of various magnesium carbonates (magnesite or dolomite), hydrates (barringtonite, etc.) or hydroxides (brucite). The EDS results also indicated that the 'stone like' product, identified as calcite, could be a mixed system with additional C-S-H or portlandite due to an abundance of calcium; the fiber-like phase could also have included portlandite, since there was an abundance of calcium but no carbon.

In a study [35], samples of ECC containing blast furnace slag and limestone powder were observed by using SEM and EDS identified the healing product to be a calcite and/or C-S-H. As with the mechanical properties, it therefore appears that the inclusion of BFS and limestone powder had little, if any, effect on the capacity of the ECC for healing. In the study [38], researchers investigated the self-healing properties of ordinary Portland cement/fly ash blends at similar ages and they found that degree of healing increased with increasing fly ash content. Therefore, the pozzolanic reaction is likely to be the cause of at least some of the healing. They concluded that fly-ash cement systems have self-healing ability for micro cracks that occur from shrinkage.

It is literally common case that with the presence of water for ECC healing products formed at the faces of cracks and completely filled the cracks which have widths less than 50 μm . Nevertheless fibers provide further encouragement for the production of healing products and are likely to provide the sites for the precipitation of those products. In most cases mechanical tests showed that self-healing products not only seal cracks but also protected steel cords and led to mechanical performance [2].

Self-healing in early age concrete

Investigations about the evidence of self-healing in early aged concrete were literally taken from Delft University of Technology studies [39-41]. In these studies different parameters were used. The amount of compressive force applied during healing was 0, 0,5, 1 and 2 MPa; the type of cement on the concrete mix was CEM III (BFSC) and CEM I 52,5 R (OPC); cracking time was at an age of 20, 27,5 (further named 1 day), 48 and 72 hours; the crack were 20, 50, 100 and 150 μm and finally specimens

were stored under water and with 95% and 60% RH respectively. The research group concluded that cracks are healed when they are made at an early age and they are closed again (a compressive stress is applied) and the specimens were stored under water. The amount of compressive stress did not seem to influence the strength recovery. The results indicate that a crack healing can occur when compressive stress is applied to close the crack, the two crack faces touch each other again or the distance between the crack faces is small enough. Crack healing takes place in both concretes made with BFSC and OPC. OPC probably has additional capacity for crack healing at a later stage when compared to BFSC-concrete because of more unhydrated cement left in the crack. With increasing age of the specimen at the moment the first crack is made, a decrease in strength recovery was found. The width of the crack did not influence the strength recovery due to healing. The tests with different crack mouth openings all show similar amounts of strength recovery. It is a must for crack healing that specimens are stored under water. Researchers also concluded that on-going hydration is the mechanism for crack healing that leads to the strength recovery in this investigation and this mechanism only works when the crack is closed again. It was shown that crack healing does take place when enough humidity is present. For the practical situation of early age surface cracks in (massive) concrete structures, from a durability point of view, this investigation shows that surface cracks can disappear again, at least under the right conditions as discussed above.

Self-healing on ultra-high performance concrete

Ultra High-Performance Concrete (UHPC) is a cementitious material which has very low water-cement ratio [2]. In a study [42] used a water-cement ratio of 0,2 and additionally silica fume in their studies. They cured the specimens after 2 days water curing with heat-cure at 90°C and 100% RH for 48 h. In the three-point bending test, the prismatic specimens with a center notch were loaded in a displacement controlled manner till the top and further until a crack mouth opening displacement of about 30 µm. Then the specimens were stored in water for a certain time. Figure 1.14 illustrates the deflection-softening behaviour of UHPC. The peak bending stress is about 7,3 MPa at 15 µm. Unloading took place at a load level of 2 kN which corresponds to a bending stress of 3,75 MPa. Reloading follows the original curve.

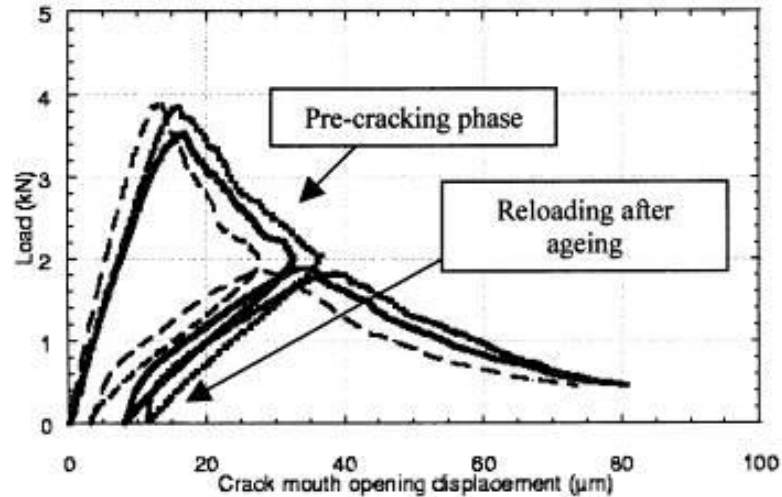


Figure 1.14 : Load-Displacement behaviour of virgin specimen (Pre-cracking phase) and reloading after 3 weeks in air [42].

The storage in water led to slightly different behaviour as shown in Figure 1.15. Water cured specimens showed an increase in bending stress compared to non-cured specimens. The initial stiffness of cracked specimens (reloading stiffness) after 10 weeks storage in water was almost the same as the one of the virgin specimens. Crack mouth opening distance decreases with increasing time of water storage. Resonance frequency and acoustic emission measurements showed that self-healing effect was present. The cause of self-healing was seen in the formation of new products in the crack due to continued hydration of fractured unhydrated cement grains [43].

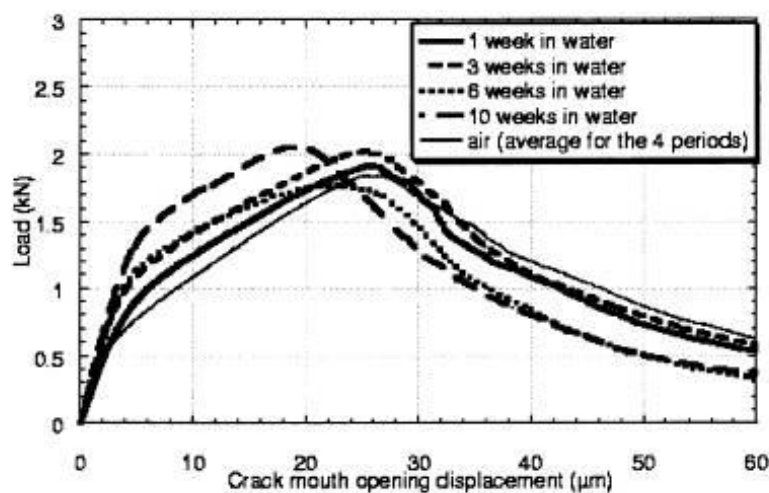


Figure 1.15 : Load-Displacement behaviour of cured specimens and non-cured ones [42].

Autonomic self-healing

There are also some other types of self-healing like adding concrete tubular encapsulated healing agents. When a crack appears, tubes break and components flow into the crack. Upon contact of both components with air, the healing agent reacts inside the crack and then can be healed. In some studies about autonomic self-healing with tubular encapsulated healing agents, self-healing properties and some regain in mechanical strength are obtained [44,45].

Another method is the application of mineral-producing bacteria, which was developed in several laboratories as a repair methodology. The application of bacteria for ecological engineering purposes like removal of chemicals from waste water streams [46], for bioremediation of contaminated soils [47] and removal of greenhouse gasses from landfills [48] is becoming popular. The applicability of specifically mineral-producing bacteria for filling of pores and cracks in concrete has been recently investigated [49-53]. Ureolytic bacteria of the Genus *Bacillus* were used as agent for the biological production of calcium carbonate based minerals in most of these studies. Enzymatic hydrolysis of urea to ammonia and carbon dioxide is the mechanism of calcium carbonate formation. When the pH-value of the equilibrium constant is near 9,2 the reaction causes a pH increase from neutral to alkaline conditions that results the formation of bicarbonate and carbonate ions which precipitate with present calcium ions to form calcium carbonate minerals. On the other hand, the method proved mechanical recovery [49,50] and decrease of permeability [51,52]. Mostly in the studies, bacteria or derived ureolytic enzymes were externally applied on cracked concrete structures or test specimens. Nevertheless, this process was labor intensive as it is repeatedly needed during the service life of a construction and is therefore expensive.

In another study [54] it is investigated the potential of bacteria to act as self-healing agent in concrete, i.e. their ability to repair occurring cracks. For this process, a specific group of alkali-resistant spore-forming bacteria related to the Genus *Bacillus* was selected. It was found that cement stone incorporated bacterial spores could convert concomitantly incorporated calcium lactate to calcium carbonate-based minerals upon activation by crack ingress water and in conclusion it is said that alkali-resistant spore-forming bacteria related to the genus *Bacillus* was suitable for application as self-healing agent in concrete and probably cement based materials.

1.2.3 Textile reinforced concrete

Textile reinforced concrete (TRC) is a composite material consisting of fine-grained concrete and high-performance filament yarns (e.g. glass, carbon) as textile reinforcement [55]. High tensile strength and pronounced pseudo-ductile behavior are the basic properties of textile reinforced concrete (TRC). Because of these excellent mechanical properties, it can be used for applications in new construction as well as in the strengthening and repair of structural elements made of reinforced concrete or other traditional materials [56]. The textile reinforcement supply good crack distribution and very effective crack bridging, leading to very narrow crack widths. There is no corrosion problem of alkali-resistant (AR) glass or carbon fibers in comparison with steel reinforcement. A concrete covering is not a must like steel reinforcement. Therefore, it is possible to design and produce extremely light, thin-walled new structures with TRC; this supplies new ways for the construction material concrete and gives architects and engineers more freedom in the design [57]. However, it is an effective way to use for repair or/and strengthening of the existing concrete structures. As concluded in the study [58] TRC can be used in structural elements. Some applications of TRC are using as repair material, protection of the existing structural members against the corrosion of concrete and using as reinforcement. As mentioned in the study [59,60] the first practical application for the strengthening of existing structures using textile reinforced concrete was carried out in 2006 for retrofitting of an RC roof shell at the University of Applied Sciences in Schweinfurt, Germany.

The 80 mm thick hypar-shell has a width of approximately 27 m and a maximum span of approximately 39 m, (Figure 1.16). A TRC layer of 15 mm thickness containing three layers of textile sheets made of carbon fiber was used to these particular areas in order to increase the load carrying capacity and to prevent further increase in deformations.

In the study [56], water absorption as well as gas and water permeability tests were performed on specimens made of TRC using both crack-free and cracked specimens with a particular focus on the effect of cracks on the transport properties. The main parameters were the fineness and coating of the yarns comprising the textile reinforcement. The capillary suction of TRC was studied for the fluid transport both parallel and perpendicular to the plane of textile reinforcement.

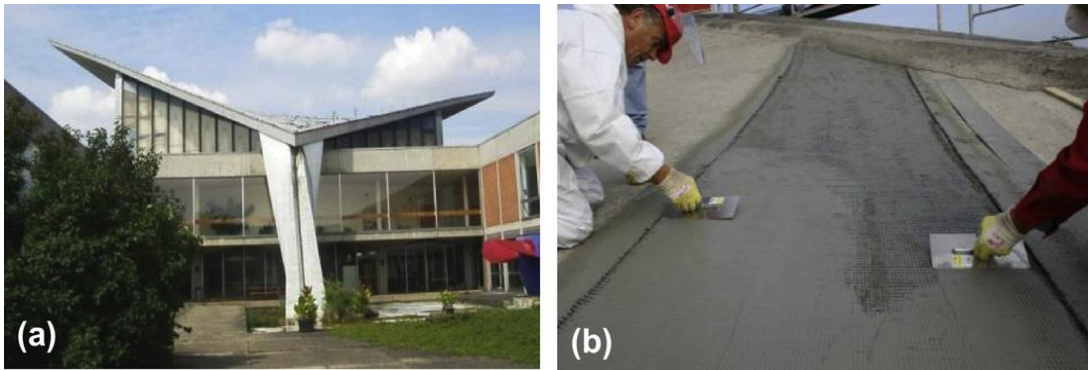


Figure 1.16 : a) Steel reinforced concrete hyper-shell at the FH Schweinfurt (Germany), b) Embedding the textile reinforcement [56].

As seen in the following figure, for permeability testing special equipment was developed to enable measurement of the water and gas transport behavior of cracked TRC in-situ, under uniaxial tension, and at chosen strain levels. The results in the study indicate a very low permeability and capillary absorption of the crack-free material and with uncoated textile increase in the fineness of the yarns showed considerable increase in water absorption. It is concluded that multiple cracking with relatively small crack widths in comparison to ordinary cracked concrete generally results the increase of ingress of corrosive substances (e.g. chlorides or sulfates) , which may lead to a deterioration of concrete and steel reinforcement. Nevertheless, the self-healing of fine cracks indicated a pronounced reduction in the transport rates of water and gas over time.

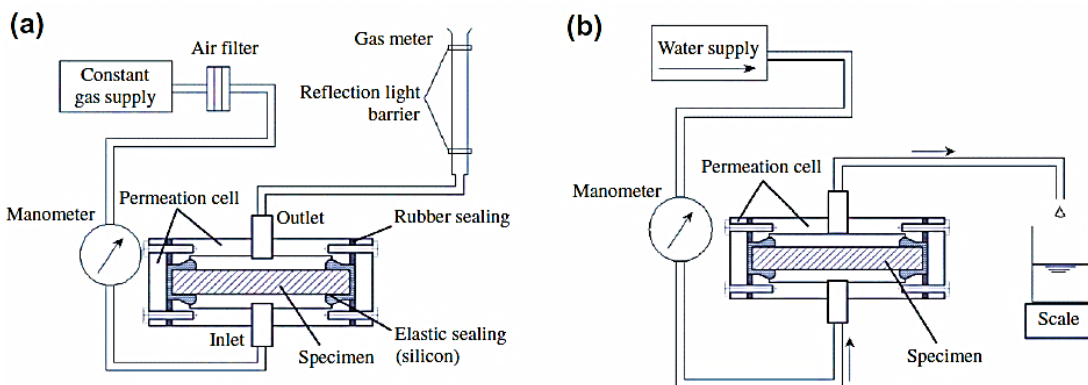


Figure 1.17 : Schematic view of the test setup for (a) gas permeability, (b) water permeability [56].

1.2.4 Superabsorbent polymers

Superabsorbent polymers (SAPs) are one of the most fascinating materials in modern polymer technology [61,62]. It is said in the state of art report of SAP [63], these polymers are able to absorb up to 1500 g of water per gram of SAP (Figure 1.18).

They were developed in the late 1980s and the first application of SAPs was in diapers.

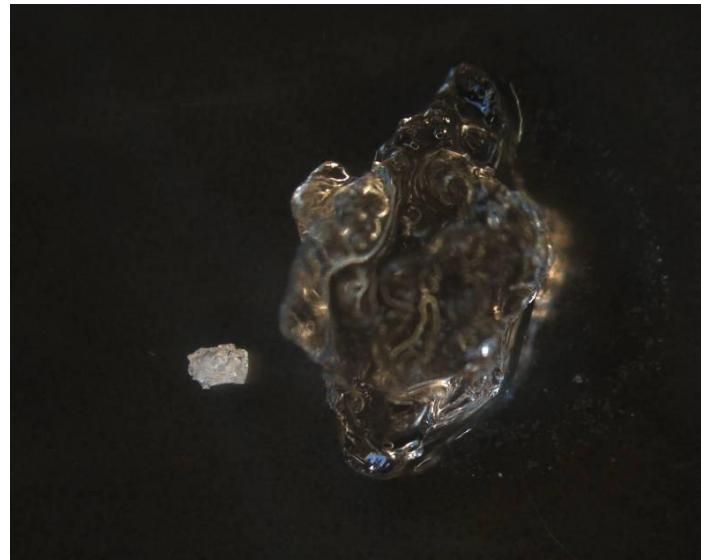


Figure 1.18 : Dry and swollen SAP particle (figures with courtesy of BASF) [63].

From a chemical point of view, SAPs are cross-linked polyelectrolytes which start to swell upon contact with water or aqueous solutions resulting in the formation of a hydrogel. In the hygiene industry only SAPs based on cross-linked poly acrylic acid are used (Figure 1.19), which is partially neutralized with hydroxides of alkali metals, usually sodium. There are traditionally two markets of SAP: Hygiene industry and technical SAPs. Technical SAPs, which can be based on acrylamide and acrylic acid, are used in landscaping, cable isolation, firefighting, food packaging.

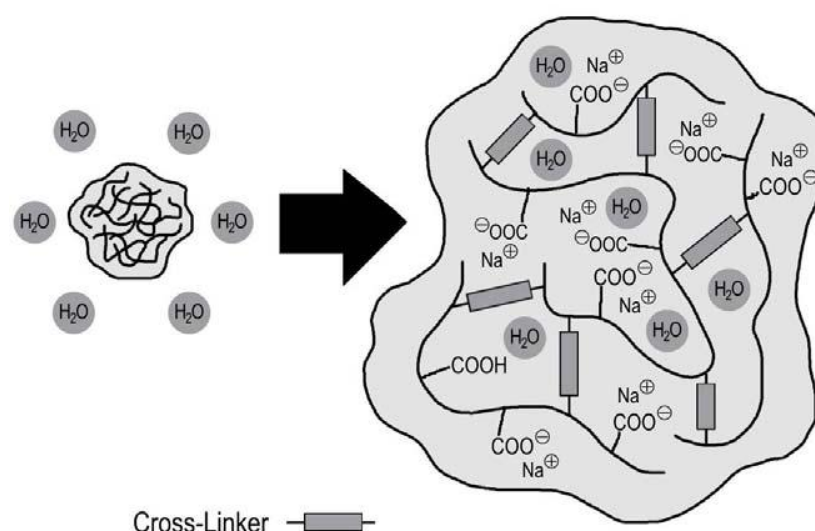


Figure 1.19 : SAP based on polyacrylic acid [63].

Swelling of SAPs depends on the osmotic pressure, which is proportional to the concentration of ions in the aqueous solution. When the ions in SAPs are forced closely together by the polymer network, there is a very high osmotic pressure inside. Because of absorption of water, the osmotic pressure is reduced by diluting the charges (Figure 1.19). Other external pressures, (e.g. if the SAP has to swell or retain water against external mechanical forces) reduce the absorption capacity as well. When all forces are even the swelling is in equilibrium. Therefore, the absorption of a SAP is strictly dependent on the concentration of ions in the swelling medium. Di- and trivalent ions, e.g. Ca^{2+} and Al_3^+ , have an additional effect on the swelling behavior of SAPs which are based on polyacrylates. Because of their complex formation with carboxylate groups, they act as additional cross-linkers dramatically reducing the absorption capacity.

Super Absorbent Polymers (SAP) appear to be most appropriate for use as a water-regulating additive. However, in some studies [64-67] various types of SAP were tested and demonstrated that certain types show a very pronounced ability to mitigate autogenous shrinkage of high-strength mortar and concrete. SAPs may be engineered for the special purposes of internal curing by designing the necessary size and shape of the particles, water absorption capacity and other properties. With only small amounts of SAP and some additional water for internal curing are added directly to the fresh mix.

In a study [68], internal curing on autogenous shrinkage as well as on the effect of SAP addition on the development of stresses due to restrained autogenous deformations of UHPC was investigated. Seven mix compositions were experimentally evaluated in the study: two reference concrete mixes with no internal curing (fine-grain reference concrete F-R and coarse-grain, fiber-reinforced concrete Cf-R) and five UHPC mixes with internal curing (fine-grain UHPC: F-S.4, F-S.3.04, F-S.3.05, and F-S.4.07; coarse-grain UHPC: Cf-S.3.04.). With regard to internal curing, the variable parameters were the amount of internal curing agent (0,3% and 0,4% SAP, related to the mass of cement) and the amount of additional water (0,04 to 0,07 in reference to the mass of cement). An exception is the mix identified as F-S.4, to which purposefully only SAP material was added but no extra water for internal curing was introduced. As seen in the following figure, it is concluded that internal curing using SAP and an extra amount of water reduces the autogenous

shrinkage of UHPC dramatically. This effect becomes even more pronounced with increasing amounts of SAP and extra water.

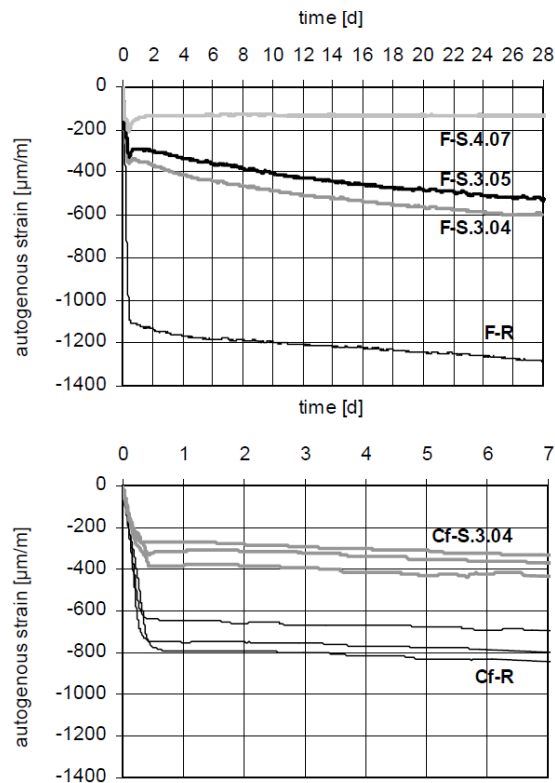


Figure 1.20 : Autogenous shrinkage of fine and coarse grained UHPC measured starting after the final set [68].

In the study [69] a new means for the prevention of self-desiccation: incorporation of superabsorbent polymer (SAP) particles in the cement-based material is described. During mixing of the concrete, the SAP will absorb water and form macro inclusions, which essentially consist of just free water. Conceptually, this is similar with air entrainment, which is used for frost protection of concrete. Thus, the described technique referred to as water entrainment. However, in another study [70] about SAP materials, it was concluded that the addition of dry SAPs caused a densification of the pore structure; the strength decrease due to SAP addition was small. The drying shrinkage was retarded, the freeze-thaw resistance increased and the chloride migration was reduced.

2. EXPERIMENTAL STUDY

In this study, there are two parts; preliminary work and final part. In both parts of the study, thin concrete plates were produced and after 28 days they were pre-cracked. The pre-cracked specimens were exposed to various cure conditions during various time periods. For both stages of study, concrete plate specimens were produced using three main mixtures. The binder materials were CEM I and CEM III however, CEM I used with and without SAP materials in two groups. SAP materials were used to observe the positive effect of them to self-healing process. In the preliminary work, the mechanical properties of specimens after self-healing curing were observed by uniaxial tensile test. In the second part of thesis, specimens were cured for longer periods and besides uniaxial test micro-structural tests and observations i.e. optical microscopy, SEM-EDX, MIP were performed.

2.1 Materials

2.1.1 Cement

Portland cement CEM I 32.5 R and CEM III/B 32,5 N-LH/HS/NA conforming to the DIN EN 197-1 [71] and DIN 1164-10 [72], respectively, were used in this thesis. Their properties are given below:

Table 2.1: Properties of cement types used in experiments.

	CEM I 32.5 R	CEM III/B 32,5
Producer	Schwenk KG, Werk Bernburg	Schwenk KG, Werk Bernburg
Density	3,15 kg/dm ³	3,15 kg/dm ³

Table 2.2 : Properties of CEM I 32.5 R.

Parameter	Unit	Limits of standard	Test results
Fineness of grind			
200 µm sieve residue	%		0,2
90 µm sieve residue	%		2,4
63 µm sieve residue	%		8,1
Blaine Specific Surface	cm ² /g		2850
Mortar Tests			
Water demand	%		26,9
Setting Time, Initial	min	≥60	160
Final	min	≤720	200
Soundness (Le Chatelier)	mm	≤10	1,1
Compression strength			
2 days	N/mm ²	≥10	22,1
28 days	N/mm ²	≥32,5; ≤52,5	49,9
Chemical Analysis			
Loss On Ignition	%	≤5	2,19
SO ₃	%	≤3,5	3,23
Cl ⁻	%	≤0,1	0,08
Insoluble Residue	%	≤5	0,28

Table 2.3 : Properties of CEM III/B 32,5.

Parameter	Unit	Test results
Mortar Tests		
Water demand	%	32
Setting Time, Initial	min	270
Compression strength		
7 days	N/mm ²	27,3
28 days	N/mm ²	46,2
Chemical Analysis		
Loss On Ignition	%	2,8
SO ₃	%	2,8
Cl ⁻	%	≤0,1
Insoluble Residue	%	≤5
Na ₂ O Equivalent	%	0,77

2.1.2 Aggregates

2.1.2.1 Sand

Three different size groups of aggregates are chosen to use in the thesis after some preliminary mixtures. Natural round shaped quartz sand (Ottendorf/Germany) aggregates were used in this study. The producer of sand is Euro Quartz GmbH, Werk Ottendorf-Okrilla, Germany and the properties about grain size distribution are given in the following table and figure.

Table 2.4 : Sieve total pass (%) of sand 0/1.

	Sieve total pass (%) through mesh sizes										D-Sum	k-value
	0,125	0,25	0,5	1	2	4	8	16	31,5	63		
Sand 0/1	1,2	8,5	45,3	85,2	98,9	100	100	100	100	100	739	1,62

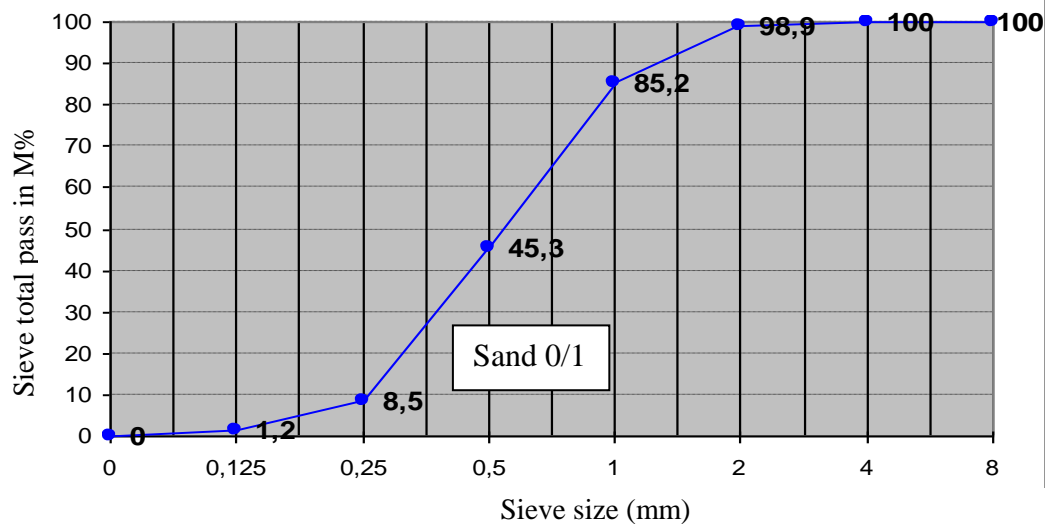


Figure 2.1 : Grain size curve of sand 0/1 mm.

Another type of quartz sand between the grades 0,06-0,2 mm is also used in this study. Quartsands are produced from prepared natural raw minerals. Properties of this sand group are given below.

Table 2.5 : Properties of quartz sand (0,06-0,2)mm.

Grain size distribution	(%)
> 0,2 mm	2
0,1-0,2 mm	86
0,063-0,1 mm	11
< 0,063	1
Bulk density (kg/m ³)	1,2
Chemical Analysis	(%)
SiO ₂	99,2
Al ₂ O ₃	0,2
Fe ₂ O ₃	0,06
TiO ₂	0,25
CaO+MgO	0,03
K ₂ O+Na ₂ O	0,01
Loss On Ignition	0,1

The last group of aggregate was a sand named Millisil which was a fine sand produced from processed silica sand by iron-free grinding with subsequent air

separation. The properties of this ground silica sand can be seen in the tables 2.6 and 2.7.

Table 2.6 : Typical grain size and grain characteristics and typical grain size related properties of Millisil.

Upper grain size $d_{95}\%$ in μm	220
Average grain size $d_{50}\%$ in μm	90
Mesh size in μm	Residue in weight-%
400	0,1
300	0,3
200	7
160	18
125	32
100	42
63	62
40	75
Grain diameter in μm	Residue in volume-%
32	71
16	82
8	90
6	92
4	94
2	97
Bulk density g/cm^3	1,35
Tapped bulk volume $\text{ml}/100\text{ g}$	52
Spec. Surface Blaine cm^2/g	1000
Oil absorption $\text{g}/100\text{ g}$	14

Table 2.7 : Physical Properties and Chemical Composition of Millisil.

Physical properties	
Density g/cm^3	2,65
pH-value	7
Hardness	7
Linear coefficient of thermal expansion α 20-300°C	$14 * 10^{-6} * \text{K}^{-1}$
Chemical Properties	
SiO ₂	99
Al ₂ O ₃	0,3
Fe ₂ O ₃	0,05
CaO + MgO	0,1
Na ₂ O + K ₂ O	0,2
Loss on ignition 1.000°C	0,25
Moisture	0,1

2.1.3 Pozzolanas

2.1.3.1 Fly Ash

In the study, in one group of mixtures, fly ash was used with CEM III and silica-

fume. The producer is BauMineral GmbH, Germany and the name of the product is EFA-Füller® HP Flugasche. Related standards about this fly ash are DIN EN 450-1 [73] and DIN 1045-2 [74]. Some properties of fly ash are given below.

Table 2.8 : Properties of fly ash.

Specific Values	
Loss on ignition	Category A ≤ 5 M.-%
Content of grains $> 45 \mu\text{m}$	17 ± 10 M.-%
Na ₂ O-Equivalent	1,10 M.-%
Bulk density (DIN 1060, 3)	1,11 t/m ³
Compacted density	$2,32 \pm 0,20$ t/m ³

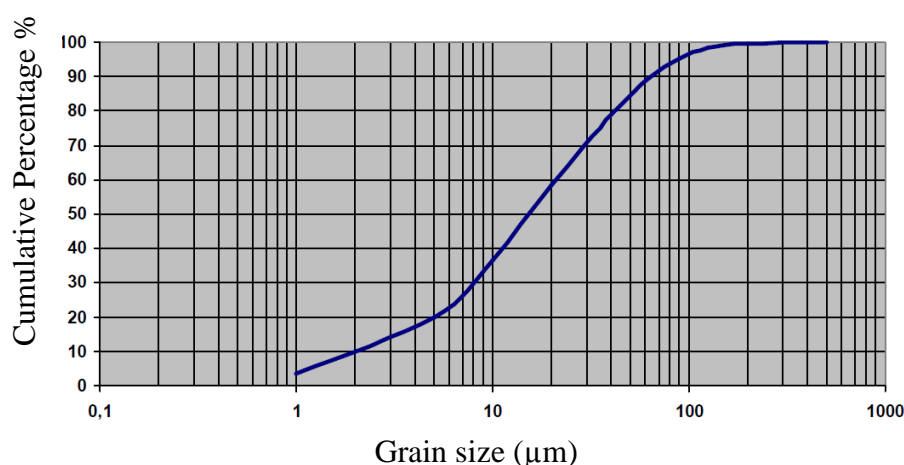


Figure 2.2 : Grain size distribution of fly ash.

2.1.3.2 Silica fume

In one of the mixture groups in this study, silica fume was used in a suspension form. Properties of silica fume can be seen in the following table.

Table 2.9 : Properties of silica fume.

Name of Product	Micro Silica Suspension EMSAC 500S
Producer	BASF AG
Solid particle content (amorphous SiO ₂)	50 % of mass 50 1,3
Density of solids	2,15 kg/dm ³
Density of suspension	1,37 kg/dm ³

2.1.4 Admixtures

Superplasticizer FM 30, a product of BASF AG, conforming to EN 934-2 [75] was used (Table 2.10). This plasticizer based on naphthalin sulfonate had a density of 1.2 kg/l. The admixture was used as 1 percent fraction of cement by weight as specified in the user manual of the admixture.

Table 2.10 : Properties of super plasticizer.

Raw material base	Naphthalinsulfonat
Color and form of delivery	Darkbrown and liquid
density (at 20°C)	1,20 ± 0,03 g/cm ³
pH (at 20°C)	7,5 ± 1,0
Maximum chlorid content	0,10 M%
Maximum alkali content	6,5 M%, as Na ₂ O-Equivalent

2.1.5 Water

Tap water conforming to EN 1008 [76] was used in the study.

2.1.6 Textile Reinforcement

In this study, textile reinforcement which is produced by ‘‘Institut für Textilmaschinen und Textile Hochleistungswerkstofftechnik der TU Dresden’’ with the name of NWM3-014-07-b1 (30%) is used. Some properties of this carbon, black textile reinforcement can be seen in the Tables 2.11 and 2.12.

Table 2.11 : Properties of textile reinforcement.

Product code	Operator	Stacking tier (°)	Material and Fineness in Textile	Separation distance (mm)	Weft-knitted fibers	Binding, stitch length (mm)	Output (m)
NMW3-014-07-b1 (30%)	SFB (A6)	90 0	TEN-CF800-02	7,2	PP-t	Tricot, 2,0	50+20

Table 2.12 : Material description and properties of commercial filament.

Glossary	Producer	Product code	Material	Appearance	Fineness	Charge Nr.
TEN-CF800-02	Tenax Fibers GmbH, Germany	Tenax HTA 5131 800 tex f6000	Carbon	Filament yarn	800	02
Code	Fineness	Density (g/cm ³)	Diameter (µm)	Expansion (%)	Strength (N/mm ²)	E-modulus (GPa)
TEN-CF800-02	800	8,07	12000	0,72	1218	209,89

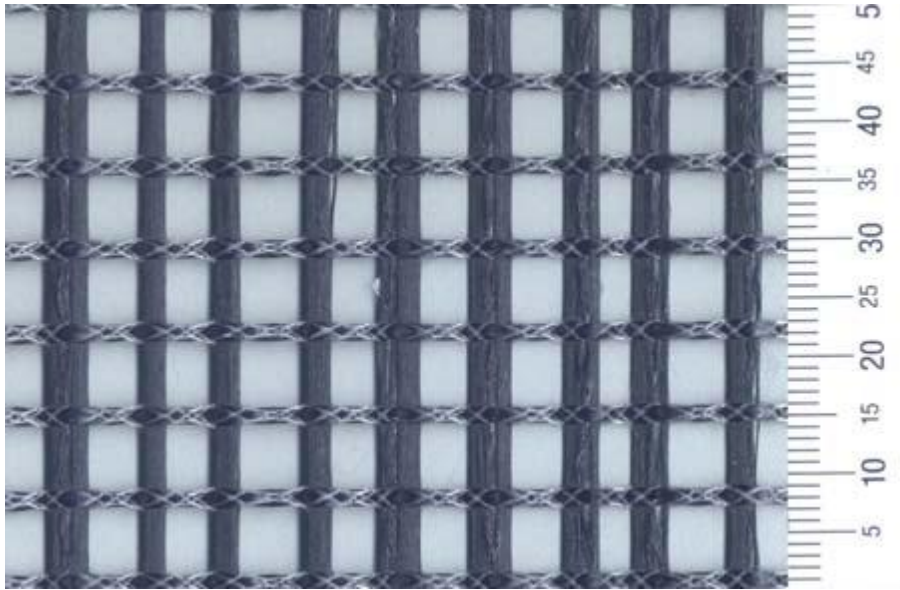


Figure 2.3 : Biaxial textile reinforcement made of carbon multifilament yarns.

2.1.7 Superabsorbent Polymer

In this thesis two SAP products were used, which are here called B3 and B4 in accordance to the studies performed by Michaela Gorges [77] in the TU Dresden Construction Materials Institute. Particle size distributions of these SAP materials are given below.

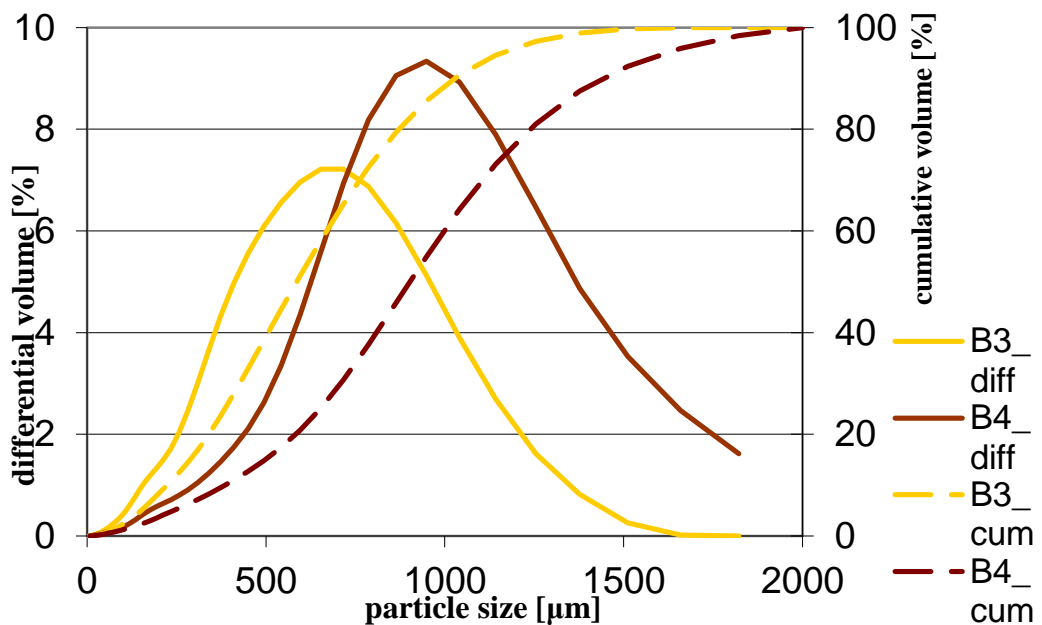


Figure 2.4 : Particle-size-distribution of SAP material.

2.2 Mixture Composition, Specimen Preparation, Curing and Testing Program

Concrete mixtures were prepared in batches of 0.08 m³ in a laboratory pan mixer. 100x500x14 mm plastic plate moulds were used for specimens and compaction was done by a vibratory table. Specimens were produced with laboratory procedure for producing TRC specimens in the laboratory of TU-Dresden Construction Materials Institute. Ingredients were mixed dry, with water and finally with admixture for defined time periods. The specimens for the investigations of self-healing processes are rectangular TRC plates 500 mm long, 100 mm wide, and 14 mm thick (Figure 2.5). The specimens are produced with 3 layers of carbon-fibre textile reinforcement in the preliminary work and 4 layers of textile reinforcement were used in the main part of thesis. The arrangement of the textile layers is symmetrical and parallel to the plate’s surface.

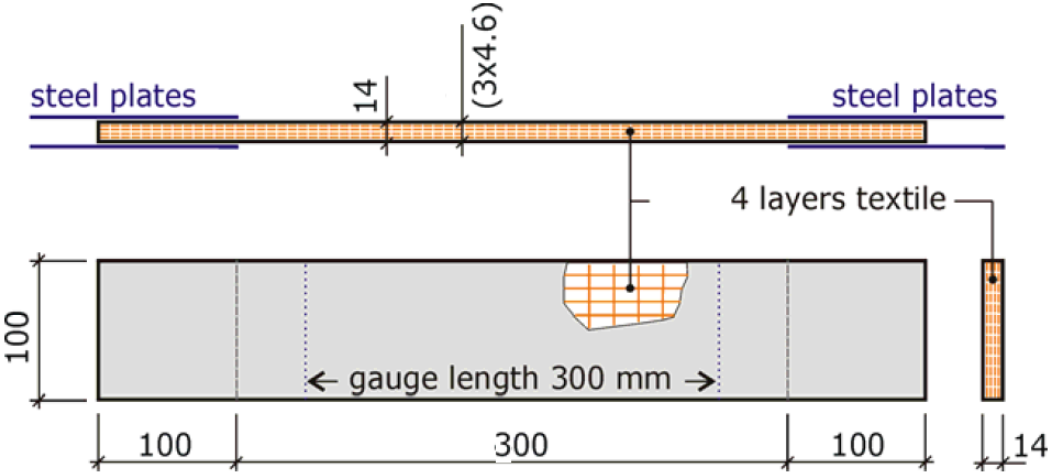


Figure 2.5 : Geometry of TRC tension test specimen.

The matrix composition is varied by the type of binder. The first matrix system is based on Portland cement (CEM I). The second mixture is comprised of blast furnace cement (CEM III) and a relatively high content of pozzolana (a mix of fly ash and silica fume). The water-to-binder ratio was below 0.40 in both matrices to guarantee a sufficient amount of non-hydrated binder. After de-moulding in the preliminary work the plates were kept in water for 28 days and in the second part of thesis they were sealed (wrapped in plastic foil) and stored in a climate-controlled room at 20°C until testing or further treatment. Thus, water release or uptake during the hardening can't be possible.

Table 2.13 : Material amounts for 1 m³ concrete mixture.

	CEM I	Sand(0/1)	Quarzsand	Millisil	Water	Plasticizer
C1	861,25	1032,5	57,5	57,5	287,5	8,75
	CEM III	Sand	Fly ash	Silica fume	Water	Plasticizer
C3	550	1101,25	247,5	55	247,5	8,75

* SAP group mixtures were same as C1 group amounts.

**All the amounts in the table are given in kg.

SAP material amounts were calculated through empiric formulas of recent studies about SAP material in the institute. Some preliminary mixtures were produced to observe appropriate amounts. Selected SAP type 0,3 of cement by weight (2,58 kg/m³) were used. However, extra water which increases w/c ratio as 0,06 was used.

In order to obtain several crack characteristics and crack widths similar to those under actual service conditions, the uniaxial tensile TRC specimens were preloaded up to two different strain levels and then unloaded to the desired crack width resulting from the remaining strain (Figure 2.6).

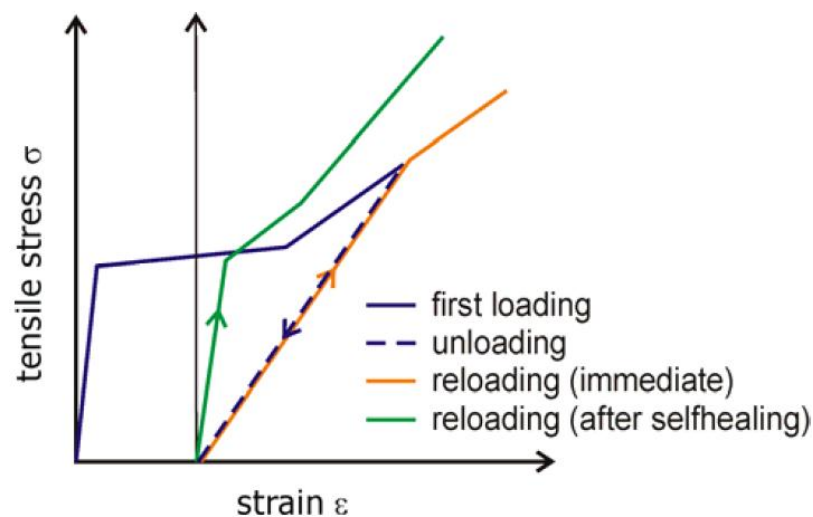


Figure 2.6 : Loading of a TRC tension test specimen.

Wetting and drying method was used to simulate outdoor environmental conditions as an accelerated method. After inducing the initial crack pattern, in the preliminary work, the cracked specimens were exposed to three different environmental conditions for 13 days: 1) lab climate (20°C, relative humidity 65%), 2) water (20°C), and 3) wetting-drying cycles (20 h in water of 20°C and 4 h in oven at 40°C), respectively. In the second part of investigation, the specimens were exposed to several climate environments to generate different self-healing conditions. The exposures were:

- storage at lab climate (20°C/65% relative humidity),

- storage in water (20°C),
- storage in a wet and dry cycle (water storage (20°C) during 1 hour, drying at lab climate (20°C) during 23 hours),
- storage in a wet and dry cycle (water storage (20°C) during 1 hour, drying at lab climate (20°C) during 71 hours).

The respective durations of the cracked specimens' exposures were to be 2 weeks and 4 weeks. For all the concrete composition and curing period groups at least 3 plates were produced and tested.

2.3 Fresh Concrete Properties

Slump test was carried out just before casting the specimens according to method that was recently used in the institute laboratory to ensure the similar workability of all concrete batches. The device which used for the test can be seen below. After placing concrete to the testing apparatus, there was a waiting period for 30 seconds. The diameter of concrete measured after 15 times manual vibrating. The average slump of fresh concrete obtained was 18 ± 2 cm.



Figure 2.7 : Slump test equipment.

2.4 Experimental Procedure

In this study, the effect of self-healing of high-performance fibre-reinforced cementitious composites is investigated. Textile Reinforced Concrete specimens were used for the investigation. In the preliminary work and second experimental part of the thesis three types of concrete mixtures are used. In the first group the

binder was pure Portland cement (CEM I). In the second batch, the binder was composed of blast furnace cement (CEM III) and pozzolana (fly ash and silica fume). The third group consisted of CEM I cement, aggregates and SAP particles. They were exposed to several conditions of curing after initial cracking. Then self-healing properties of specimens are investigated with mechanical test and microstructural analysis.

2.4.1 Uniaxial Tension Tests

First cracks have to be made in the concrete in a controlled way. Tensile test was chosen for this controlled pre-cracking. Test machine, which can be seen in the following figure, was used for uniaxial tension tests and its properties are listed below:

Servo-hydraulic test machine,

- type: INSTRON 8501
- Load measuring range: 100 kN
- Displacement capacity of hydraulic jaw: 250 mm
- Electronic capture of load, deformation of machine
- Measurement of specimen deformation by means of 2 lateral fixed LVDT
- Measuring range of LVDT is 10 mm.



Figure 2.8 : Uniaxial tension test machine.

In the preliminary work, at an age of 28 days, a crack pattern was generated by means of straining TRC samples up to 3 mm/m. Subsequently a second load cycle was performed to measure the stress-strain curve in the cracked state. Eventually, the samples were loaded again up to a strain of 3 mm/m. Two load cycles were applied and the stress-strain curves recorded. Similarly, in the second part of experimental studies, uniaxial tension tests were done for pre-cracking and investigation of mechanical properties before and after self-healing. However, at least 3 specimens were tested for each group.

2.4.2 Microscopic Analyses

Microscopic analysis was done to view the cracks' conditions before and after self-healing curing via the optical microscope and also electron scanning microscope to observe self-healing effect on cracks. EDX investigations were coupled with ESEM pictures to identify the self-healing products in the cracks of specimens. Optical microscopy is also used to investigate cracks and thin sections which are prepared from cured and non-cured specimens.

To have information about pore sizes and distribution of them in several self-healing curing conditions, MIP tests were also done to some specimens. The specimens were prepared according to apparatus and testing machines. All the microscopic analyses were done in the second experimental part of the investigation.

2.4.2.1 Electron Scanning Microscopy

Electron scanning microscope was used to view the process of further hydration or newly formed self-healing products on the crack surfaces of the specimens through the self-healing procedure. The model of the machine and the producer were XL30 ESEM, Company FEI, (ESEM stands for Environmental Scanning Electron Microscope). The electron beam is produced using a Tungsten cathode. The pictures were taken at different magnifications. Small specimens of 1cm³ were cut and dried in oven and both crack surface and sliced surface is investigated. The situation of the cracks was investigated comparing the specimen before and after self-healing cure.

2.4.2.2 Optical Microscopy

Microscopic analysis was done using an optical microscope with 5 to 50 times magnifying. The optical microscope used is a ZEISS Microscope. The pictures were

taken from the microscope using a digital camera. The cracks were observed before and after self-healing cures. The crack size changes before and after cure was measured.

Some horizontal and vertical thin sections are prepared from specimens before and after self-healing cures. Specimens were cut, grinded, and polished until a final thickness and during the process the thin section is mounted upon an object glass. Pictures were taken under UV lights; also those thin specimens were observed with the optical microscope. Thin-section concrete petrography is most suited to general examinations of concrete to see the pores and crack pattern. The aim of the research was to take advantage of the optical microscopy results on thin sections, and carry out a study to determine the microstructures of concrete-pastes/aggregates, micro voids/cracks as well as the quantification of the crack patterns.

2.4.2.3 Mercury Intrusion Porosimeter Test

Mercury intrusion test was done by introducing mercury under pressure into the concrete pores and the extrusion. With the pressure and the quantity of the mercury pore diameters and sizes can be analysed. The MIP tests have been performed using a configuration of two mercury porosimeters. The first one, working in the pressure range from 13.3 kPa - 300 kPa, is for evacuating and filling the sample holders with mercury and for measuring the bigger pores. The second one, working in the pressure range from 100 kPa - 200 MPa is for measuring the finer pores. Using the two porosimeters, a pore size range from 7.5 μm up to 112 μm can be measured. From the detected values of pressure and increased mercury, the pore size distribution is calculated by the Washburn equation. Finally volume/pressure and total pore size distribution curves were gained.

2.4.2.4 EDX analysis

The EDX-detector (Energy Dispersive X-ray) is installed inside the ESEM and detects the X-ray emitted by the sample. Because the x-ray is characteristically for each element, it is possible to get information of the element composition of the sample investigated. In the study it is used a RÖNTEC EDX- detector. EDX investigations were coupled with ESEM pictures to identify the self-healing products in the cracks of specimens.

3. EXPERIMENTAL RESULTS AND DISCUSSION

The purpose of this thesis is to investigate self-healing of different concrete mixtures by mechanical and microstructural tests. The tests which were done on specimens are explained previously. Before and after curing, effects of self-healing due to different curing applied to the specimens were investigated.

The test program consisted of testing 50x100x14 cm rectangular concrete prisms which were cured in water and in a plastic folio for 28 days. Concrete under uniaxial tension test and some other micro-structural test were done before and after curing.

At the first stage of this study, after 28 days curing in water tank, specimens were subjected to uniaxial tension test to make initial cracks and after self-healing cure for two weeks, they were tested in the same machine to observe the effects of the self-healing on mechanical properties. Photographic methods were also used to observe the cracks and crack pattern.

At the second stage of testing, some of the specimens were sealed by plastic folio thus, water release or uptake during the hardening can be avoided and they are kept in a climate-controlled room at 20°C for 28 days and after initial cracking they were exposed to different curing conditions for 2 and 4 weeks. Finally they are tested to identify the changes occurred in some mechanical and micro-structural properties of concrete. The tests applied were uniaxial tension, mercury intrusion and additionally optical and electron microscopy observations.

3.1 Mechanical Properties of Specimens

Uniaxial tension tests were performed to make initial cracks and to observe self-healing effect of specimens. Specimens are loaded up to the deformation 3 mm/m and then reloaded. To see the uniaxial tension behaviour of cracked specimens, they were loaded for the second time. Mostly the second curve was the similar to tension curve of textile reinforcement. This loading regime was performed for both initial cracking and ultimate loading of specimens.

3.1.1 Preliminary work

In the preliminary work, three concrete mixtures were used. The first binder for the first group was pure Portland cement CEM I and then CEM III, fly ash and silica fume were the binder materials for the second group. Additionally, in the third group pure Portland cement CEM I and SAP materials were used together. The curing period was 13 days and fixed for all groups.

Table 3.1 : Table of specimens’ naming according to various concrete composition and curing conditions.

Composition/Curing Conditions	Wet-Dry Cycle	Air Curing	Water Curing
CEMI	C1WD	C1A	C1W
CEMIII	C3WD	C3A	C3W
SAP	SAPWD	SAPA	SAPW

*Number ‘2’ in front of these codes indicates the second loading after the self-healing curing.

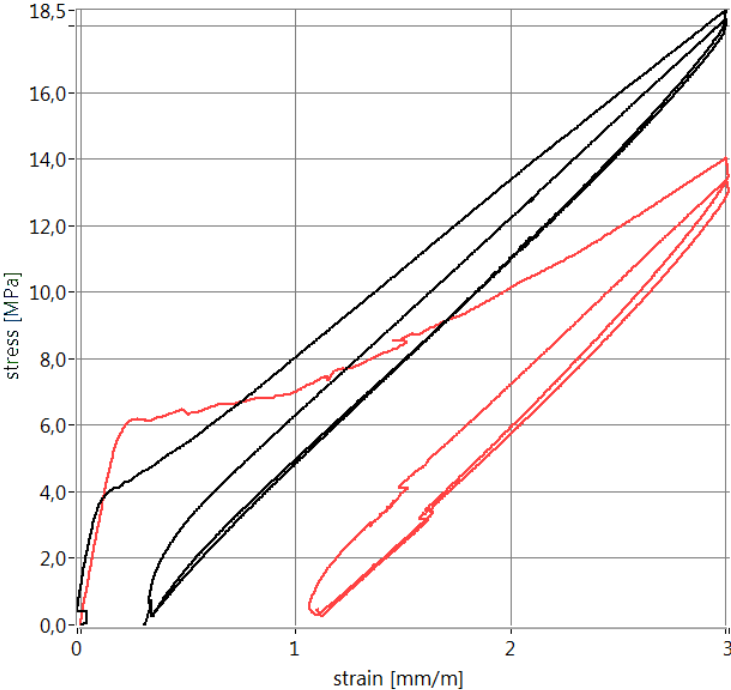


Figure 3.1 : Stress-strain curve of C1WD and 2C1WD.

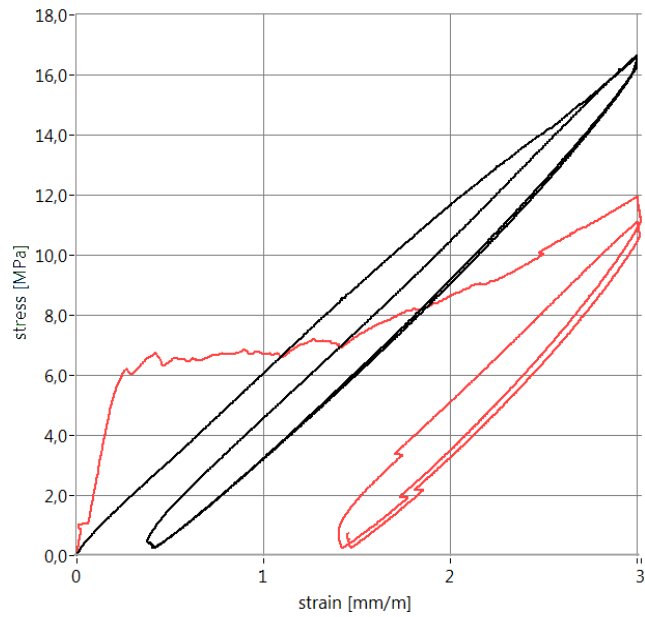


Figure 3.2 : Stress-strain curve of **C1A** and 2C1A.

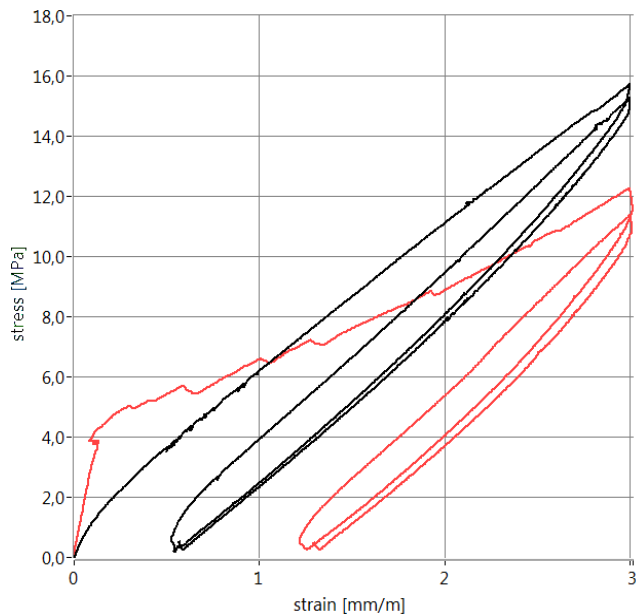


Figure 3.3 : Stress-strain curve of **C1W** and 2C1W.

In the first group (C1) specimens, the most visible self healing effect can be easily seen in the wet-dry cycle curing condition. In this group of curing, there are newly formed self-healing products which has a stress up to 4 Mpa. In the water curing conditions, specimens showed relatively less self-healing behaviour. As it can be seen in the previous figures (3.1, 3.2, 3.3), second curve that is loading curve after self-healing cure reached greater stress levels than the air cured group. Nearly no self-healing effect can be seen in the last group of specimens. The second loading curve is so similar the second part of first loading curve. That means, there was no

newly formed self-healing product which create an extra stress, however initially cracked and air cured concrete curves are so similar with the textile reinforcement.

The cement is replaced with fly ash and silica fume in the second group of concrete mixtures. Fly ash reacts with Ca(OH)_2 from cement hydration and produces C-S-H gel. It is thought to be less influenced by the availability of free water than the hydration reaction of cement. Specimens are exposed to same curing conditions that are air, water curing and wet-dry cycling. In the following figures (3.4, 3.5, 3.6) stress-strain curves of mixtures can be seen. The wet-dry cycling group seems to be best self-healing effect as in the pure Portland cement group. Nevertheless self-healing ability of the specimens made of CEM III and pozzolana led to much less pronounced crack bridging. The brief self-healing period was too short to generate a sufficient amount of hydration products in the slow hydrating binder combination. The self healing behaviour of such a mixture are studied again in the final part of the thesis again. It can be said for the air curing group that there was no self-healing products which are effects the machanical properties of specimens. Water curing group also showed a self-healing behaviour mechanically, however this effect was less than wet-dry cycling group. It has to be mentioned that some newly formed self-healing products that have a stress level less than 1,5 MPa; were present in the specimens.

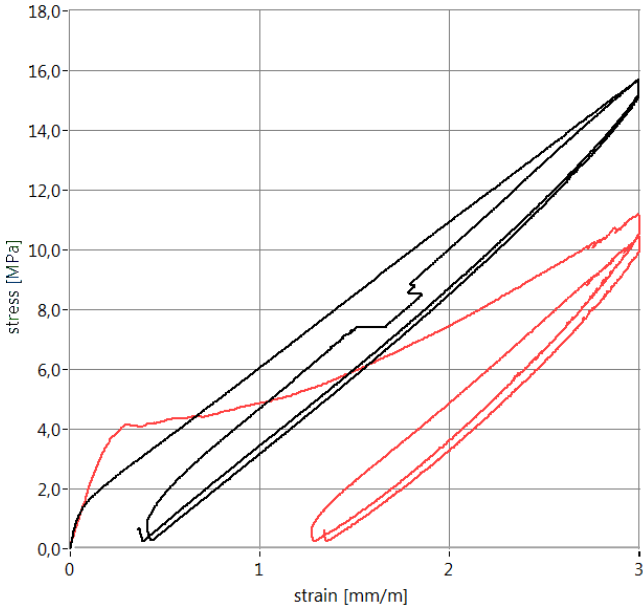


Figure 3.4 : Stress-strain curve of C3WD and 2C3WD.

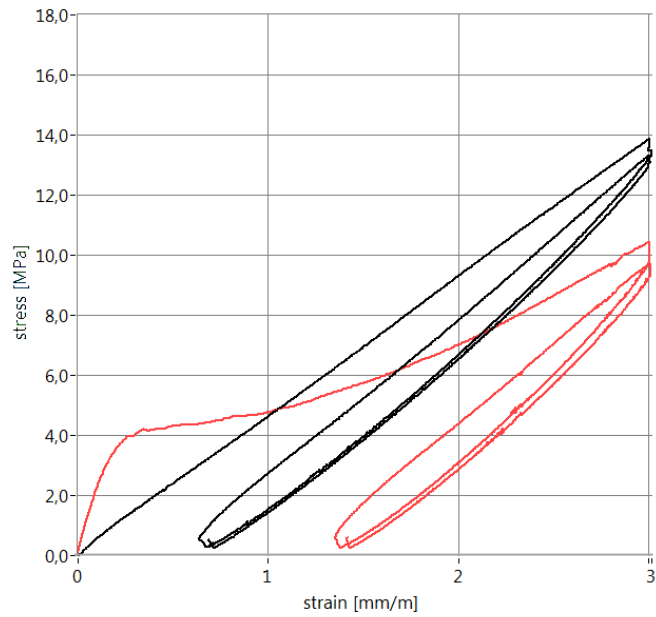


Figure 3.5 : Stress-strain curve of **C3A** and 2C3A.

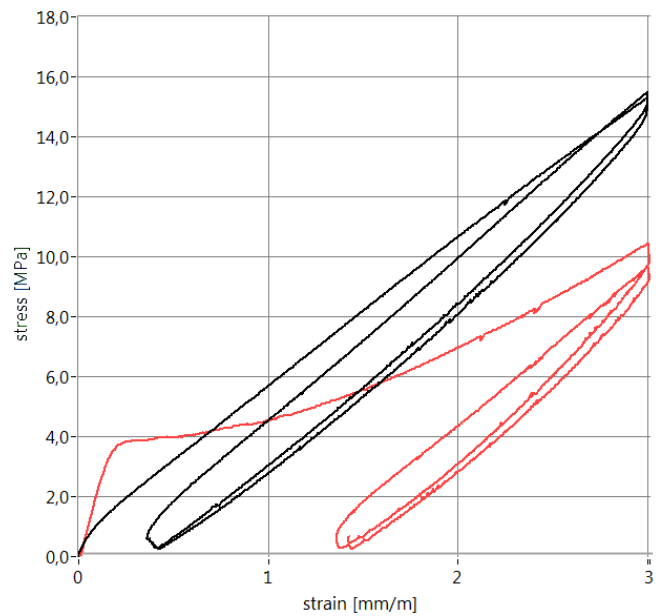


Figure 3.6 : Stress-strain curve of **C3W** and 2C3W.

The third group in the preliminary work of this thesis was the concrete mixtures that contained CEM I as a binder and SAP materials. As it can be seen in the figures 3.7, 3.8 and 3.9, wet-dry cycled specimens showed a clear self-healing about mechanical properties. On the other hand the mechanical self-healing degree was less than the specimens that have binder CEM I and consist no SAP materials. There was no mechanical self-healing effect in air cured group. Finally the specimens that were cured in the water showed self-healing less than the wet-dry cycled specimens.

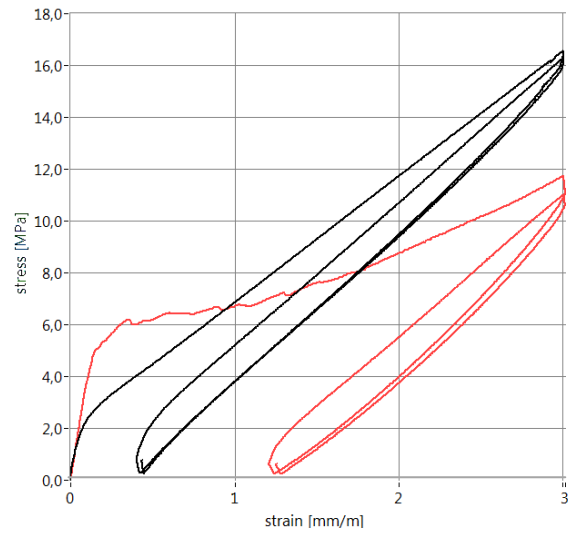


Figure 3.7 : Stress-strain curve of **SAPWD** and 2SAPWD.

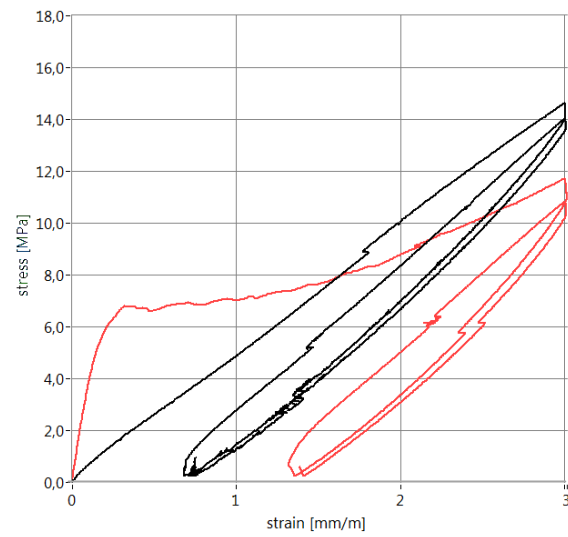


Figure 3.8 : Stress-strain curve of **SAPA** and 2SAPA.

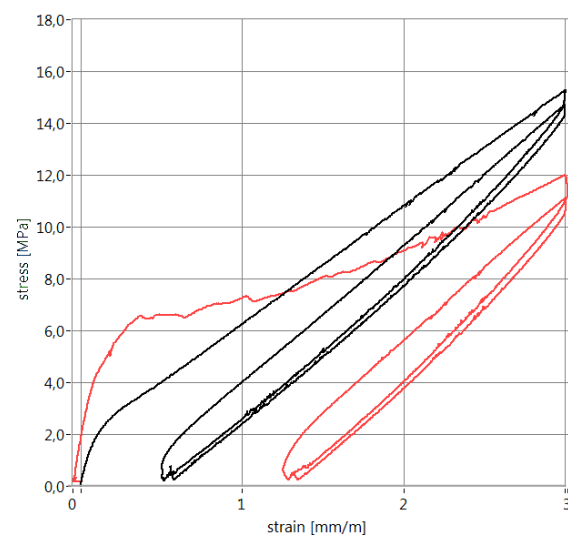


Figure 3.9 : Stress-strain curve of **SAPW** and 2SAPW.

3.1.2 Final work

In the final work, same concrete compositions as the preliminary work were used. After production, specimens are demoulded on the following day and they were wrapped in plastic foil and stored in a climate-controlled room at 20°C for 28 days until testing or further treatment. In addition, there were two types of curing periods which are 2 and 4 weeks. The four curing conditions were air curing in a climate-controlled room, curing in water, wet-dry cycling-1 (water storage (20°C) for 1 hour, drying at lab climate (20°C) for 23 hours) and wet-dry cycle-2 (water storage (20°C) for 1 hour, drying at lab climate (20°C) for 71 hours). In the following figures it can be seen that specimens had not any mechanical self-healing effect after air curing however, the second loading line in the ultimate loading are so similar to second loading of initial loading (pre-cracking) that is like textile reinforcement loading curve. Thus these specimens can be considered to be references.

Table 3.2 : Table of specimens' naming according to various concrete composition, curing conditions and durations.

Compositio n/ Curing Conditions	Air Curing	Water Curing	Wet-Dry Cycle-I	Wet-Dry Cycle-II	Curing Conditions/Duratio n
CEMI	C1A2	C1W2	C1WD12	C1WD22	2 Weeks Time Curing
CEMIII	C3A2	C3W2	C3WD12	C3WD22	
SAP	SAPA2	SAPW2	SAPWD12	SAPWD22	
CEMI	C1A4	C1W4	C1WD14	C1WD24	4 Weeks Time Curing
CEMIII	C 3 A 4	C 3 W 4	C 3 W D 1 4	C 3 W D 2 4	
SAP	SAPA4	SAPW4	SAPWD14	SAPWD24	

* After these codes, the last digit points the number of specimens.

**Number '2' in front of these codes indicates the second loading after the self-healing curing.

As it can be seen in the figures 3.10-15, there was no self healing effect. For air curing, time period of curing, the binder type and SAP usage did not matter for self-healing. It is because of absence of water.

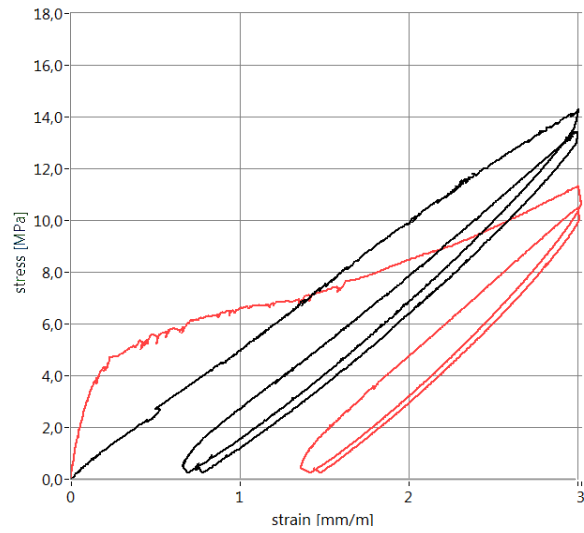


Figure 3.10 : Stress-strain curve of **C1A22-2C1A22**.

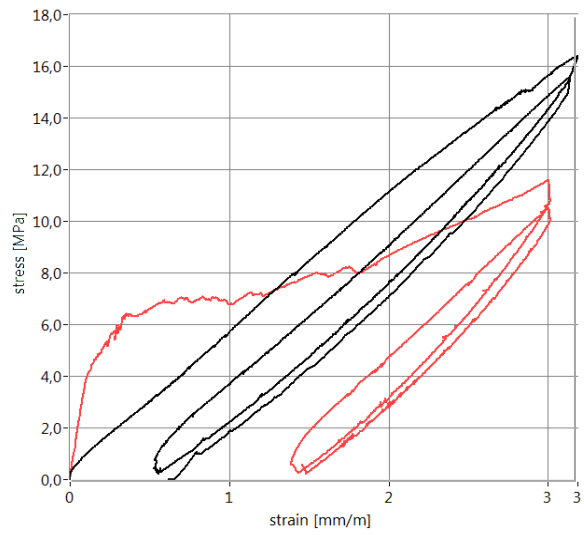


Figure 3.11 : Stress-strain curve of **C1A42-2C1A42**.

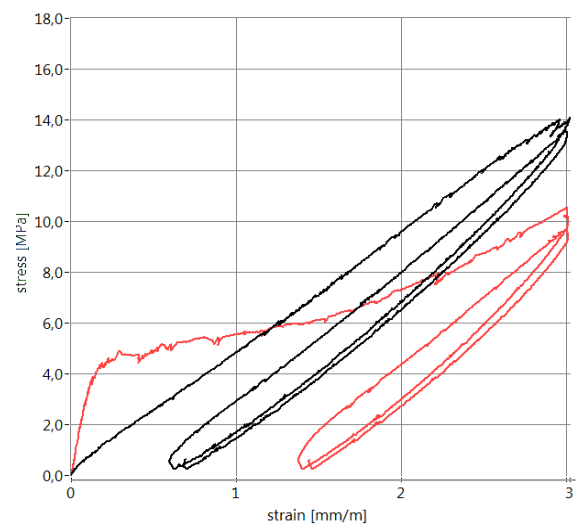


Figure 3.12 : Stress-strain curve of **C3A21-2C3A21**.

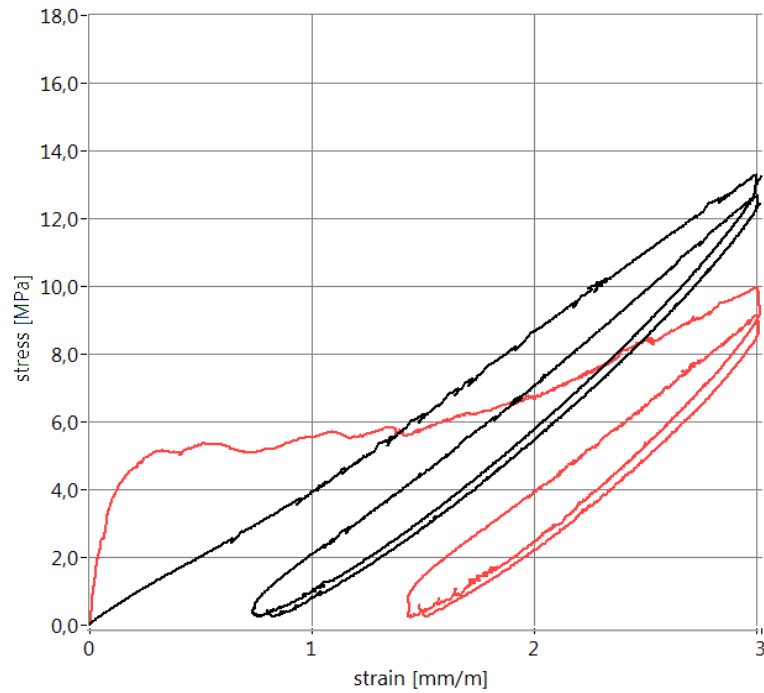


Figure 3.13 : Stress-strain curve of **C3A41-2C3A41**.

SAP materials was unable to absorb water during the period that specimens were exposed to air conditions. However, SAP materials did not show any effect on self-healing properties.

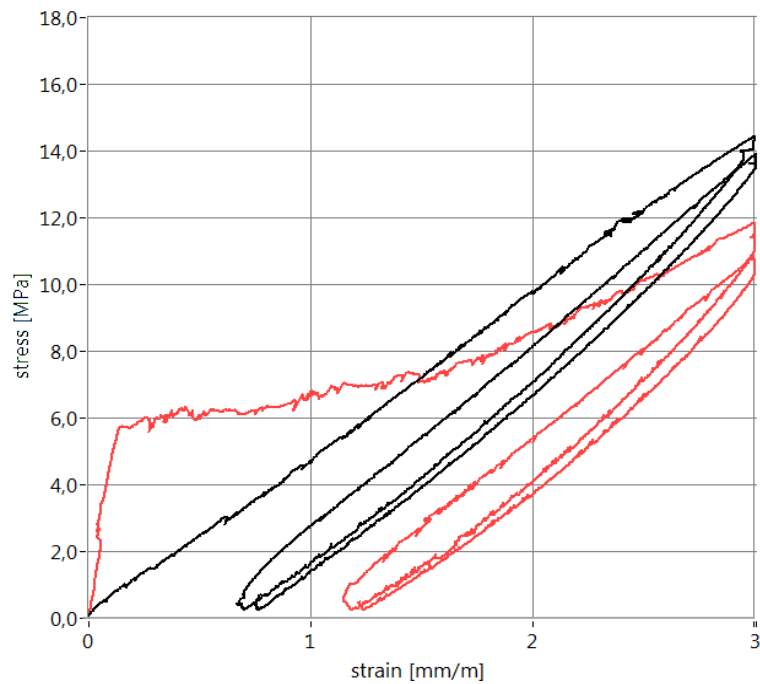


Figure 3.14 : Stress-strain curve of **SAPA21-2SAPA21**.

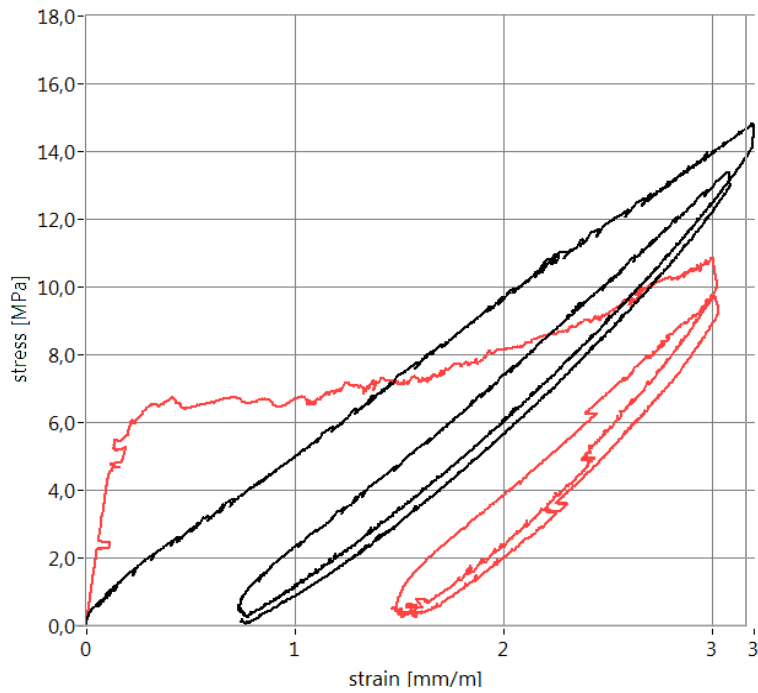


Figure 3.15 : Stress-strain curve of **SAPA41-2SAPA41**.

All water cured specimens are exposed to water curing at 20°C. The three groups of concrete mixtures were kept in water curing for 2 and 4 weeks.

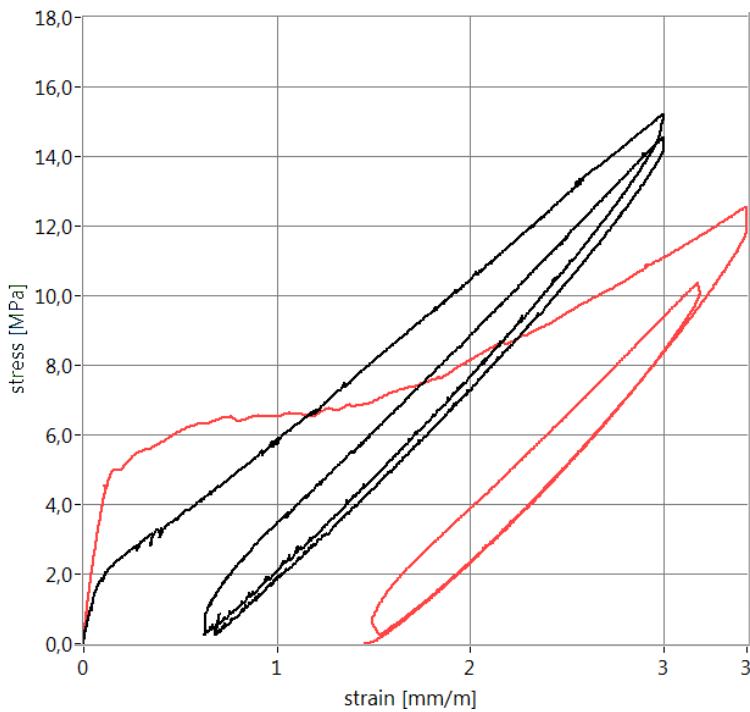


Figure 3.16 : Stress-strain curve of **C1W22-2C1W22**.

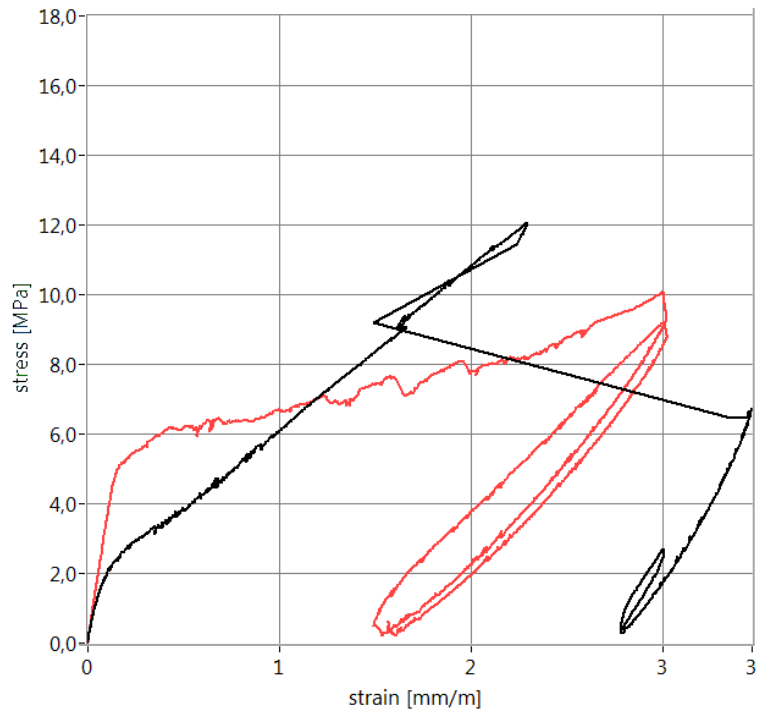


Figure 3.17 : Stress-strain curve of C1W41-2C1W41.

As it can be seen in the figures 3.16-21, specimens made of CEM I cement have showed higher tensile strength recovery after curing. However, as expected, specimens that are cured for 4 weeks had higher degree of self-healing on mechanical properties than 2 weeks cured specimens.

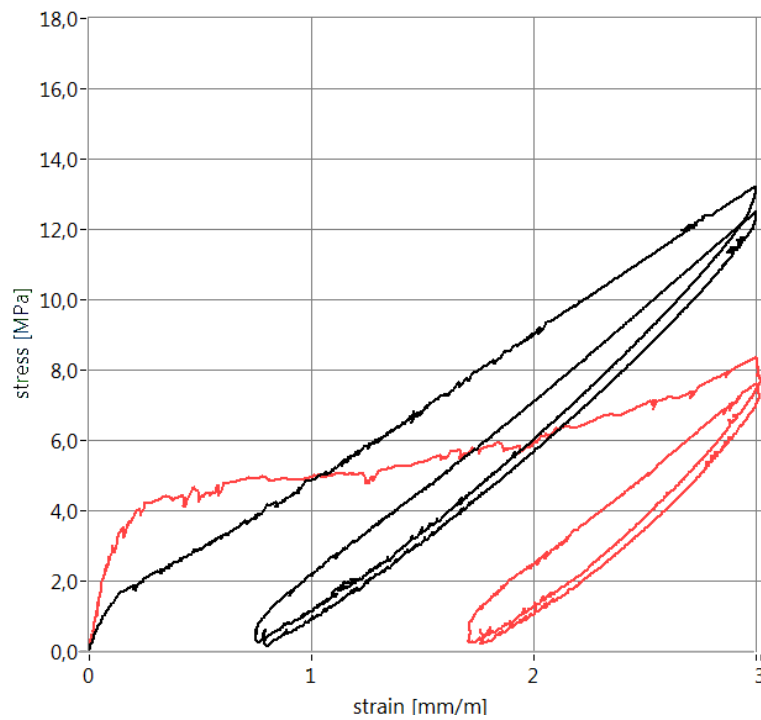


Figure 3.18 : Stress-strain curve of C3W22-2C3W22.

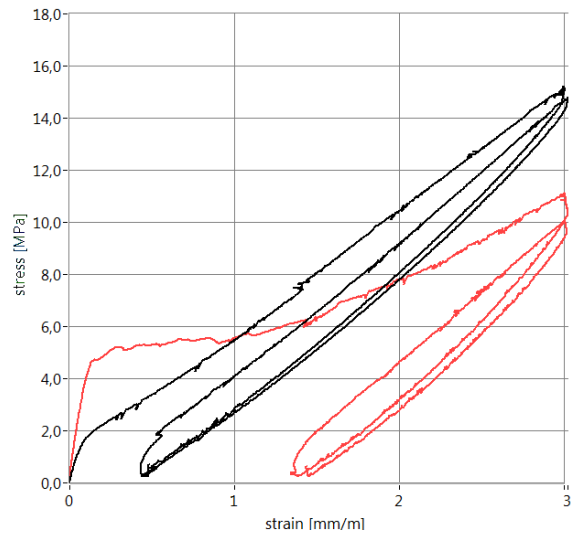


Figure 3.19 : Stress-strain curve of **C3W43-2C3W43**.

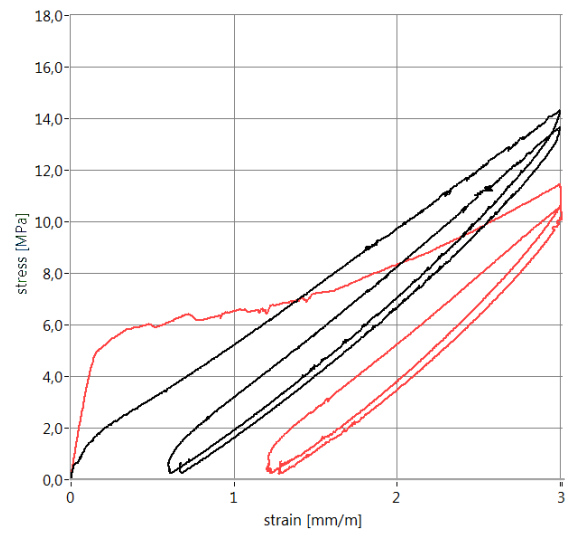


Figure 3.20 : Stress-strain curve of **SAPW21-2SAPW21**.

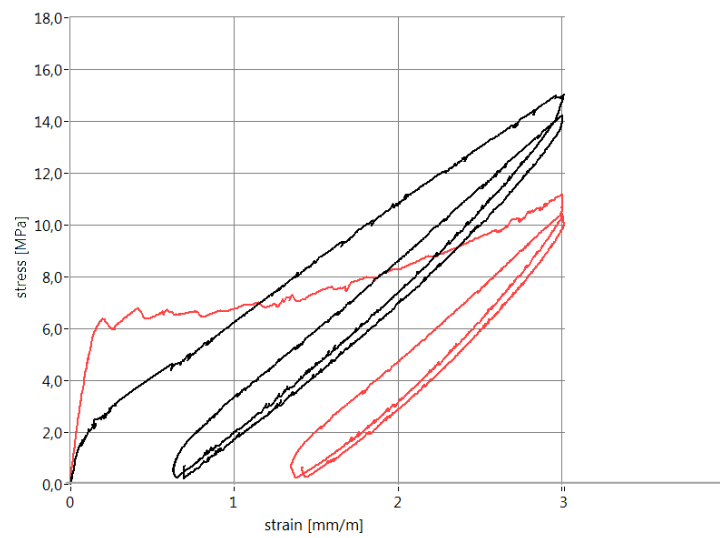


Figure 3.21 : Stress-strain curve of **SAPW43-2SAPW43**.

Similarly, the wet-dry cycle-1(water storage (20°C) for 1 hour, drying at lab climate (20°C) for 23 hours) cured specimens that were cured for 4 weeks have showed better mechanical properties recovery than 2 weeks cured ones. Because of the composition of concrete, mixtures with CEM I showed the highest strength. As it can be seen in the following 6 figures, CEM I group specimens that were cured for 4 weeks reached the maximum mechanical self-healing.

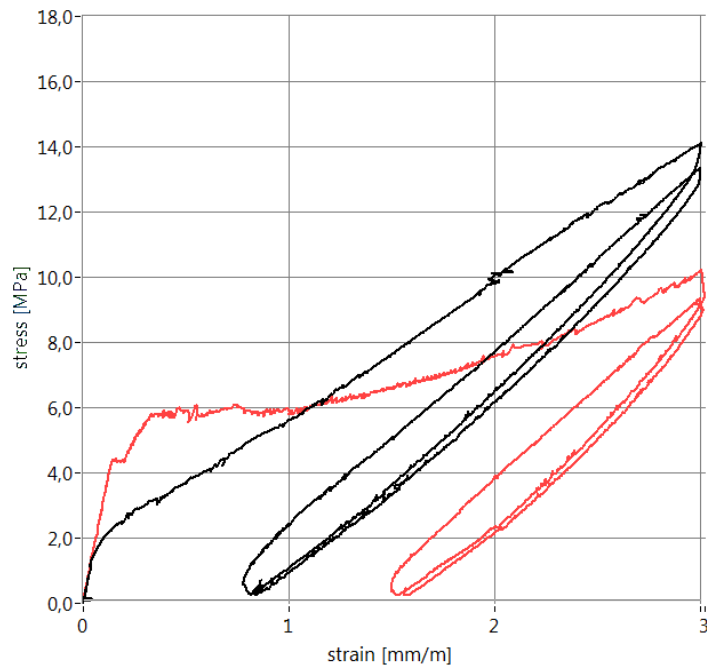


Figure 3.22 : Stress-strain curve of C1WD121-2C1WD121.

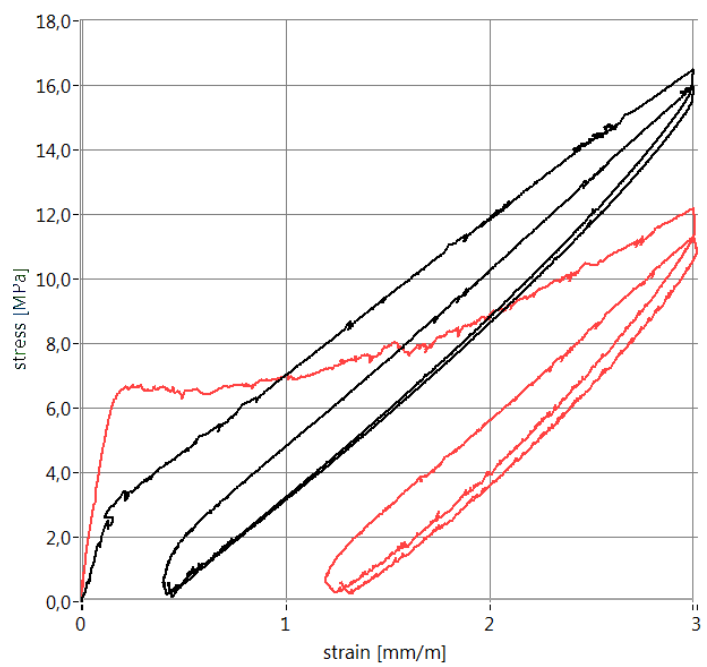


Figure 3.23 : Stress-strain curve of C1WD142-2C1WD142.

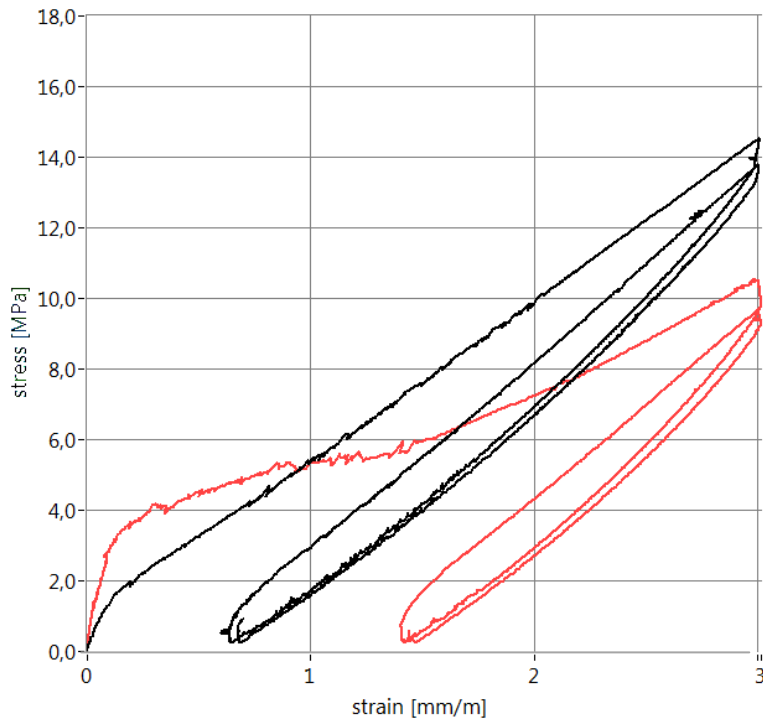


Figure 3.24 : Stress-strain curve of C3WD123-2C3WD123.

Concrete specimens gained nearly 60% of their initial tensile strength. CEM III group specimens had less initial tensile strength but the effect of self-healing was clear. SAP materials did not give any positive effect in comparison to the pure CEM I group.

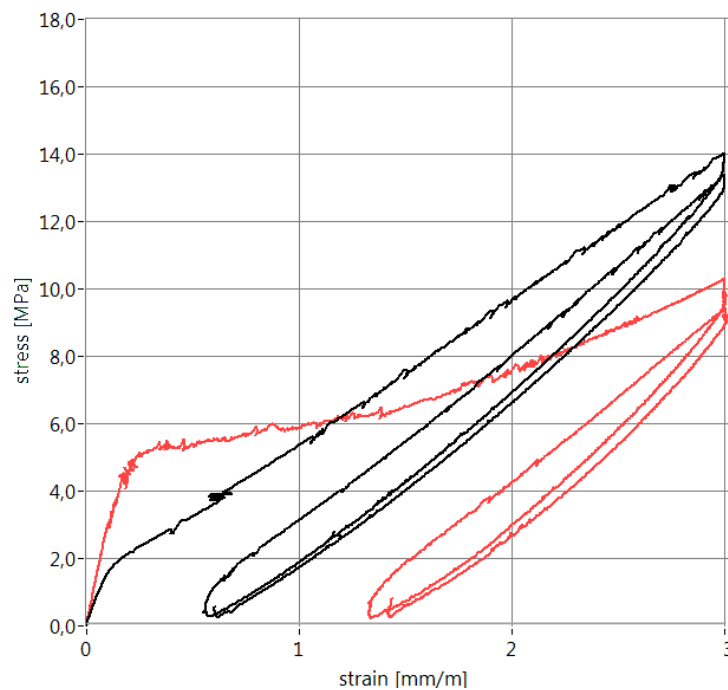


Figure 3.25 : Stress-strain curve of C3WD142-2C3WD142.

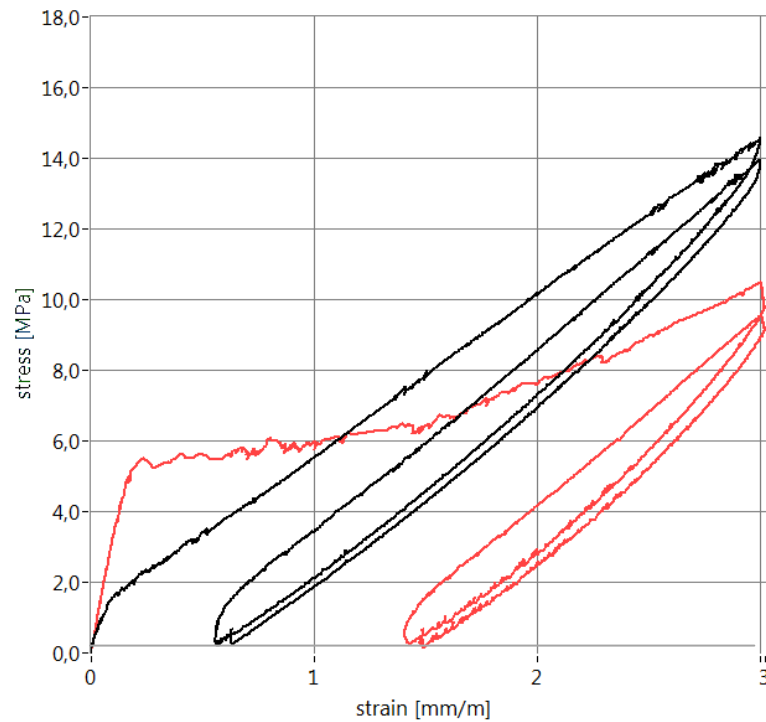


Figure 3.26 : Stress-strain curve of **SAPWD121-2SAPWD121**.

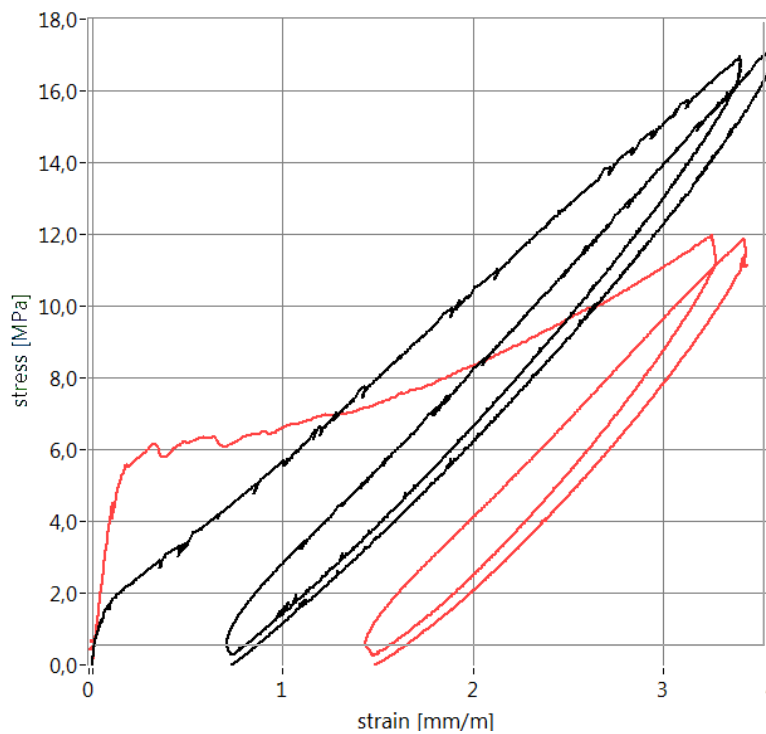


Figure 3.27 : Stress-strain curve of **SAPWD141-2SAPWD141**.

The second group of wet-dry cycle was storage in water (20°C) during 1 hour, drying at lab climate (20°C) during 71 hours. As it can be seen in the following 6 figures, as the all other types of curing and concrete composition groups, it was clear that 4 weeks curing is better than 2 weeks curing for recovery of mechanical properties.

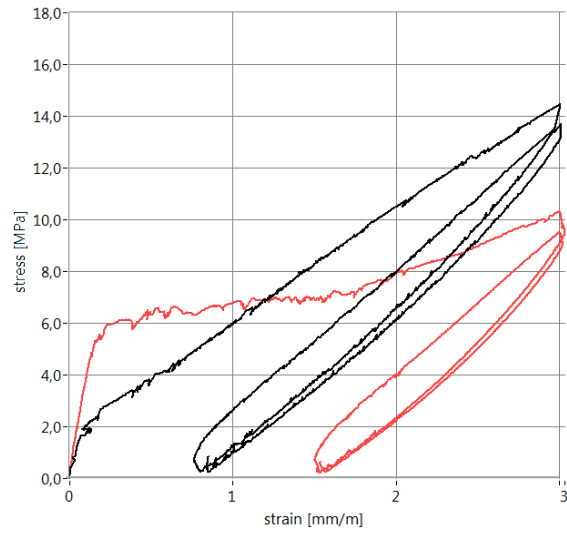


Figure 3.28 : Stress-strain curve of **C1WD223-2C1WD223**.

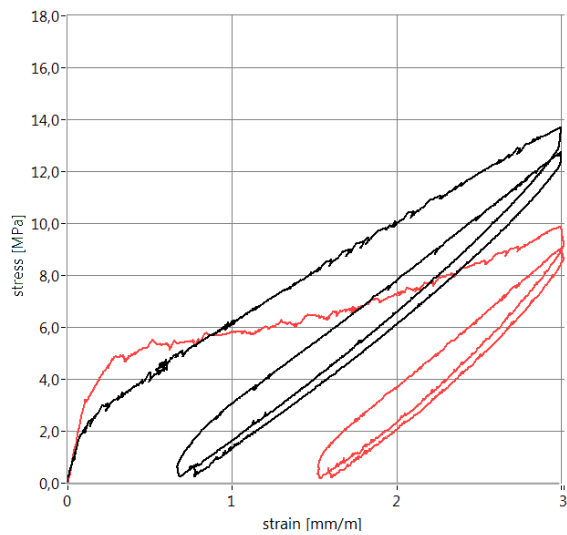


Figure 3.29 : Stress-strain curve of **C1WD24-2C1WD243**.

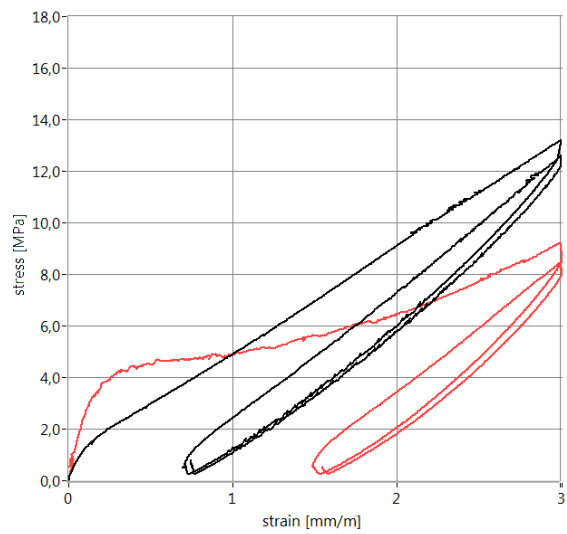


Figure 3.30 : Stress-strain curve of **C3WD221-2C3WD221**.

In this group of curing, there was no negative effect in the concrete specimens that contain CEM III and some other pozzolanas. It can be mentioned 4 weeks curing for this wet-dry cycle in CEM III group was enough to have same mechanical self-healing recovery as CEM I group. For all the groups 4 weeks cured specimens, the tensile strength of newly formed self-healing products till the first cracking of concrete was over 2 MPa. It can be also seen that concrete specimens with SAP materials did not show any decrease in tensile strength and also for the 4 weeks cured group the recovery rate of mechanical properties seems to be higher than the specimens without SAP materials.

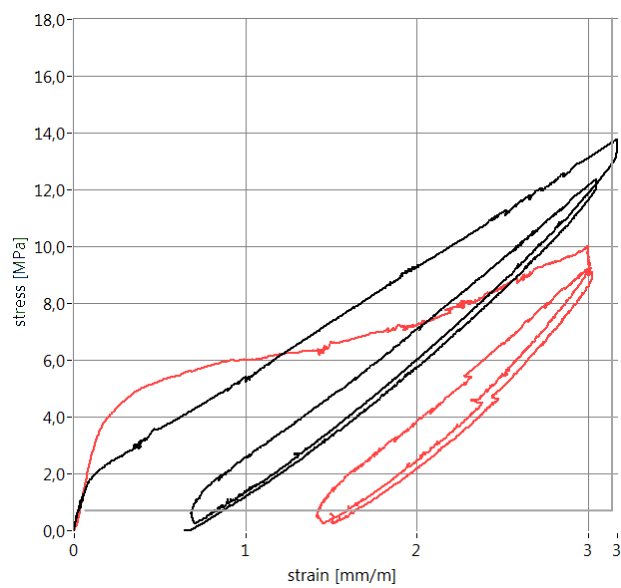


Figure 3.31 : Stress-strain curve of C3WD243-2C3WD243.

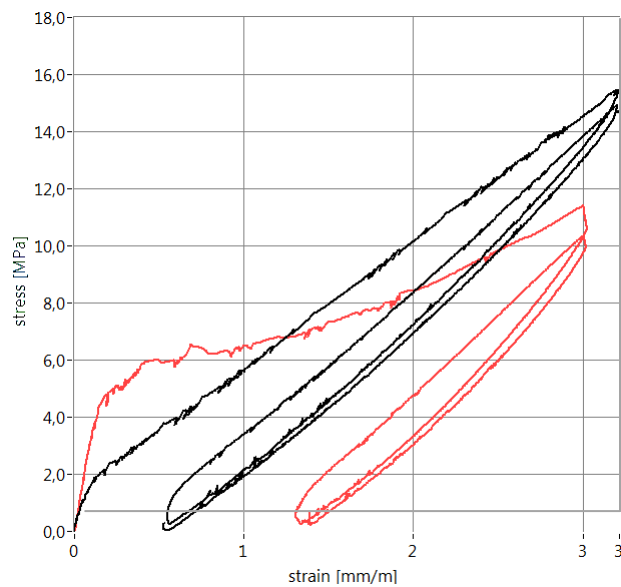


Figure 3.32 : Stress-strain curve of SAPWD223-2SAPWD223.

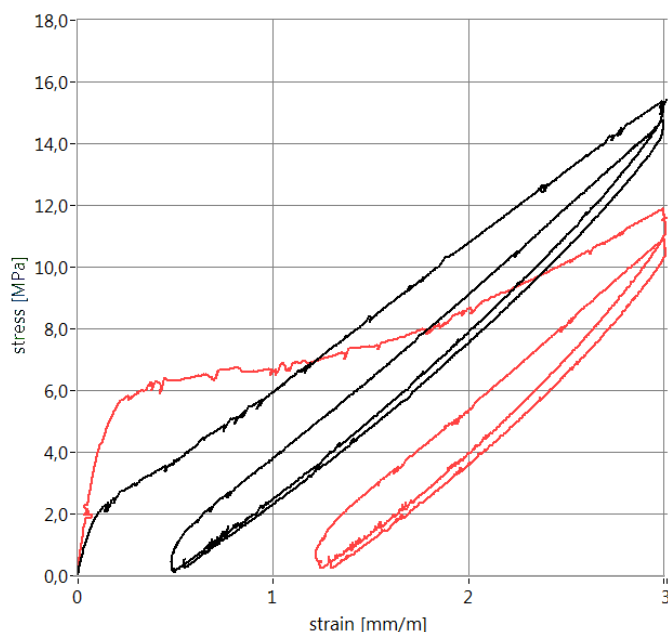


Figure 3.33 : Stress-strain curve of **SAPWD243-2SAPWD243**.

3.2 Microscopic Analyses

Microscopic analysis was performed in the second experimental part of the study to observe the cracks' conditions before and after self-healing curing. Electron scanning microscopy, EDX, optical microscopy and MIP tests were done for the microscopic analysis.

3.2.1 Optical microscopy analysis

Observation of the samples that exposed various curing types and durations are observed in the optical microscopy analysis. In addition, thin sections that were prepared from the surfaces of specimens were photographed under UV light and were also investigated. Lots of photos were taken and typical examples of each group are shown below.

3.2.1.1 Two weeks curing

The first group of specimens are exposed air, water curing and two types of wet-dry cycling for 2 weeks. The following photos are grouped according to same concrete compositions. As it can be seen in the photos, for the specimens which are produced with pure Portland cement showed no self-healing in the air curing group. The edges of the cracks which are mostly about 20 μm are clean. Water cured specimens showed relatively better self-healing behaviour but it was not enough to close all the

cracks totally. As it can be seen in the photos below, cracks are partially closed. Most cracks were nearly closed in the wet-dry cycle-1 group. It is possible to see the crack that had an initial width of 20 μm were closed up to 2,2 μm . The typical photo of the second wet-dry cycled group shows fully closed cracks which had 20 μm initial crack width.

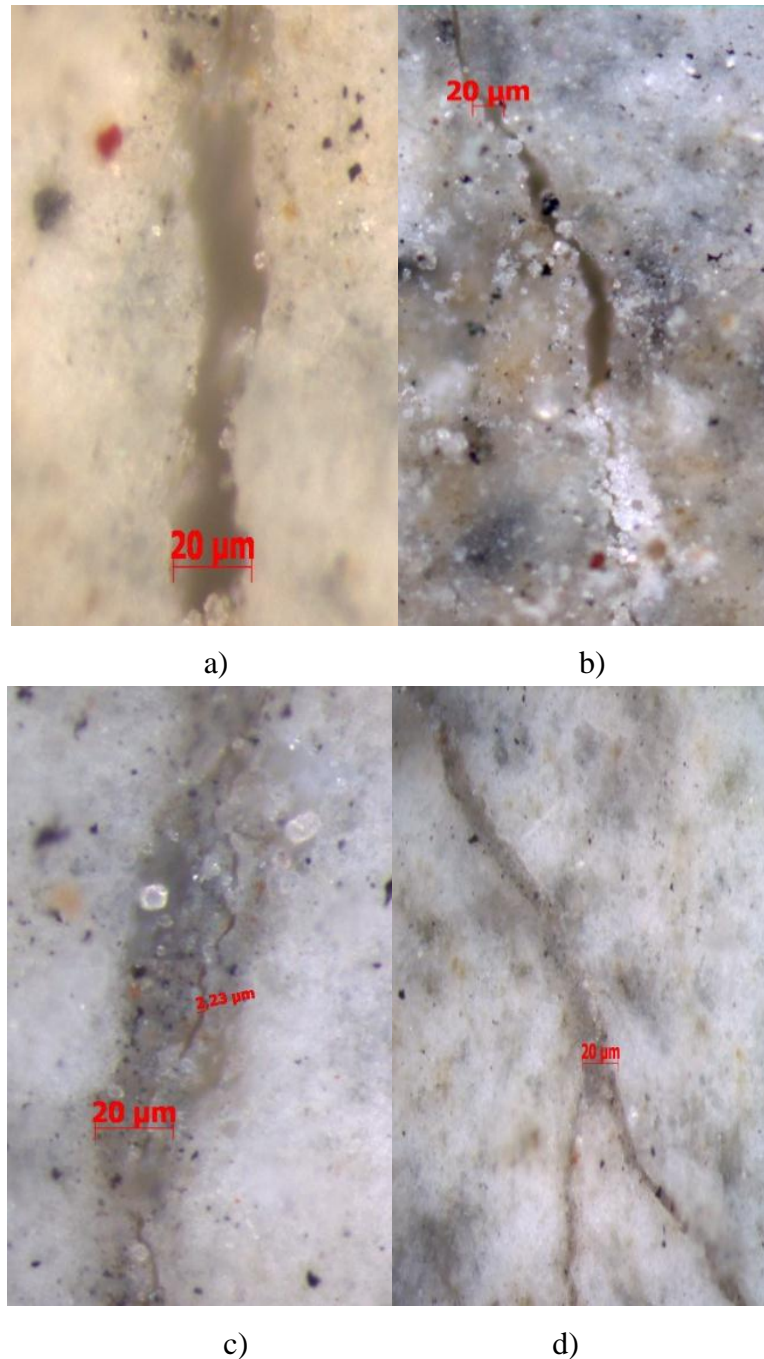
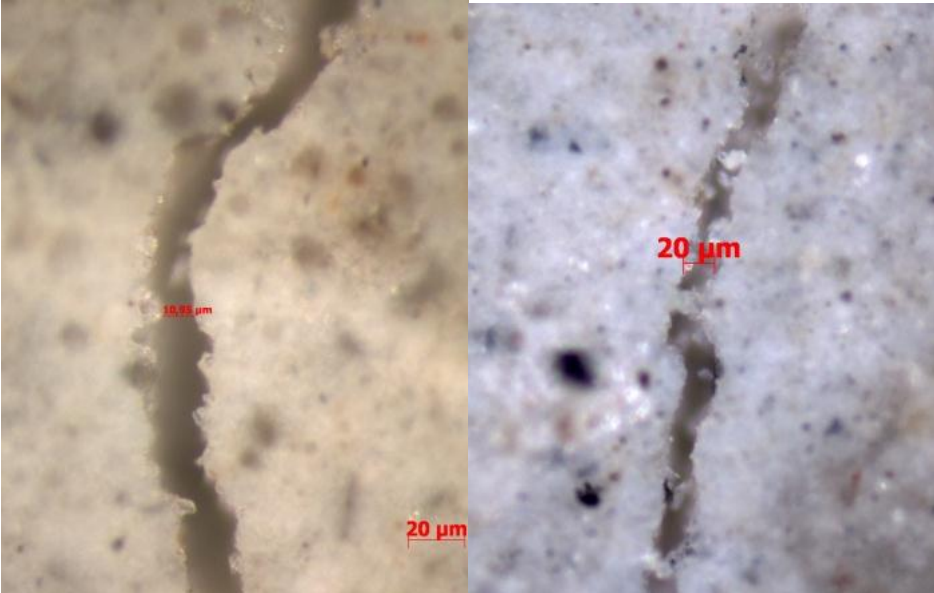


Figure 3.34 : Optical microscope photos of a) C1A, b) C1W, c) C1WD1 and d) C1WD2 specimens.

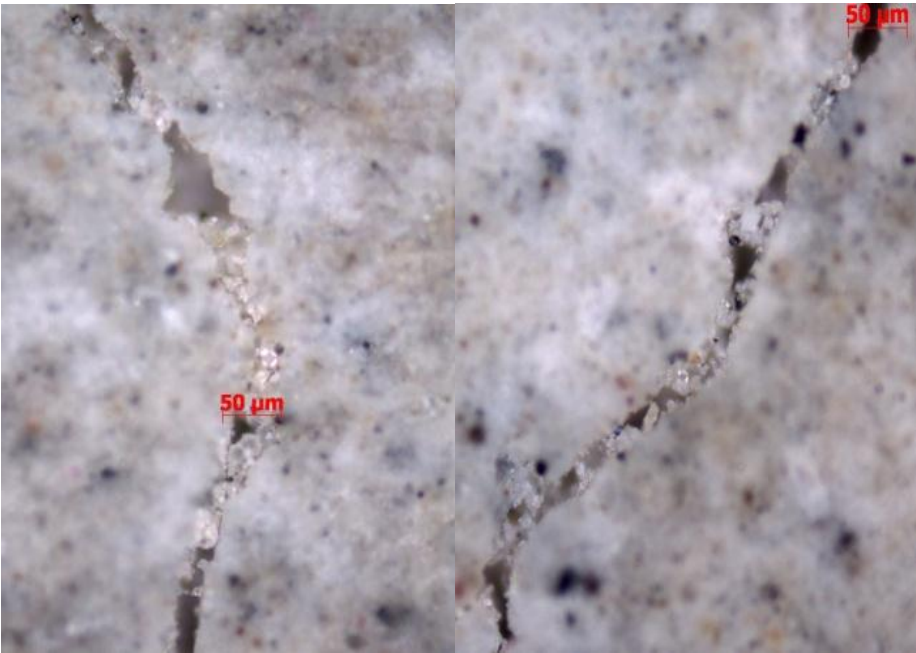
It can be said that for all the group of specimens that are produced with CEM III and pozzolanas have showed less self-healing behavior than the first group. As it can be

seen in the following photos, cracks were not closed totally. It has to be mentioned that specimens that were exposed to second wet-dry cycle, showed the best crack closing capacity.



a)

b)

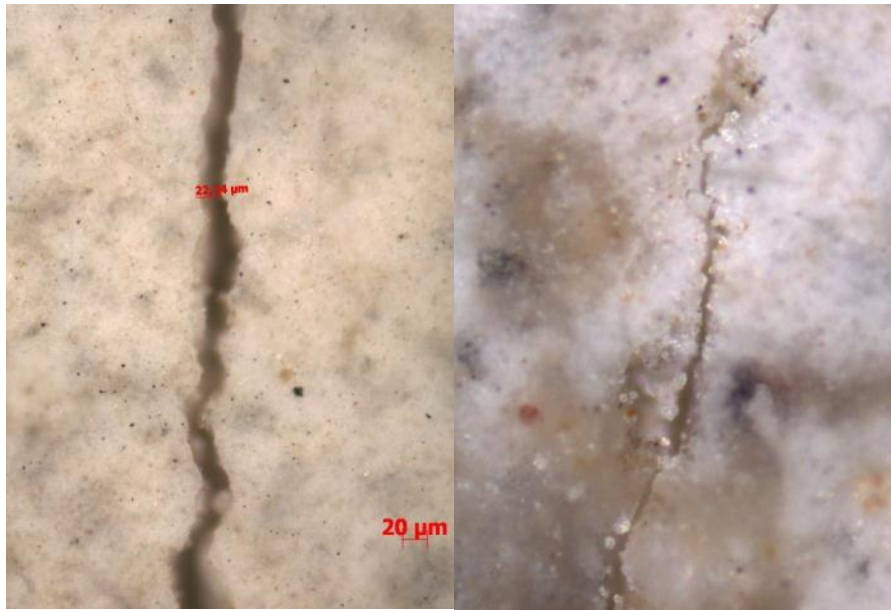


c)

d)

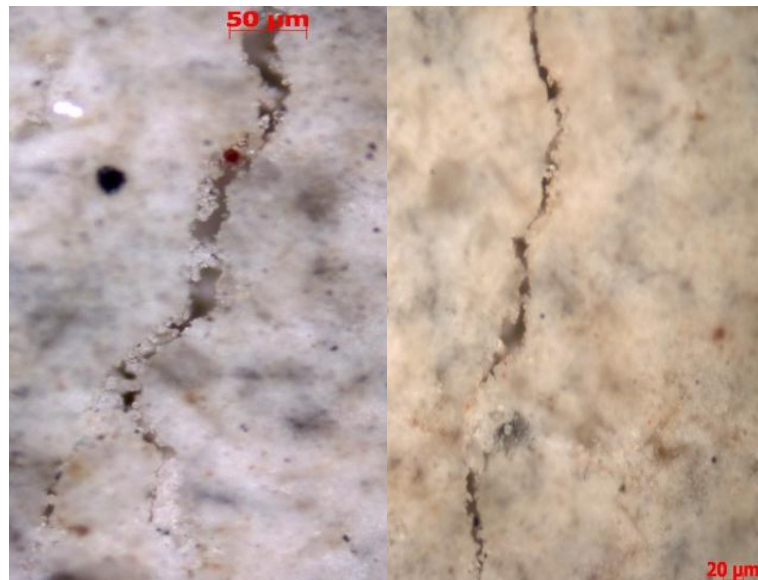
Figure 3.35 : Optical microscope photos of a) C3A, b) C3W, c) C3WD1 ve d) C3WD2 specimens.

Specimens with SAP materials were also not as good as the first group of specimens. There were some weak self-healing products at the edges of cracks (Figure 3.36). However these products were not much enough to close the cracks totally.



a)

b)



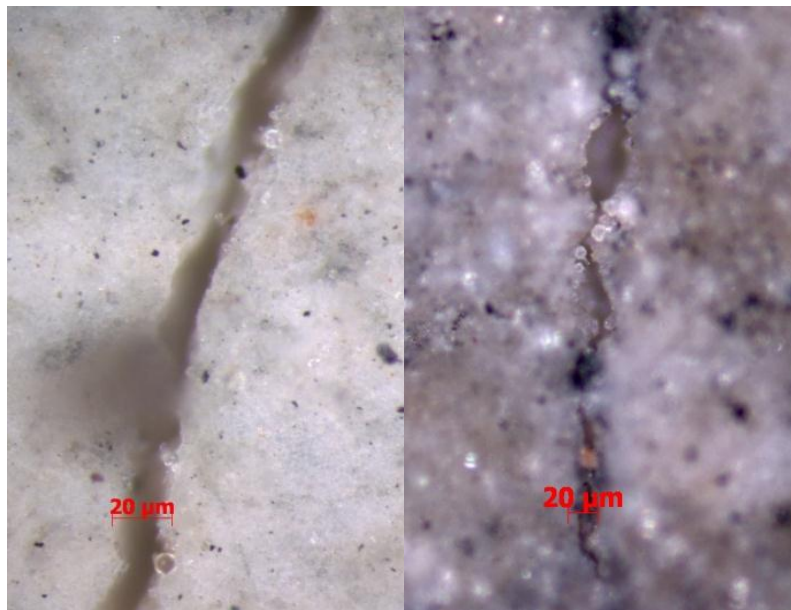
c)

d)

Figure 3.36 : Optical microscope photos of a) SAPA, b) SAPW, c) SAPWD1 ve d) SAPWD2 specimens.

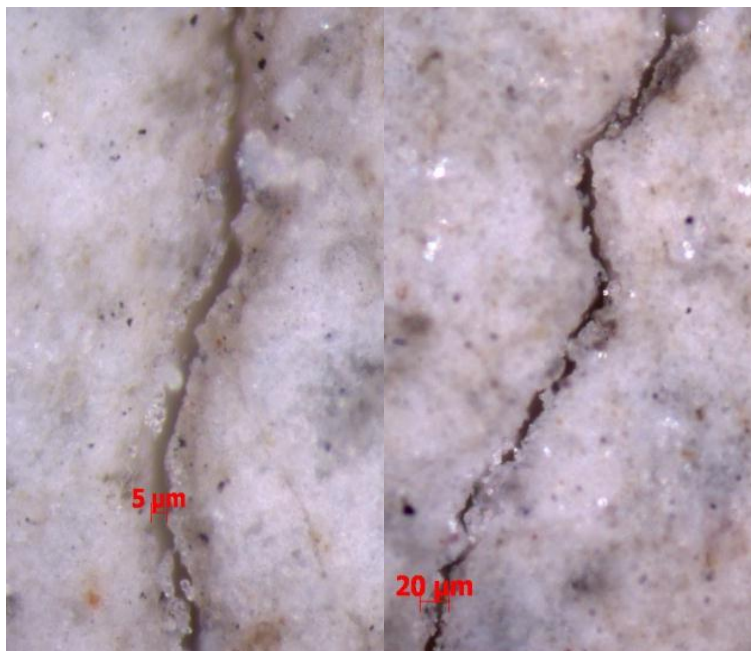
3.2.1.2 Four weeks curing

As expected specimens that are cured for 4 weeks showed better self-healing than 2 weeks curing time except the first CEM I group. It can be seen in the following figure, both wet-dry cycle groups of specimens were not be able to close the cracks totally. Mostly there were crack openings up to 5 μm after curing. It has to be also mentioned for specimens that are exposed to water and wet-dry cycles, it was also possible to see fully closed cracks.



a)

b)



c)

d)

Figure 3.37 : Optical microscope photos of a) C1A, b) C1W, c) C1WD1 ve d) C1WD2 specimens.

In the CEM III group, there were more fully closed than partially closed cracks for the water cured specimens. As it can be clearly seen in the following pictures a crack that had a 20 μm opening is totally closed by newly formed self-healing products. In the next photo, the crack opening of 20 μm were closed up to 5 μm . The second wet-dry cycled specimens were not mostly able to close the cracks as the first wet-dry cycle group.

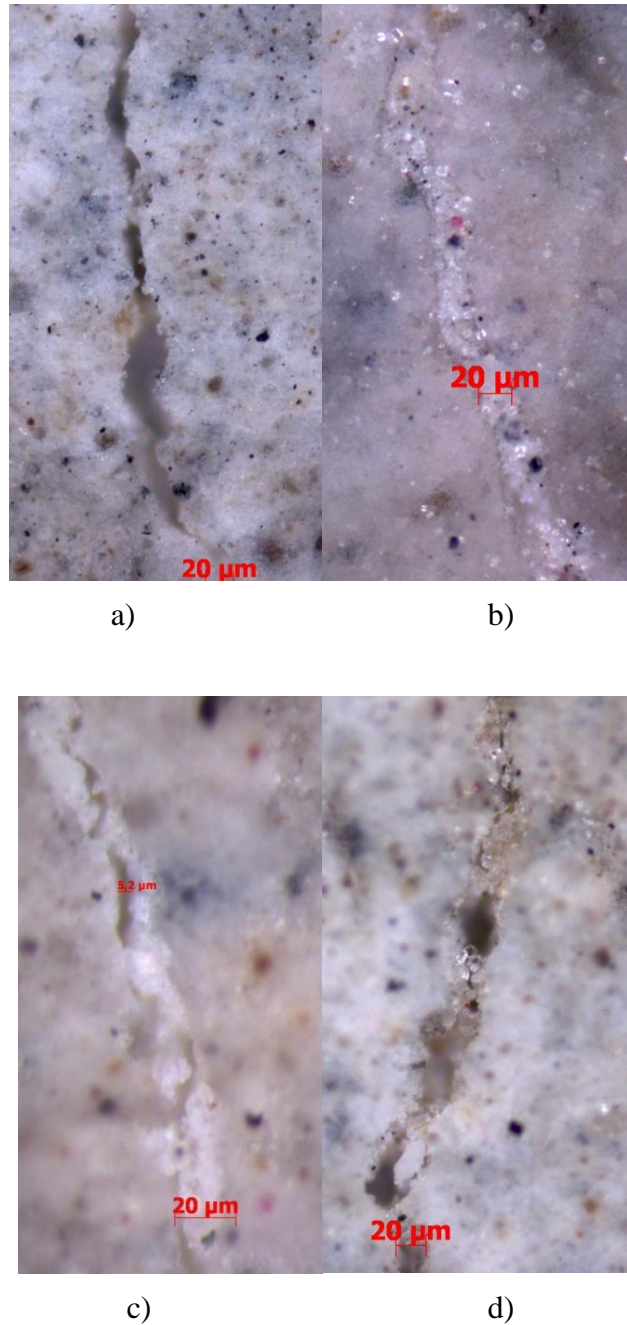
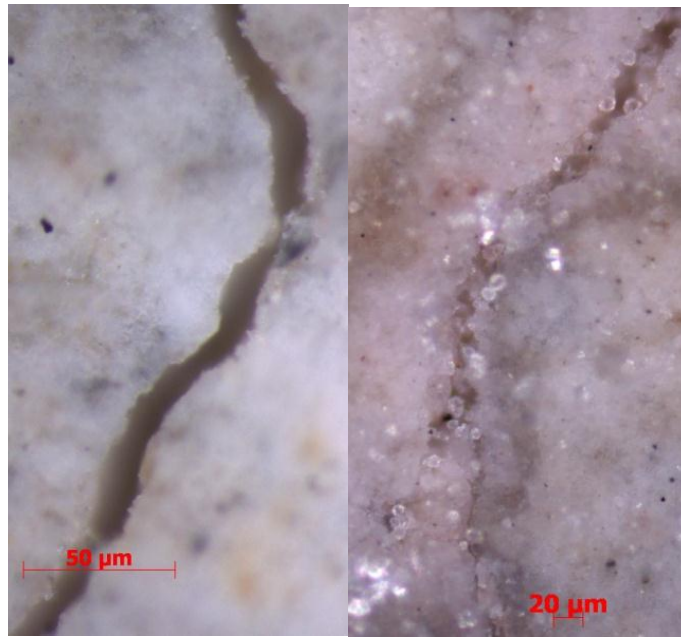


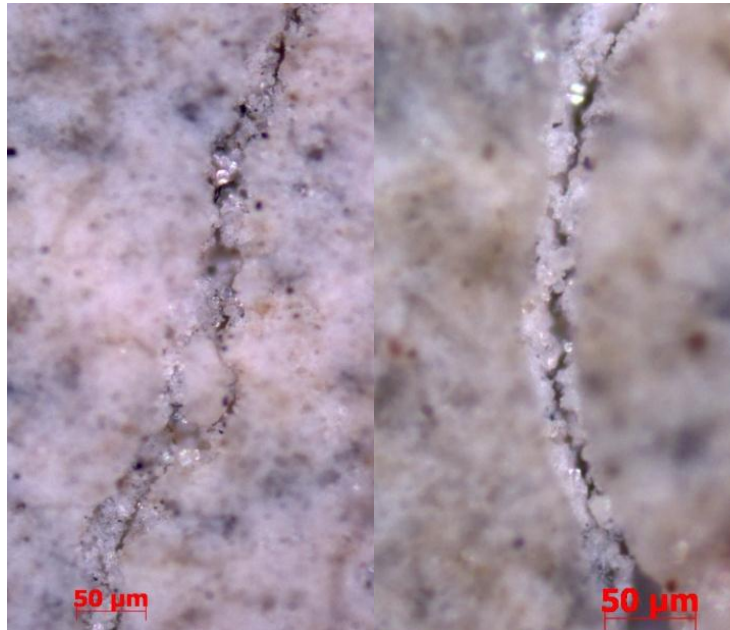
Figure 3.38 : Optical microscope photos of a) C3A, b) C3W, c) C3WD1 ve d) C3WD2 specimens.

It was expected for the specimens that include SAP materials to show better self-healing, but for both curing groups and durations the self-healing ability of those specimens were not as better as the specimens that don't include SAP materials. As it can be also seen in the following pictures, the cracks were not totally closed; however the closing rate was higher than the 2 weeks cured specimens.



a)

b)



c)

d)

Figure 3.39 : Optical microscope photos of a) SAPA, b) SAPW, c) SAPWD1 ve d) SAPWD2 specimens.

3.2.1.3 Thin Sections

In this study, some photographs of the sections that are prepared from the surfaces were taken under UV lights and some of thin sections were also photographed under microscope with up to 50 times magnifying. The green parts of the photos which were taken under UV light are voids and cracks, nevertheless in the photographs which were taken under optical microscope voids and cracks are seen yellow under microscope light. After pre-cracking multiple cracks were occurred and cracks that

are vertical to cross section of specimens can be seen in the pictures. As it can be seen in the figures below, specimens for the pure Portland cement group after water and wet-dry cycles curing vertical cracks were mostly closed as parallel with the optical microscopy photographs and there is no visible vertical cracks on the thin sections. Photos below were chosen among more numbers of photos.

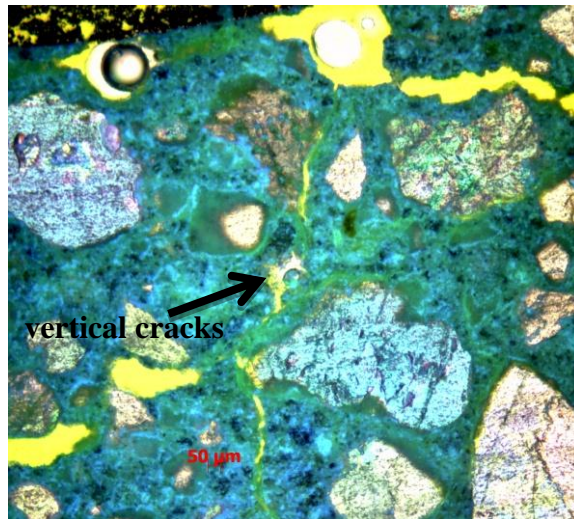
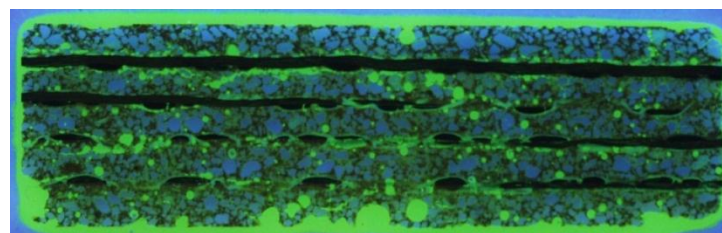
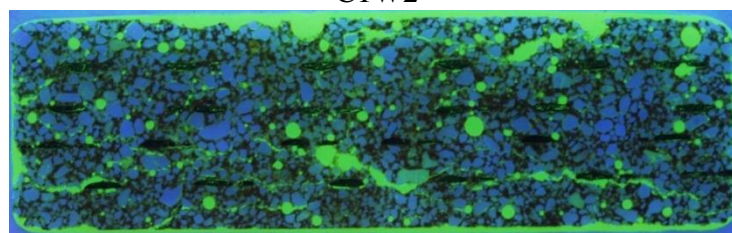


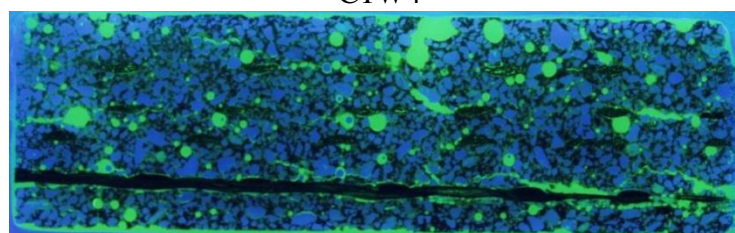
Figure 3.40 : The optical microscope photo of CEM I reference (pre-cracked and no cured) specimen.



C1W2

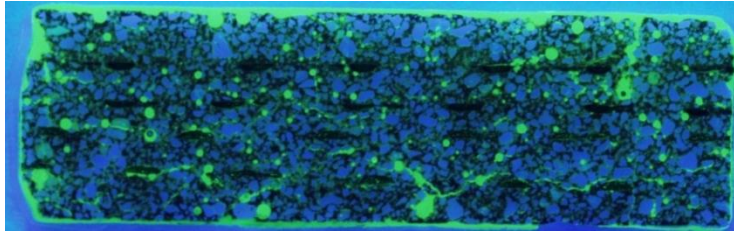


C1W4



C1WD22

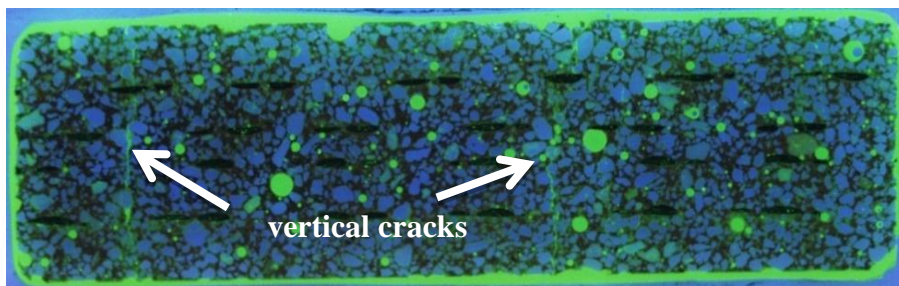
Figure 3.41 : The photos of CEM I specimens exposed to water and wet-dry curing for 2 and 4 weeks, which were taken under UV light.



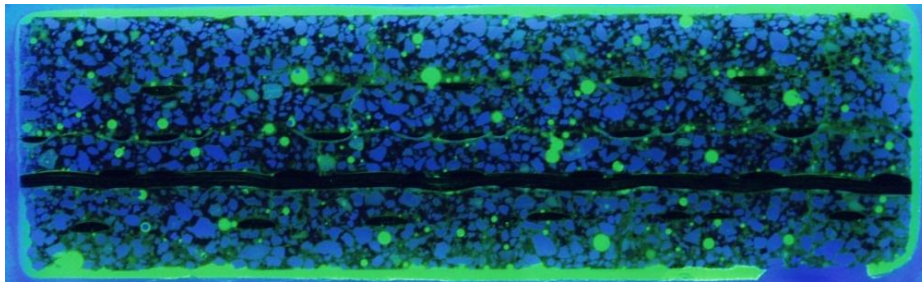
C1WD24

Figure 3.41 (continued) :The photos of CEM I specimens exposed to water and wet- dry curing for 2 and 4 weeks, which were taken under UV light.

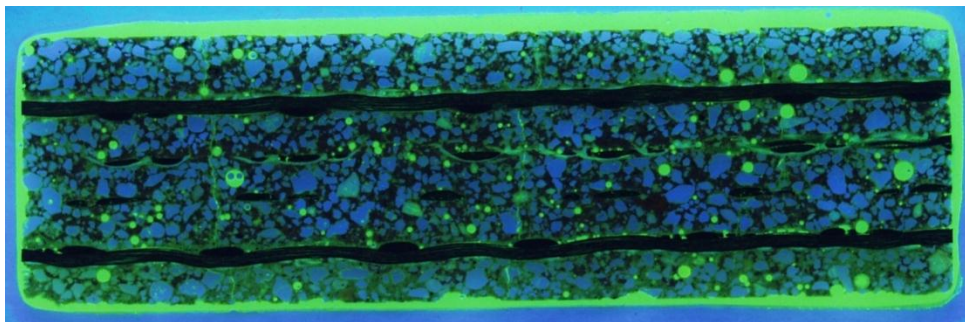
In the second part of thin sections' investigation, specimens that were produced with CEM III and pozzolanas were observed. Vertical cracks which occurred after pre-cracking were narrower and partially closed after self-healing as it can be clearly seen in the optical microscope photos. However in the photos that were taken under UV light, cracks were visible in the reference specimen.



REFC3

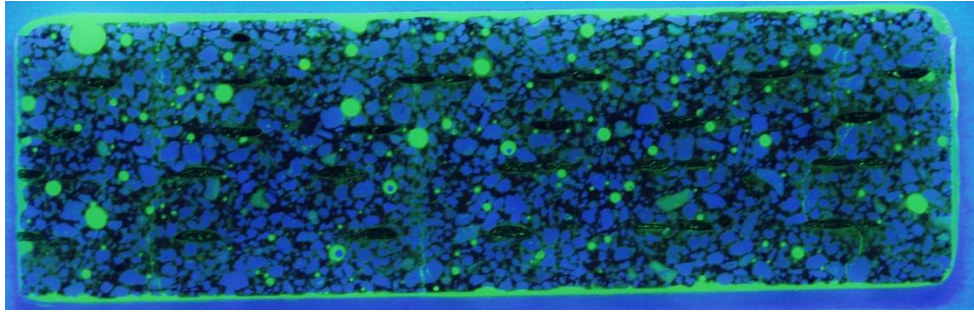


C3WD22

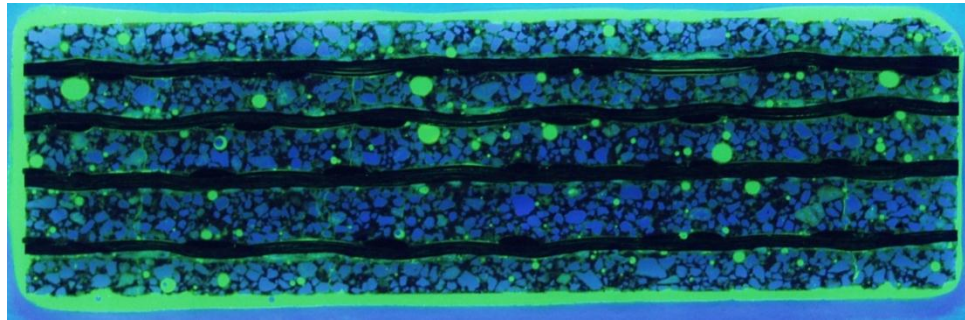


C3WD24

Figure 3.42 : The photos of CEM III specimens exposed to water and wet-dry curing for 2 and 4 weeks, which were taken under UV light.



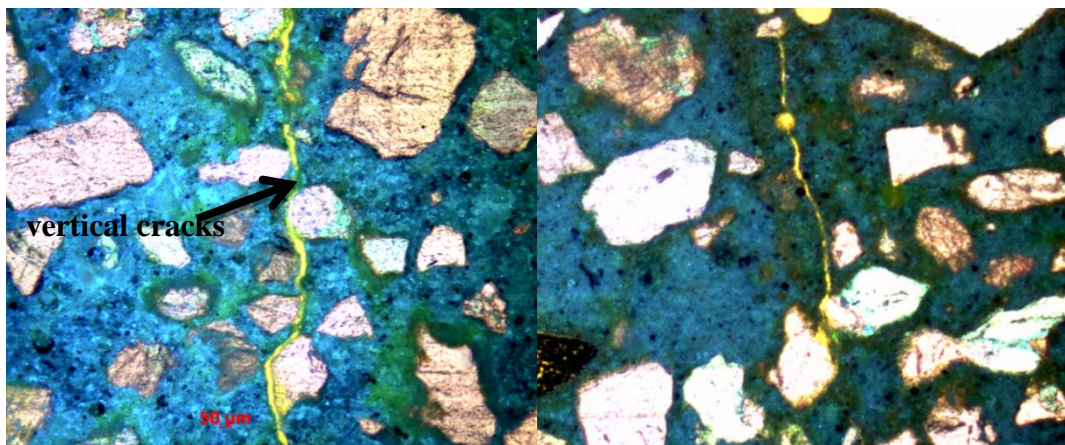
C3W2



C3W4

Figure 3.42 (continued) :The photos of CEM III specimens exposed to water and wet-dry curing for 2 and 4 weeks, which were taken under UV light.

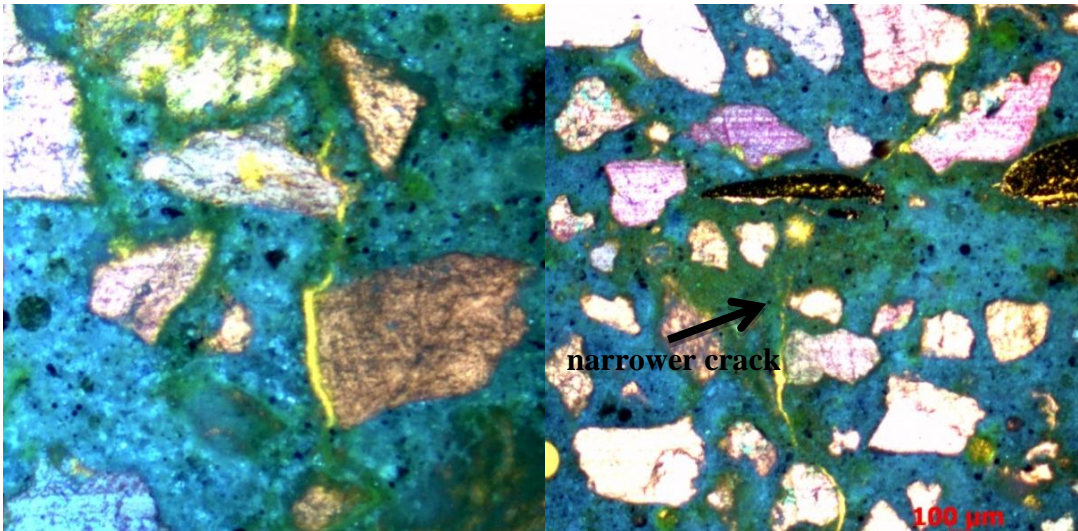
Vertical cracks were still visible but also smaller in the specimens that were exposed to water curing and wet-dry cycle-II for 2 and 4 weeks. These results are also parallel with optical microscopy photos and it was because of 2 and 4 weeks self-healing curing was not enough to close cracks totally.



REFC3

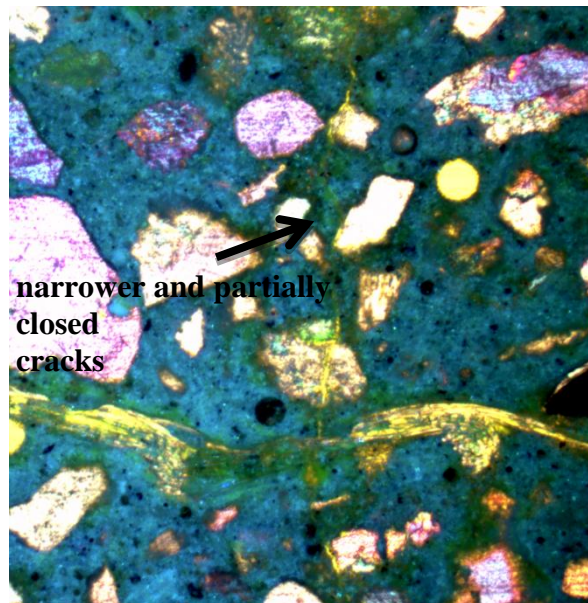
C3W2

Figure 3.43 : The optical microscope photos of CEM III specimens after various exposures.



C3W4

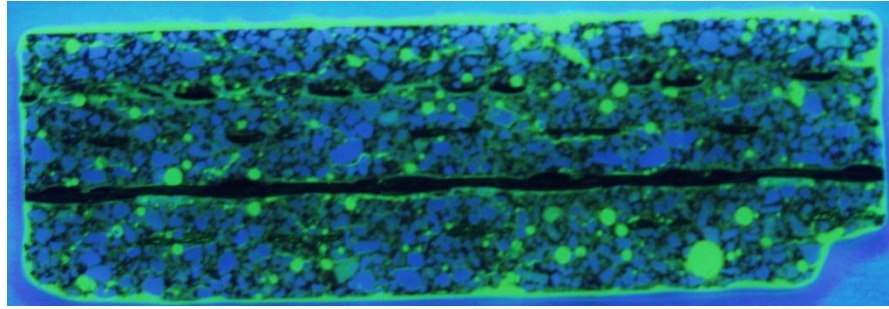
C3WD22



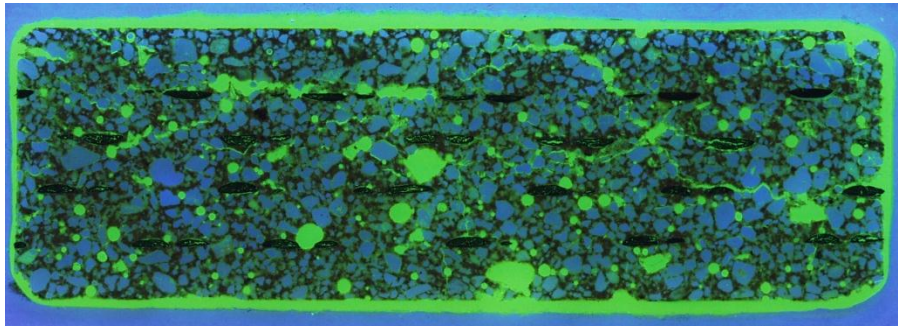
C3WD24

Figure 3.43 (continued):The optical microscope photos of CEM III specimens after various exposures.

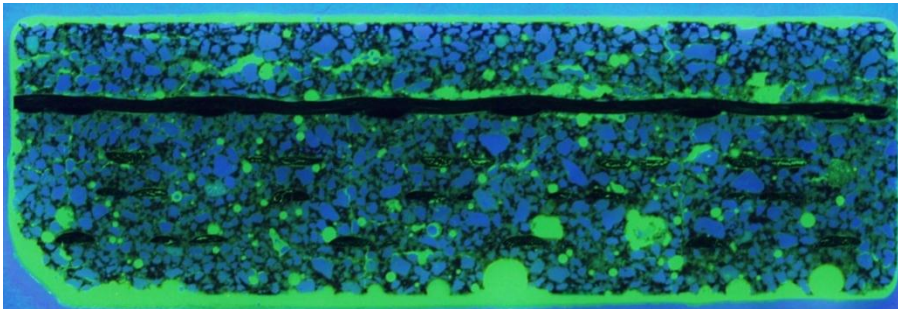
The last group for the thin section observation was SAP group. As it mentioned before the specimens were produced with Portland cement CEM I as binder and SAP materials were added directly to the mixture. There were no clearly visible cracks in UV light photos of thin sections as it can be seen below.



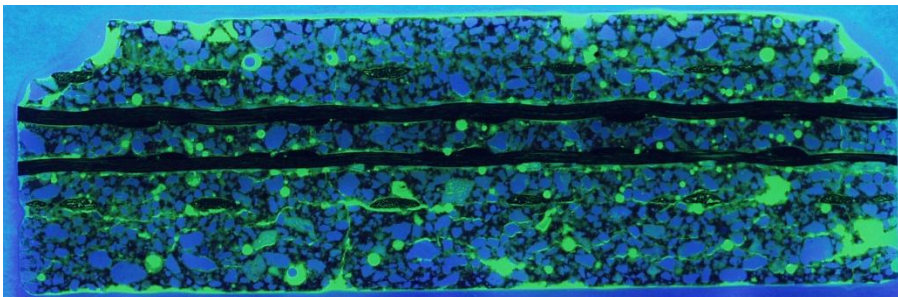
SAPW2



SAPW4



SAPWD22



SAPWD24

Figure 3.44 : The photos of CEM III specimens exposed to water and wet-dry curing for 2 and 4 weeks, which were taken under UV light.

In the light microscope photos of thin section photos of reference specimens, cracks were clearly visible as it can be seen as yellow line. For both 2 and 4 weeks water cured specimens cracks were totally closed. However, as it can be seen in the second picture below the crack pattern was visible as a green line. It means the thickness of thin section at that crack was smaller than the third picture. It can be concluded that 4 weeks curing made thin section specimens thicker than 2 weeks water curing.

Finally, in the photos of thin section specimens which were exposed to 2 and 4 weeks wet-dry cycle-II, cracks were not totally closed.

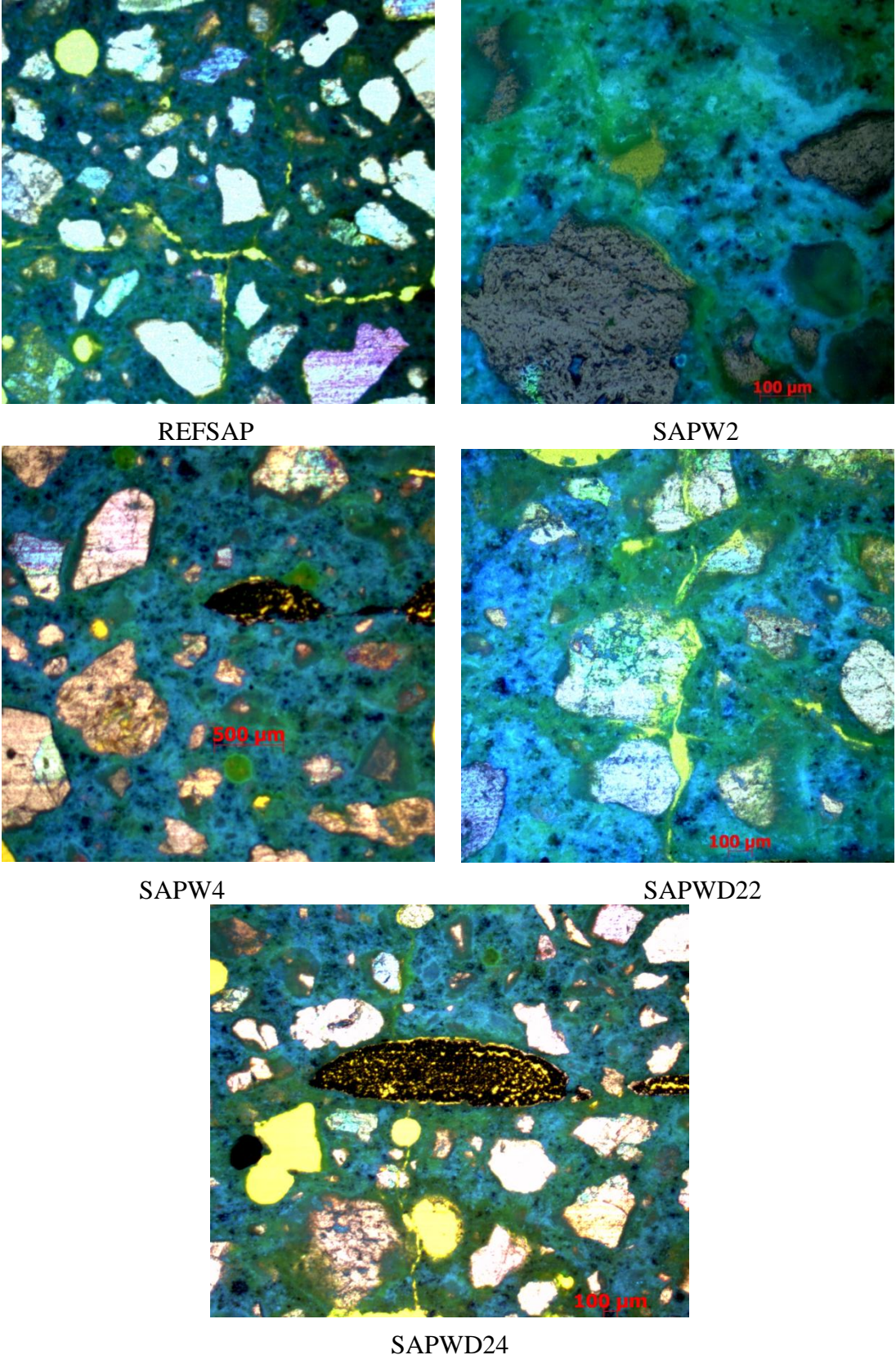


Figure 3.45 : The optical microscope photos of SAP group specimens after various exposures.

3.2.2 SEM and EDX analysis

Analysis of SEM pictures and EDX was an investigation to monitor self-healing and to understand the chemical composition of self-healing products. Many SEM pictures were taken from various points of specimens and with different magnitudes. The best and typical pictures were showed below; however some of them were chosen to couple with EDX analysis. For all the EDX analysis it was hard to distinguish self-healing products as calcites and C-S-H phases.

For the SEM picture which are showed below, it is clear to see the original width and the healed part of the specimen. The specimen was exposed to water curing for 4 weeks. Some parts of the specimen were totally closed. In the EDX analysis it can be said that there was a good combination of C-S-H phases and calcites.

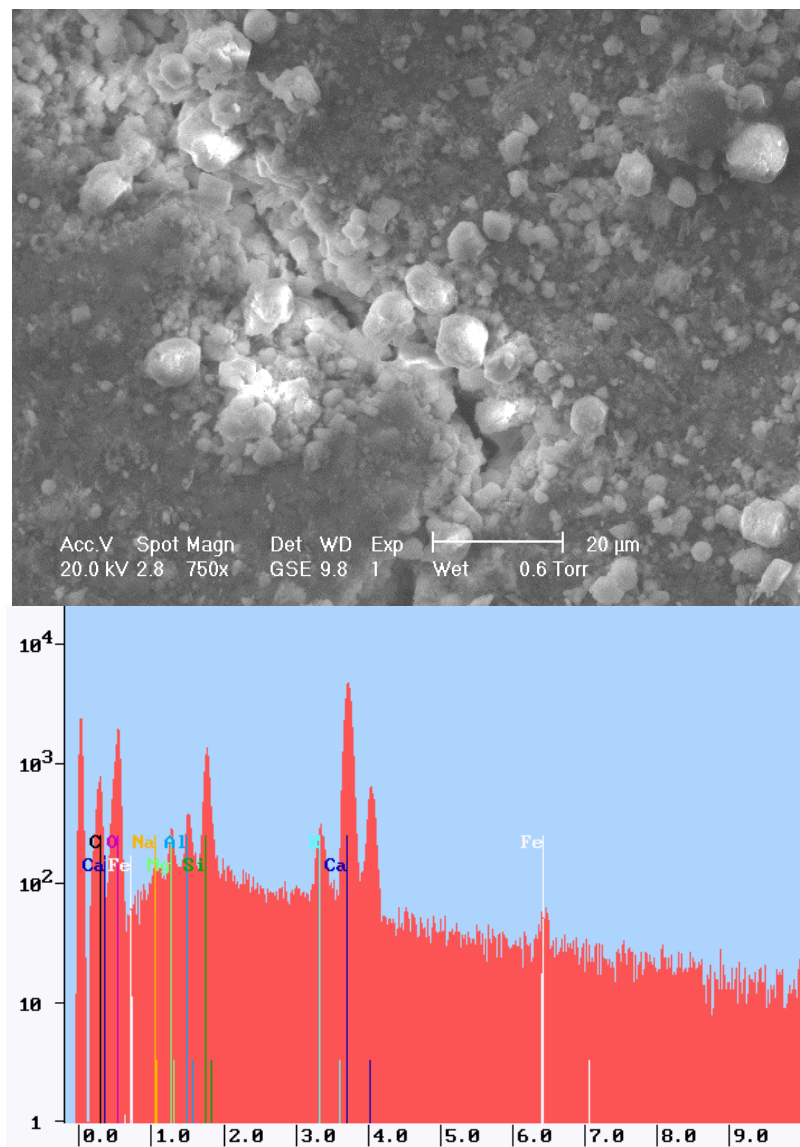


Figure 3.46 : SEM picture of a crack and EDX analysis of the specimen C1W4.

In the EDX analysis picture below for the specimen that was produced with CEM I and was exposed to wet-dry cycle-I for 4 weeks, the parallel behaviour is present. Furthermore calcites were slightly dominant.

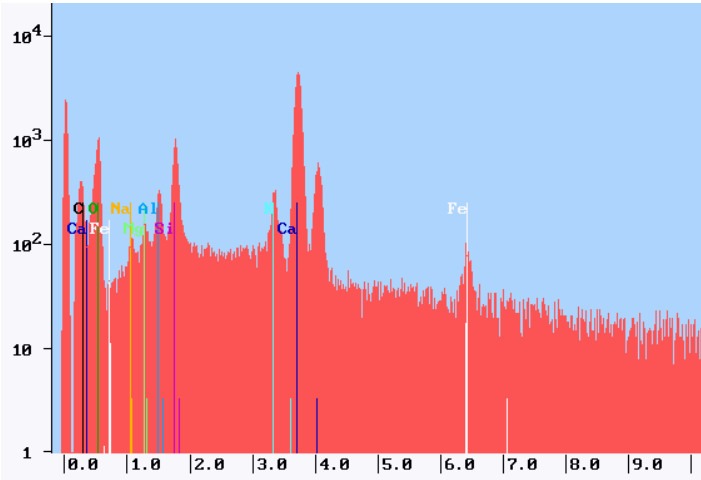


Figure 3.47 : EDX analysis of the specimen C1WD14.

The next specimen was produced with CEM III and pozzolanas and was exposed to water during 4 weeks. The remain width of the healed crack was below 5 μm . Self-healing products seem to be combination of calcites and C-S-H phases.

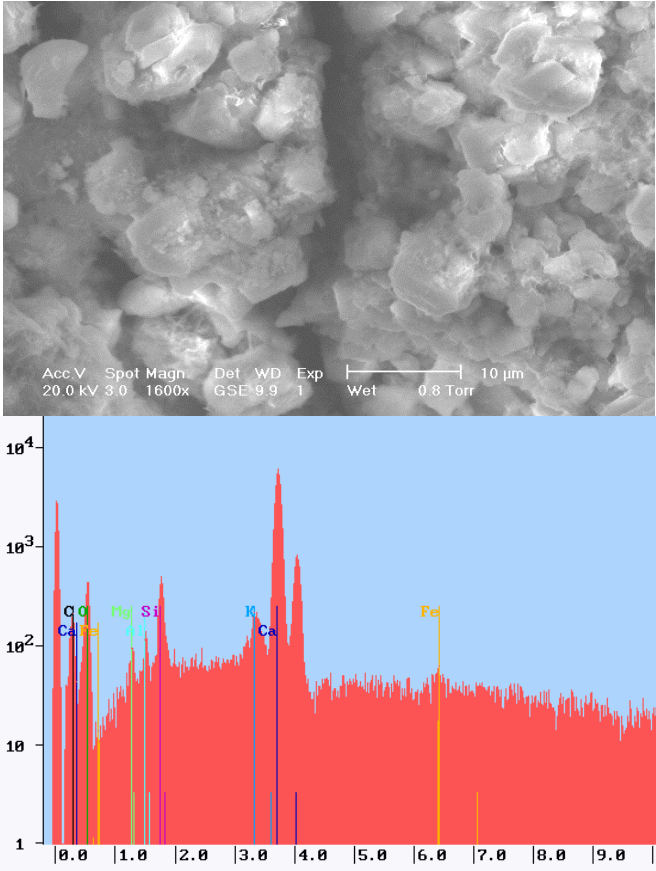


Figure 3.48 : SEM picture of a crack and EDX analysis of the specimen C3W4.

SAP materials were used for the production of last specimen for EDX analysis. The specimen was cured in water during 4 weeks. As it can be seen in the SEM picture crack was partially closed and in the EDX analysis, self-healing products were mostly calcites. Moreover C-S-H phases were also present.

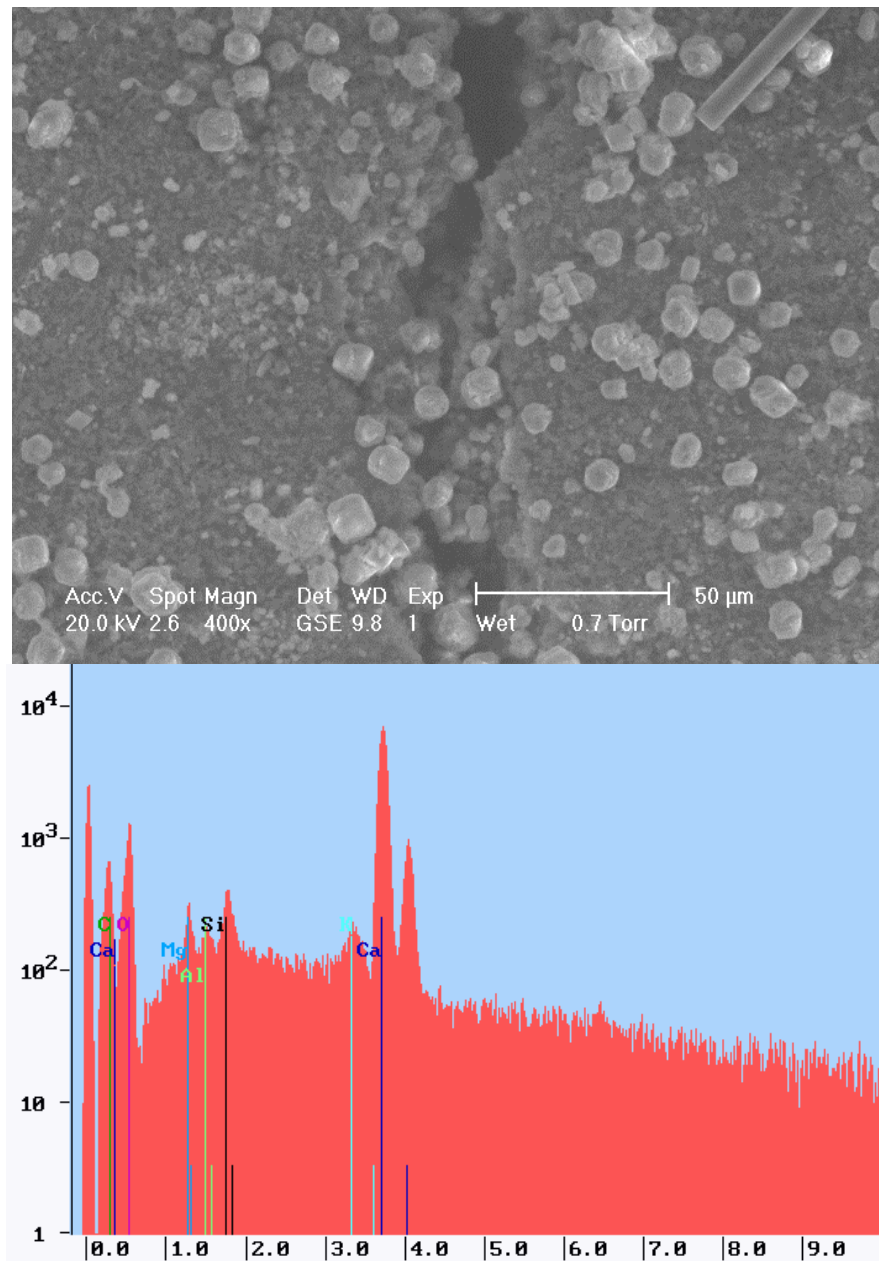


Figure 3.49 : SEM picture of a crack and EDX analysis of the specimen SAPW4.

For all cured specimens the crack width was decreased after self-healing. There was mostly combination of C-S-H phases and calcites; however for the CEM I group C-S-H phases which are important for mechanical self-healing, were more than other groups. In the following part SEM pictures of the specimens that were exposed to various conditions were showed. The group pictures that seen below are the SEM

picture of CEM I for various exposures and time. As it can be seen in the first picture the reference specimen has crack width over 20 μm , the edges of the crack was clear and there is no self-healing product. For the next specimen which was exposed to air curing for 2 weeks, there was nearly no self-healing and the crack width was nearly original crack width. Specimens that were cured in water for 2 and 4 weeks have narrower cracks. In the picture of 2 weeks cured specimen, a calcite form and in the 4 weeks cured specimen totally closed part of crack can be clearly seen. The cracks of wet-dry cycled specimens are partially closed and the combination of C-S-H phases dominantly and calcites was observed.

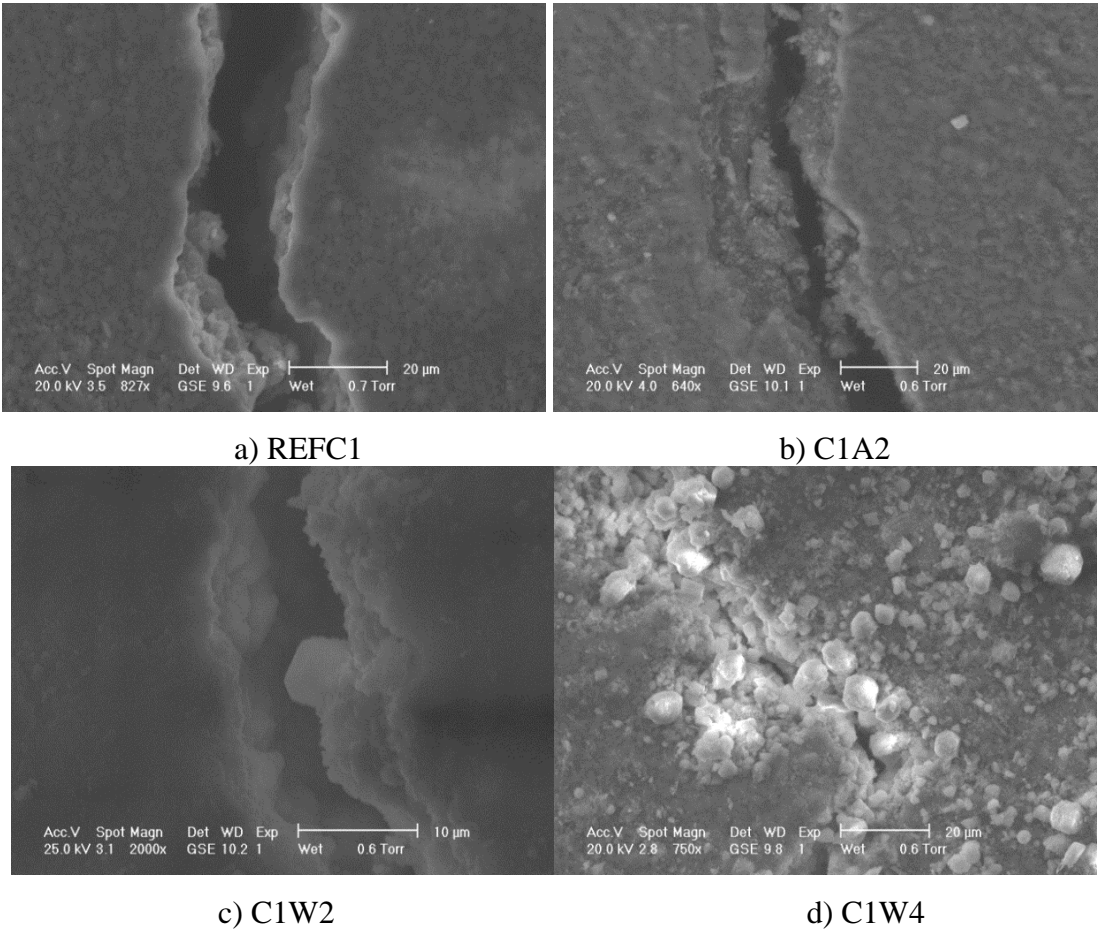
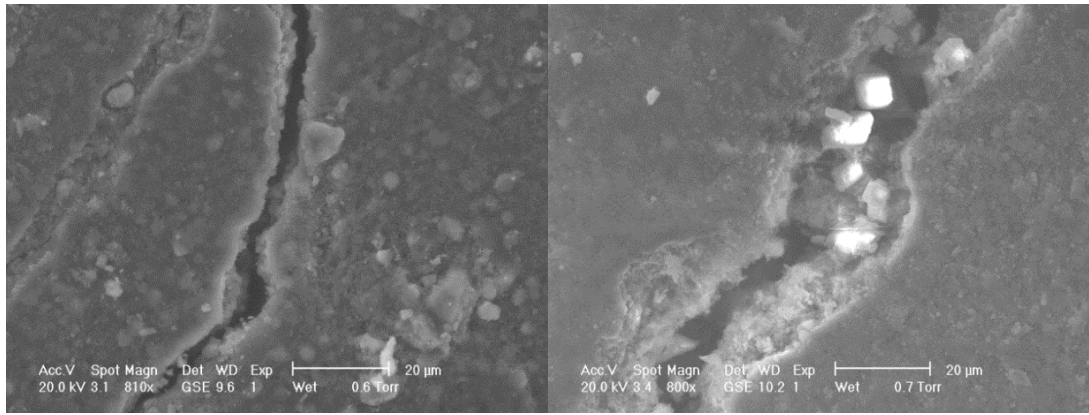
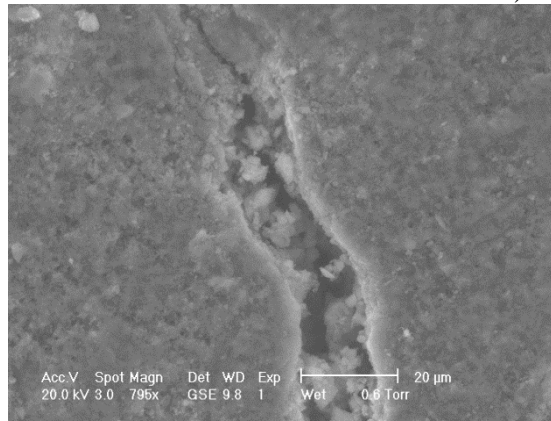


Figure 3.50 : SEM pictures of CEM I group specimens.



e) C1WD22

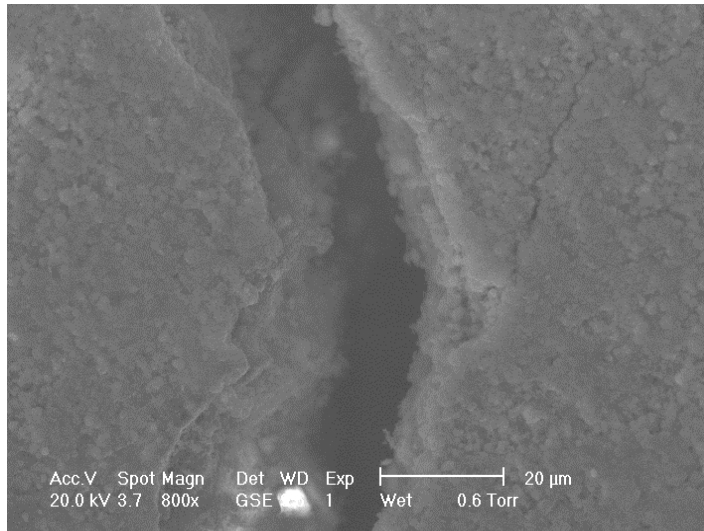
f) C1WD24



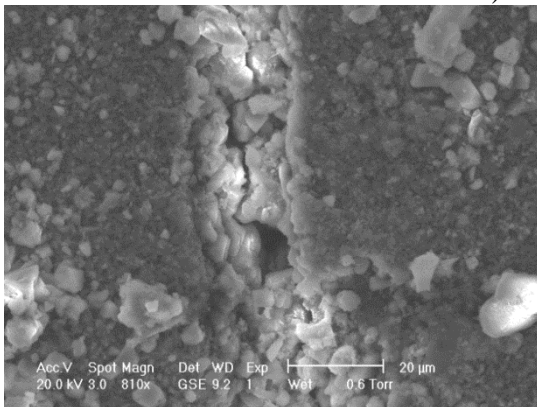
g) C1WD12

Figure 3.50 (continued) : SEM pictures of CEM I group specimens.

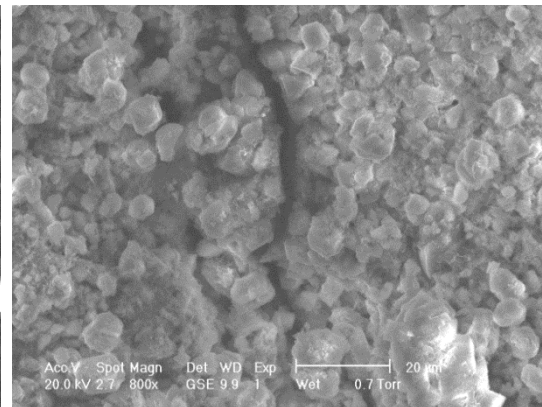
The next group of SEM pictures are pictures of specimens which were produced with CEM III and pozzolanas. The reference specimen was covered and kept in desiccator after pre-cracking to prevent any chemical activity as other reference specimens. As the first reference picture it seems no self-healing in the crack. The specimens that were exposed to water curing have nearly closed cracks; as it can be seen in the pictures below the crack widths were smaller than 2 μm . Wet-dry cycled specimens have cracks as narrow as the water cured specimens. Finer C-S-H phases and mostly calcites can be seen in the pictures.



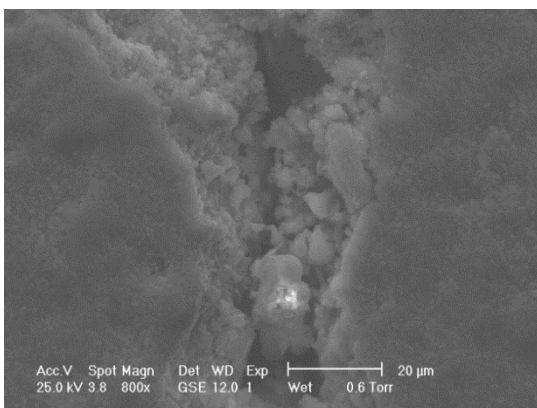
a) RC3



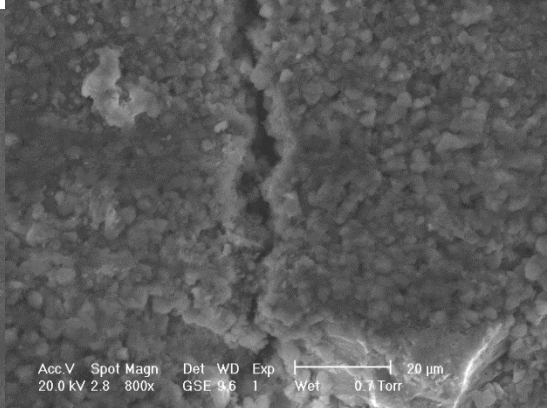
b) C3W2



c) C3W4



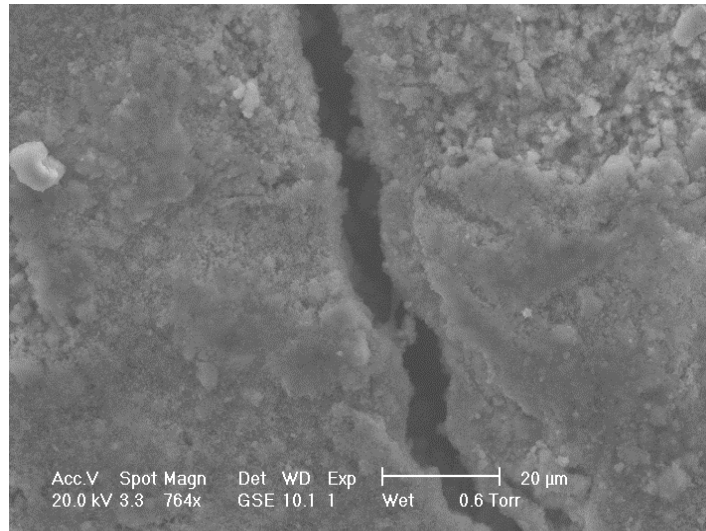
d) C3WD22



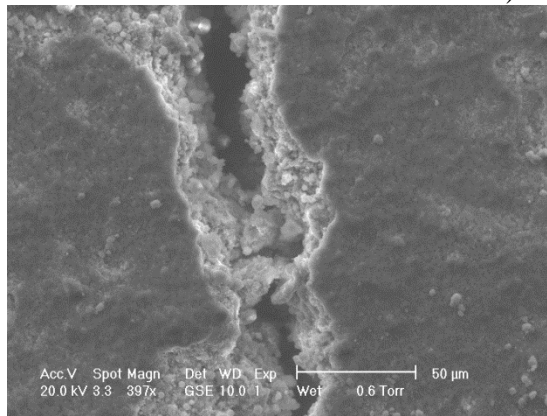
e) C3WD24

Figure 3.51 : SEM pictures of CEM III group specimens.

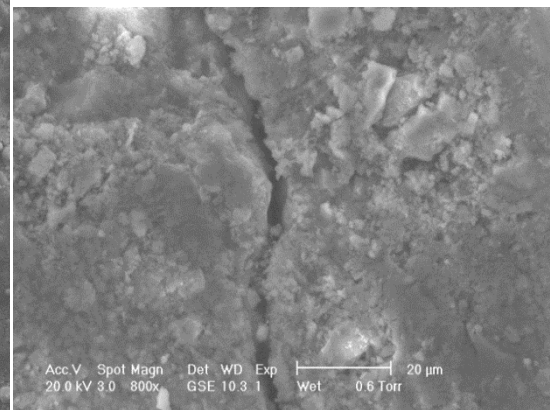
For the specimens that were produced with SAP materials it can be said that the self-healing ability of water cured specimens were better than the specimens which were exposed to wet-dry cycles. Fiber like C-S-H phases and stone like calcites were the self-healing products in the cracks.



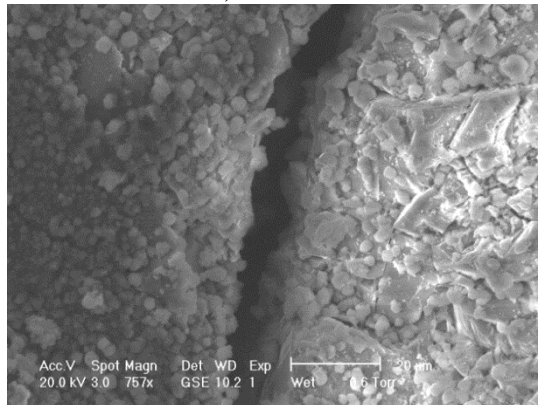
a) RSAP



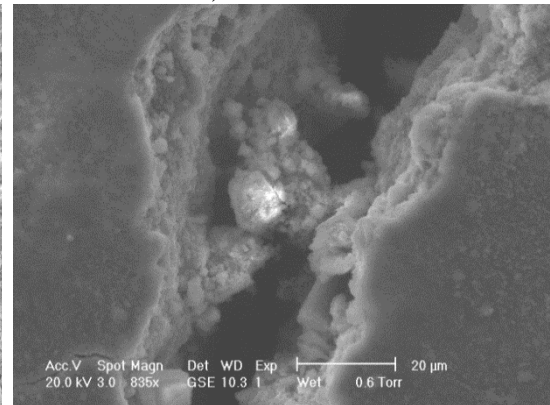
b) SAPW2



c) SAPW4



d) SAPWD22



e) SAPWD24

Figure 3.52 : SEM pictures of CEM III group specimens.

3.2.3 MIP analysis

For the MIP analysis 3 groups of specimens were produced and wrapped in plastic foil for 28 days. After pre-cracking specimens were cut according to the suitable dimensions for the test machine. All the tests were performed before and after self-

healing curing. The tests were done to have an idea about the distribution of cracks and pores for the entire structure of the specimens.

As it can be seen in the first figure, all curing types have showed a decrease in pore sizes. Moreover, water curing and wet-dry cycle-2 groups have showed smaller pore size distribution.

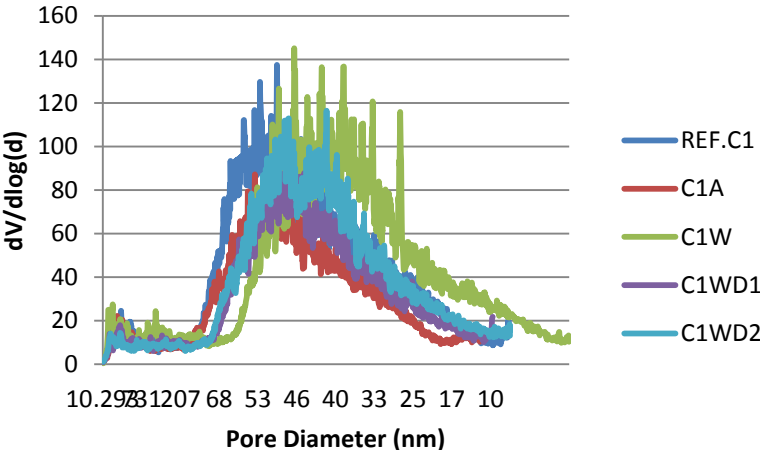


Figure 3.53 : Total pore size distribution of C1 group specimens.

In the C3 group specimens, there is nearly same distribution for the reference and air cured specimens. As the first figure, the finer pore size distribution was for the water cured and wet-dry cycled-2 specimens. It can be also said that the pore size distribution for C3 specimens were finer than C1 specimens. It may be because of totally closed cracks in the C1 group specimens. The range of pore size distribution for water cured group was 50-25 nm.

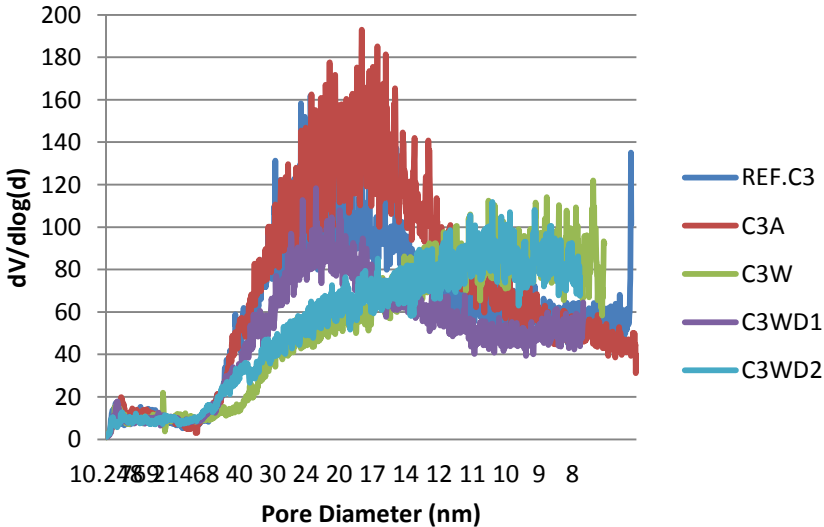


Figure 3.54 : Total pore size distribution of C3 group specimens.

The last group of was the specimens that were produced with SAP materials. As the C1 group all curing types have finer pore size distribution than reference specimens. Nevertheless, the finest distribution was for the wet-dry cycle-1 group. The pore size distribution range decreased to 32-26 nm.

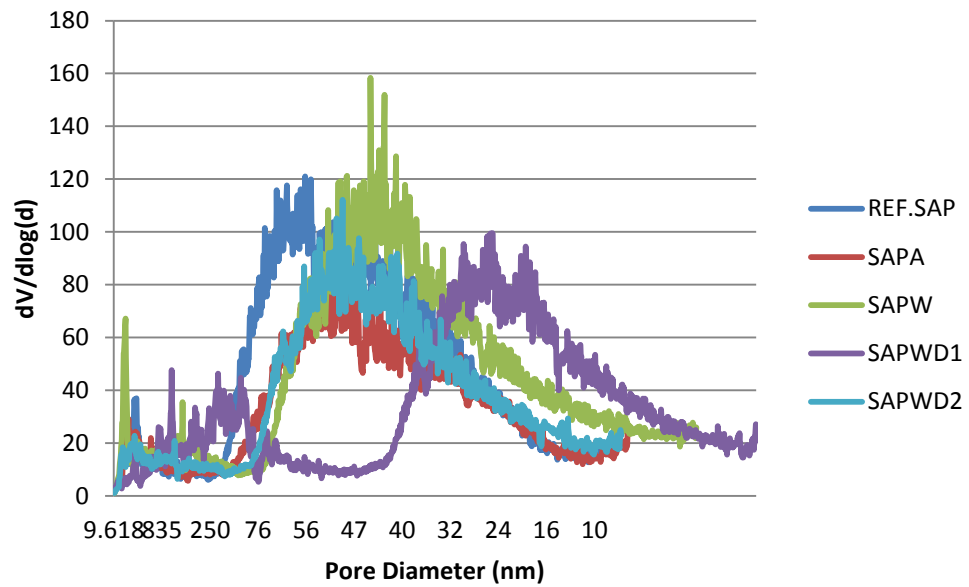


Figure 3.55 : Total pore size distribution of SAP group specimens.

4. CONCLUSIONS AND RECOMMENDATIONS

In this study, self-healing properties of high performance textile reinforced concrete, which was exposed to air and water curing and wet-dry cycles for different periods, were investigated. The effect of different types of binders was also investigated. Mechanical tests and microscopic analysis were used.

Mechanical test results can be concluded as follows;

- Self-healing products, which are attached to cracks after water and wet-dry exposures, are leading to recovery of mechanical performance. Air curing showed nearly no self-healing for all groups of specimens and time periods. Longer curing is increasing mechanical healing performance for water curing and wet-dry cycling.
- Specimens that were produced with CEM I cement and cured for longer time had the best self-healing behavior. This concrete had a large amount of unhydrated cement left after hydration and this indicates that continued hydration was the main reason for recovery of mechanical properties.
- Addition of SAP materials into the concrete mixture supported further hydration and showed positive mechanical effect for less wet-dry cycle.

Some conclusions drawn from microscopic study are:

- Water in the crack is the most important factor for self-healing. There was no self-healing and sealing of cracks without water because water is needed for the chemical reactions in self-healing and for the transport of fine particles in self-closing.
- The continued hydration of unreacted cement was present in all binders based on Portland cement. For cementitious systems containing blast furnace slag and in concrete mixtures with significant additions of pozzolanic materials such as fly ash and silica fume, the pozzolanic reaction may also provide a degree of self-

healing capacity. However, the healing capacity for pure Portland cement was the highest because of the highest amount of unreacted cement particles.

- There was no clear distinguishing but self-healing products for the crack closing were mostly combination of C-S-H phases and calcites.
- Newly formed products after all type of exposures affected the entire structure of the specimens positively for self-healing according to MIP results. Denser structures were observed after self-healing exposures.

Evaluation and discussion of the experimental results of the study indicates that self-healing of high performance fiber reinforced composites is a clear issue if water is present cracks. However, for effective self-healing there has to be enough amounts of unreacted cement particles in concrete.

REFERENCES

- [1] **Gordon, J.E.**, 1968, The new science of strong materials, or why you don't fall through the floor. Princeton University Press, Princeton, USA.
- [2] **RILEM Report**, 2011, State-of-the-Art Report of RILEM Technical Committee 221-SHC : Self-Healing phenomena in Cement-based materials.
- [3] **Taşdemir M. A., Bayramov F., Kocatürk A. N. and Yerlikaya M.**, (n.d.), Betonun Performansa Göre Tasarımı: Performans Sınıfları.
- [4] **DuraCrete**, 1997 : “Design Framework”, Document BE95-1347/R1, The European Union – Brite EuRam III, Contract BRPR- CT95-0132, Project BE95-1347, CUR, Gouda.
- [5] **(EN 1991-1, EN 1994)** Eurocode 1 - Actions on structures - Part 1-1: General actions - Densities, self-weight and imposed loads for buildings.
- [6] **Yunovich, M., Thompson, N.G.**, 2003, Corrosion of highway bridges: Economic impact and control methodologies. Concrete Int., Vol. 25, 1, pp. 52-57.
- [7] **DTI**, 2006, Construction statistics annual report. London TSO.
- [8] **Zwaag, S. van der (ed.)**, 2007, Self-healing materials, an alternative approach to 20 centuries of materials science. Springer Series in Materials Science no. 100. Springer, Dordrecht, The Netherlands.
- [9] **Mihashi, H., Kaneko, Y., Nishiwaki, T. and Otsuka, K.**, 2000, Fundamental study on development of intelligent concrete characterized by self-healing capability for strength. Transactions of the Japan Concrete Institute, vol. 22, pp. 441-450.
- [10] **Yang, Y. et al.**, 2009, Autogenous healing of engineered cementitious composites under wet-dry cycles. Cement and Concrete Research, vol 39 [5], pp. 382-390.
- [11] **Edvardsen, C. K.**, 1996, Water permeability and self-healing of through-cracks in concrete (in German).DAfStb Bull. 455, Berlin.
- [12] **Edvardsen, C.**, 1999, Water permeability and autogenous healing of cracks in concrete. ACI Materials J. 96, No. 4, pp 448-454.
- [13] **Wagner, E.F.**, 1974, Autogenous healing of crack in cement-mortar linings for gray-iron and ductile-iron water pipe. In: Journal of the American water works association 66, Nr. 6, S. 358-360.
- [14] **Hannant, D.J., Keer, J.G.**, 1983, Autogenous healing of thin cement based sheets. Cement and concrete research 13, Nr. 3, S. 357-365.
- [15] **Dhir, R.K., Sangha, C.M., Munday, J.G.L.**, 1973, Strength and deformation properties of autogenously healed mortars. Journal of the ACI, Nr. 3, S. 231-236.

- [16] **Clear, C.A.**, 1982, Leakage of cracks in concrete - summary of work to date. Cement and concrete association, internal publication.
- [17] **Ripphausen, B.**, 1989, Untersuchungen zur Wasserdurchlässigkeit und Sanierung von Stahlbetonbauteilen mit Trennrissen. Dissertation RWTH Aachen.
- [18] **Meichsner, H., Wuenschig, R.**, 1991, Institut für Ingenieur- und Tiefbau: Die Selbstdichtung von Rissen in Beton- und Stahlbetonbauteilen. Stuttgart, IRB-Verlag.
- [19] **K. Van Tittelboom and N. De Belie**, 2009, Autogenous healing of cracks in cementitious materials with varying mix compositions, Proceedings of the Second International Conference on Self-Healing Materials, Chicago.
- [20] **Jacobsen, S., Sellevold, E.J.**, 2006, Self-healing of high strength concrete after deterioration by freeze/thaw. Cement and Concrete Research 26, No. 1, pp. 55-62.
- [21] **Jacobsen, S., Marchand, J., Hornain, H.**, 1995, Sem observations of the microstructure of frost deteriorated and self-healed concrete. Cement and Concrete Research 25, Nr. 8, pp 1781-1790.
- [22] **Jacobsen, S.; Marchand, J.; Gerard, B.**, 1998, Concrete Cracks I : Durability and Self-Healing – a Review. In: Gjorv, O.E.; Sakai, K.; Banthia, N. (Eds.): Concrete under Severe Conditions 2, CONSEC '98 : Environment and Loading ; Proceedings of the 2. International Conference; Tromso, Norway, June 21-24, 1998. London ; New York : E & FN Spon, S. 217-231.
- [23] **Meichsner, H.**, 1992, Über die Selbstdichtung von Trennrissen in Beton. Beton- und Stahlbetonbau 87, No. 4, pp 95-99.
- [24] **Edvardsen, C.**, 1999, Self-healing of concrete cracks. Concrete 33, April.
- [25] **Kenneth, R. L., and Floyd, O. S.**, 1956, "Autogenous Healing of Cement Paste," ACI JOURNAL, Proceedings V. 52, No. 6, June, pp. 52-63.
- [26] **Kan, L.-L. et al.**, 2010, Self-healing characterization of engineered cementitious composites (ECC) materials.
- [27] **Taylor, H.F.W.**, 1990, Cement Chemistry , San Diego: Academic Press. p. 475.
- [28] **Homma, D., Mihashi, H., Nishiwaki, T. and Mizukami, T.**, 2008, Experimental study on the self-healing capability of fiber reinforced cementitious composites, Proc. BEFIB 2008, RILEM, 769-774.
- [29] **Edvardsen, C.**, 1999, Water permeability and autogenous healing of cracks in concrete. ACI Materials Journal, vol. 96 [4], pp. 448-454.
- [30] **Jacobsen, S. Marchand, J. and Hornain, H.**, 1995, SEM observations of the microstructure of frost deteriorated and self-healed concretes. Cement and Concrete Research, vol. 25 [8], pp. 1781-1790.
- [31] **Reinhardt, H.-W. and Jooss, M.**, 2003, Permeability and self-healing of cracked concrete as a function of temperature and crack width. Cement and Concrete Research, vol. 33 [7], pp. 981-985.

- [32] **Li, V. and Yang, E. H.**, 2007, Self-healing in concrete materials, in Self-healing materials: An alternative approach to 20 centuries of materials science, S. van der Zwaag, Editor. 2007, Springer Science: Dordrecht, The Netherlands, p. 388.
- [33] **Li, V.C.**, 2003, On engineered cementitious composites (ECC): A review of the material and its applications. *Journal of Advanced Concrete Technology*, vol. 1 [3], pp. 215-230.
- [34] **Homma, D., Mihashi, H. and Nishiwaki, T.**, 2009, Self-healing capability of fibre reinforced cementitious composites. *Journal of Advanced Concrete Technology*, vol. 7 [2], pp. 217-228.
- [35] **Qian, S., Zhou, J., Rooij, M.R. de, Schlangen, H.E.J.G., Ye, G. and Breugel, K. van**, 2009, Self-healing behavior of strain hardening cementitious composites incorporating local waste materials. *Cement and Concrete Composites*, vol. 31 [9], pp. 613-621.
- [36] **Yamamoto, A., Kan, L.-L. and Li, V.C.**, 2009, Self-healing behaviors of engineered cementitious composites under different number of wet-dry cycle, in 11th International Summer Symposium of the Japan Society of Civil Engineers. 2009: Tokyo, Japan.
- [37] **Lepech, M.D. and Li, V.C.**, 2009, Water permeability of engineered cementitious composites. *Cement and Concrete Composites*, vol 31 [10], pp. 744-753.
- [38] **Termkhajornkit, P. et al.**, 2009, Self-healing ability of fly ash-cement systems. *Cement and Concrete Composites*, vol. 31 [3], pp. 195-203.
- [39] **Schlangen, E., ter Heide, N., van Breugel, K.**, 2006, Crack healing of early age cracks in concrete. *Proceedings ECF16, Alexandroupolis*.
- [40] **Heide, N. ter, Schlangen, E., Breugel, K. van**, 2005, Experimental study of crack healing of early age cracks. *Proceedings Knud Højgaard conference on Advanced Cement-based Materials, Denmark*.
- [41] **Heide, N. ter, Schlangen, E.**, 2007, Self-healing of early age cracks in concrete. *Proc. of the First Intern. Conf. on Self-Healing Materials, 18-20 April 2007, Noordwijk aan Zee, The Netherlands* (eds. A.J.M. Schmets & S. van der Zwaag), Springer 2007.
- [42] **Granger, S., Loukili, A., Pijaudier-Cabot, G. & Chanvillard, G.**, 2005), Mechanical characterization of the self-healing effect of cracks in Ultra High Performance Concrete (UHPC)” in *Proceedings Third International Conference on Construction Materials, Performance, Innovations and Structural Implications. Con- Mat’05, Vancouver, Canada, August 22-24, 2005*.
- [43] **Granger, S., Loukili, A., Pijaudier-Cabot G. and Behloul, M.**, (n.d.), Self-healing of cracks in concrete: from model material to usual concretes’, Pre-print.
- [44] **Van Tittelboom, K. and De Belie, N.**, (n.d.), Self-healing concrete: suitability of different healing agents, *International Journal of 3R’s*, submitted.
- [45] **Van Tittelboom, K. and De Belie, N.**, 2009, Self-healing concrete by the internal release of adhesive from hollow glass tubes embedded in the

matrix, Proceedings of the Second International Conference on Selfhealing Materials, Chicago.

- [46] **Gross, A., Kaplan, D., Baker, K.,** 2007, Removal of chemical and microbiological contaminants from domestic grey water using a recycled vertical flow bioreactor (RVFB). *Ecol. Eng.* 31, 107–114.
- [47] **Chaturvedi, S., Chandra, R., Rai, V.,** 2006, Isolation and characterization of *Phragmites australis* (L.) rhizosphere bacteria from contaminated site for bioremediation of colored distillery effluent. *Ecol. Eng.* 27, 202–207.
- [48] **Jugnia, L.B., Cabral, A.R., Greer, C.W.,** 2008, Biothic methane oxidation within an instrumented experimental landfill cover. *Ecol. Eng.* 33, 102–109.
- [49] **Bang, S.S., Galinat, J.K., Ramakrishnan, V.,** 2001, Calcite precipitation induced by polyurethane-immobilized *Bacillus pasteurii*. *Enzyme Microb. Technol.* 28, 404–409.
- [50] **Ramachandran, S.K., Ramakrishnan, V., Bang, S.S.,** 2001, Remediation of concrete using micro-organisms. *ACI Mater. J.* 98, 3–9.
- [51] **De Muynck, W., Debrouwer, D., De Belie, N., Verstraete, W.,** 2008a, Bacterial carbonate precipitation improves the durability of cementitious materials. *Cement Concrete Res.* 38, 1005–1014.
- [52] **De Muynck, W., Cox, K., De Belie, N., Verstraete, W.,** 2008b, Bacterial carbonate precipitation as an alternative surface treatment for concrete. *Constr. Build. Mater.* 22, 875–885.
- [53] **Ramakrishnan, V.,** 2007, Performance characteristics of bacterial concrete—a smart biomaterial. In: Proceedings of the First International Conference on Recent Advances in Concrete Technology, Washington, DC, 2007, pp. 67–78.
- [54] **Jonkersa H. M., Thijssena A., Muiyzerb G., Copuroglu O. and Schlangen E.,** 2010, Application of bacteria as self-healing agent for the development of sustainable concrete. *Ecological Engineering* 36, p. 230–235.
- [55] **Lieboldt M., Mechtcherine V. and Hampel U.,** (n.d.), Protective behavior of textile reinforced concrete in the repair and strengthening of structural concrete members.
- [56] **Lieboldt M., Mechtcherine V. and Hampel U.,** 2011, Permeation of water and gases through cracked textile reinforced concrete, *Cement & Concrete Composites* 33, p.725–734.
- [57] **Hegger J., Will N., Rüberg K.,** (n.d.), Textile Reinforced Concrete – A new Composite Material, Institute of Structural Concrete, RWTH Aachen University.
- [58] **Hegger J, Will N, Aldea C, Brameshuber W, Brockmann T , Curbach M , Jesse J.,** 2006, Applications of Textile Reinforced Concrete. In: Brameshuber W. (ed) RILEM State of the Art Report on Textile Reinforced Concrete, Aachen, pp 237–270.

- [59] **Weiland, S., Ortlepp, R., Hauptenbucher, B. and Curbach, M.**, 2007, “Textile Reinforced Concrete for Flexural Strengthening of RC-Structures - Part 2: Application on a Concrete Shell,” in: Aldea, C.-M. (ed.), Design & Applications of Textile-Reinforced Concrete. Proc. of the ACI Fall Convention, Puerto Rico, SP-251, CD-Rom.
- [60] **Ortlepp, R.; Weiland, S. and Curbach, M.**, 2008, “Restoration of a hyper concrete shell using carbon-fibre textile reinforcement concrete,” in Limbachiya, M.C. & Kew, H.Y. (eds), Proceedings of the International Conference Excellence in Concrete Construction through Innovation, September 9–10, London, Taylor & Francis Group, pp. 357-364.
- [61] **Buchholz F.L. and Graham A.**, 1998, Modern Superabsorbent Polymer Technology, Wiley VCH.
- [62] **Frank M.**, 2009, “Superabsorbents” in “Ullmann’s Encyclopedia of Technical Chemistry”, 7th edition, electronic release, Verlag Wiley-VCH.
- [63] **Friedrich S.** (Coordinator), (n.d.), State of Art Report CHAPTER 3 – SUPERABSORBENT POLYMERS (SAP), BASF Construction Chemicals GmbH.
- [64] **Jensen, O.M, Hansen, P.F.**, 2002, Water-entrained cement based materials- II. Experimental observations. Cement and Concrete Research (32) 973-978.
- [65] **Lura, P. et al.**, 2006, Autogenous strain of cement pastes with superabsorbent polymers. Volume Changes of Hardening Concrete: Testing and Mitigation. RILEM Proceedings PRO 52, O. M. Jensen et al. (eds.), RILEM Publications S.A.R.L., 57-66.
- [66] **Mechtcherine, V. et al.**, 2006, Internal curing by Super Absorbent Polymers – Effects on material properties of self-compacting fibre-reinforced high performance concrete. RILEM Proceedings PRO 52, O. M. Jensen et al. (eds.), RILEM Publications S.A.R.L., 87-96.
- [67] **Mechtcherine, V., Dudziak, L., Hempel, S.**, 2009, Mitigating early age shrinkage of concrete by using Super Absorbent Polymers (SAP). In: CONCREEP-8, T. Tanabe et al. (eds.), Taylor & Francis Group, London, 847-853.
- [68] **Dudziak L. and Mechtcherine V.**, , 2010, Reducing the cracking potential of Ultra-High Performance Concrete by using Super Absorbent Polymers (SAP) Institute of Construction Materials, TU Dresden, Germany In: Advances in Cement-based Materials, G. van Zijl and W.P. Boshoff (eds.), Taylor & Francis Group, London, pp. 11-19.
- [69] **Jensen O. M. and Hansen P. F.**, 2001, Water-entrained cement-based materials I. Principles and theoretical background, Cement and Concrete Research 31, p. 647-654.
- [70] **H. W. Reinhardt, Assmann A. and Mönnig S.**, 2008, Superabsorbent Polymers-An Admixture To Increase The Durability Of Concrete, 1.International Conference on Microstructure Related Durability of Cementitious Composites, 13-15 October, Nanjing, China.

- [71] **EN 197-1** Cement- Part 1: Compositions and conformity criteria for common cements.
- [72] **DIN 1164-10** Composition, requirements and conformity evaluation for special common cement.
- [73] **DIN EN 450-1** Fly ash for concrete – Part 1 : Definition, specifications and conformity criteria.
- [74] **DIN 1045-2** Concrete, reinforced and prestressed concrete structures - Part 2: Concrete - Specification, properties, production and conformity - Application rules for DIN EN 206-1.
- [75] **TS EN 934-2** Kimyasal katkıları-Beton,harç ve şerbet için-Bölüm 2: Beton kimyasal katkıları-Tarifler,gerekler,uygunluk, işaretleme ve etiketleme.
- [76] **EN 1008** Beton-Karma Suyu-Numune Alma, Beton Karma Suyu Olarak Uygunluğunun Tayini.
- [77] **Gorges M.**, quotation of her study about SAP materials in Construction Materials Institute at TU Dresden.

CURRICULUM VITAE

Name Surname: Ömer Kaya

Place and Date of Birth: Haymana-02.10.1983

Address: 69 Ada 1/16 34758 Istanbul

E-Mail: omerkaya83@hotmail.com

B.Sc.: Yıldız Technical University-Istanbul

Professional Experience and Rewards: - Civil Engineer, Giba Insaat (2006-2007)

- R&D Engineer, Iston Corp. (2007-2010)